EFFECTS OF BIODIESEL BLENDING ON EXHAUST EMISSIONS

By

Jing Guo

Submitted to the graduate degree program in Department of Civil, Environmental, and Architectural Engineering and the Graduate Faculty of the University of Kansas in partial fulfillment of the requirements for the degree of Doctor of Philosophy.

Chairperson Edward Peltier

Ray E. Carter

Dennis Lane

Chris Depcik

Glen Marotz

Date Defended: June 9, 2011

The Dissertation Committee for Jing Guo
certifies that this is the approved version of the following dissertation:

EFFECTS OF BIODIESEL BLENDING ON EXHAUST EMISSIONS

Chairperson: Edward Peltier

Date approved: June 9, 2011

EFFECTS OF BIODIESEL BLENDING ON OFF-ROAD ENGINE EMISSIONS

JING GUO

Abstract

Rising fuel costs and energy demands, combined with growing concern over health related and environmental concerns, have led to increased interest in the use of biodiesel. Biodiesel can be utilized as a direct replacement for conventional petroleum diesel or mixed with it to create blended fuels. This latter practice is quite common, as many existing engines are only certified for use with fuels containing a maximum of 5-20% biodiesel. Fuel blending results in the production of a fuel with chemical makeup and combustion properties that may differ significantly from either original source. Understanding the effects of this blending process on engine exhaust composition is an important component of assessing the suitability of these fuels for use in on- and off-road diesel engines.

Research shows that the use of biodiesel made from various feedstocks can reduce the emission of total hydrocarbons (THC), carbon monoxide (CO), and particulate matter (PM), but there is often some increase in nitrogen oxides (NO_X) emissions. Since the composition of this biodiesel may vary depending on the specific feedstock used, it is important to determine the relationship between fuel composition and the resulting emissions of regulated and particle-bound air pollutants during combustion.

The goal of this study is to assess the effect of increased biodiesel concentration,

and the resulting changes in fuel properties on criteria pollutants and particle-bound metal emissions from three off-road diesel engine emissions, which include a lawn mower, a diesel generator, and a switching locomotive. The dissertation is comprised of three sections. In the first section, the lawn mower and the diesel generator were powered by used cooking oil based biodiesel blending, while the emissions profiles for CO_2, CO, NO_X, THC and PM-bound chemicals were measured. The results show that both the engine and fuel properties affected the NO_X and THC emissions, which decreased with increasing biodiesel percentage in the test fuels from both engines. In the second section, up to B20 blends of two kinds of biodiesel (soybean and tallow) were used successfully for extended periods of time in currently-operating locomotives without engine modifications. Biodiesel generally had a lower heating value and less THC emissions. There was no apparent trend for NO_X emissions. In the last section, a rapid-assessment method using LA-ICP-MS method was developed to directly analyze the particle-bound metal for diesel and biodiesel particulates at two running conditions.

Acknowledgements

In my endeavor that has taken so long to complete, there have been more people who have contributed than can be mentioned, but I would be remiss not to acknowledge the contributions of the following individuals.

I am greatly appreciative of the guidance and encouragement of my major advisor, Dr. Edward Peltier. He generously gave me not only his time and expertise, but also of his friendship.

Dr. Ray Carter should also be acknowledged for his contributions throughout this study, especially in the early stages of method development and in understanding the operation of the GC-MS instrument. I thank Dr. Chris Depcik for his insightful comments and suggestions on the research.

I also appreciate the help, advice and patience of the other members of my committee, Dr. Dennis Lane and Dr. Glen Marotz. Each made valuable contributions at appropriate times.

I would like to thank Dr. Susan Williams who provided the biodiesel for this study. Any instrumental in this study was Dr. Gwen Macpherson, who helped me a lot on the LA-ICP-MS method development.

Financial support was obtained from University of Kansas, Transportation Research Institute from Grant # DT0S59-06-G-00047, provided by the US Department of Transportation – Research and Innovative Technology Administration.

Without the people who made it enjoyable to come into the lab or office each day, I would not have endured long enough to finish this thesis. Among many others, I

extend my gratitude to Jay Bernard, Carrie Hohl, Alex Krejci, Pavan Llipilla, Sergio Guerra, Wen Zhang, Si Chen, Xiaolu Chen, Michael Mangus, and Ron Wilson.

I would also like to acknowledge the help, trust and support of my family and friends, especially and posthumously my parents, Qian Shi and Yijing Li.

Table of Contents

List of Figures

List of Tables

Nomenclature

ASTM	American Society for Testing and Materials
ANOVA	Analysis of Variance
BaP	Benzo[a]pyrene
BSE	Brake Specific Emissions
CO	Carbon Monoxide
DI	Direct Injection
EGR	Exhaust Gas Recirculation
EI	Electron Ionization
EISA	Energy Independence and Security Act
EPA	Environmental Protection Agency
FAME	Fame Fatty Acid Methyl Ester
FID	Flame Ionization Detector
FSN	Filter Smoke Number
FTT	Feedstock to Tailpipe
GC-MS	Gas Chromatograph-Mass Spectrometry
GF-AAS	Graphite Furnace Atomic Absorption Spectrometry
IDI	Indirect Injection
HC	Unburned Hydrocarbons
HCN	Hydrogen Cyanide
HF	Hydrofluoric Acid
KU	University of Kansas
LA-ICP-MS	Laser Inductively Coupled Plasma Mass Spectroscopy
LDL	Low Detection Limit
LNT	Lean NO_X Trap
MTBE	Methyl Tertbuty Ether
NDIR	Non-dispersive Infrared Spectroscopy
NDUV	Non-dispersive Ultraviolet Spectroscopy
NO	Nitric Oxide
NO_2	Nitrogen Dioxide

NO_X	Nitrogen Oxides
O_2	Oxygen
O_3	Ozone
PAHs	Polycyclic Aromatic Hydrocarbons
PCBs	Polychlorinated Biphenyls
PCDDs	Polychlorinated Dibenzodioxins
PM	Particulate Matter
RF	Response Factor
ROFA	Residual Oil Fly Ash
ROS	Reactive Oxygen Species
RSD	Relative Standard Deviation
SCR	Selective Catalytic Reduction
SOF	Soluble Organic Fraction
THC	Total Hydrocarbon
ULSD	Ultra-low Sulfur Diesel
VGT	Variable Geometric Turbocharger
VOCs	Volatile Organic Compounds
WCO	Waste Cooking Oil
WVO	Waste Vegetable Oil

Chapter I. Introduction

I.1 Diesel Exhaust

Diesel engines play a vital role in transportation, power generation and industrial activities. The primary advantages of the diesel engine over the gasoline spark ignition engine include its durability, reduced fuel consumption, and lower emissions of carbon monoxide (CO) and unburned hydrocarbons (HC). However, diesel exhaust is also a major source of air pollutants, especially nitrogen oxide (NO_X) and particulate matter (PM) due to the high flame temperature and diffusive combustion in the engine combustion chamber. This results in growing health-related and environmental concerns.

Diesel exhaust can have serious adverse effects on the environment and human health. Nitric oxide (NO) and nitrogen dioxide (NO_2), the primary nitrogen oxides (NO_X) produced by diesel engines, are precursors of ground level ozone. When NO_X and volatile hydrocarbons emitted from the diesel exhaust react in the presence of sunlight, ozone is formed (Fernando et al., 2005). Ozone is a strong oxidizer that affects the respiratory system, leading to damage of lung tissues. $NO_{X,}$ in the form of nitric acid, is a contributor to acid rain, which damages human-made structures and vegetation. In addition, it increases the acidity of waterways, making them unsuitable for aquatic life. NO_X emissions also contribute to the eutrophication of rivers, lakes, and streams.

Diesel exhaust is a major source of fine particles in the atmosphere that can deposit in lungs and exacerbate respiratory and allergic diseases. In addition, they

have a major impact on air quality issues because they scatter and absorb radiation, reduce visibility, damage materials, and soil monuments and other architectural structures (Pöschl, 2002). There are various experimental observations explaining the mechanism of pulmonary toxicity from air particulates: direct chemical interaction in airways and alveoli and transport of toxic chemicals which adsorbed onto the surface of the particle (Vallyathan et al., 1994). The particle-bound transition metal content is considered to be responsible for hydroxyl radical production. These radicals induce activation of transcription factors, leading to airway inflammation in asthmatics (Baulig et al., 2004).

A growing recognition of the harmful effects of diesel emissions on air quality and human health has led the U.S. EPA to propose new diesel engine standards for light-duty, on-road heavy-duty, and non-road heavy-duty mobile sources. This major regulatory initiative addresses the problem of carbon monoxide (CO), nitrogen oxides (NO_X), total hydrocarbons (THC) and particulate matter (PM) emissions by setting much stricter engine emission standards (U.S. Environmental Protection Agency, 2009). The current final rule establishes standards for different diesels by adopting different tiered programs and projects to a certain time frame in order to better control the emissions.

I.2 Alternative Fuels

Increasing liquid fuel prices and supply shortage in the last decade have promoted an interest in the development of alternative fuels to control diesel automotive emissions and provide energy independence from imported petroleum sources

(Nwafor, 2004). Oxygenated fuels have a history of reducing exhaust emissions from motor vehicles. Additions of methyl tert-butyl ether (MTBE) and ethanol have been successful in reducing CO and non-evaporative hydrocarbon emissions from gasoline engines (Cardone et al., 2002; U.S. Environmental Protection Agency, 2010). The success of oxygenated gasoline has sparked an interest in the use of oxygenated compounds as emission-reducing additives in diesel fuels.

Biodiesel, a promising oxygenated fuel, is increasingly examined as a potential substitute for conventional high-pollutant fuels because it is a biodegradable, non-toxic, and relatively clean-burning fuel generated from natural and renewable sources such as vegetable oils, animal fats, recycled restaurant greases and waste cooking oil. The chemical structure of the feedstock and biodiesel itself both can affect the emissions. Biodiesel is currently produced from high quality food-grade vegetable oils using methanol and an alkaline catalyst through a transesterification process. Researchers are currently investigating strategies for producing bio-derived lipids to make biodiesel. Algae have shown promise for increasing the available volume of biodiesel, since the lipid yield per unit area per unit time for algae can be one to two orders of magnitude greater than that for a typical oilseed crop, such as soybeans or rapeseed (Hu et al., 2008)

It has been well documented that the use of biodiesel in diesel engines, either in its neat form or as a blend with diesel fuel, is effective in reducing carbon monoxide (CO), hydrocarbons (HC), and particulate matter (PM) under most conditions (Yang et al., 2007). However, most studies have shown that NO_X emissions from diesel

engines increase when the percentage of biodiesel in the fuel blend is increased (Lapuerta et al., 2008). Despite recent advances in toxicological research in the field of air pollution, further assessment of health and environmental impacts associated with biodiesel blends emissions is generally required.

The University of Kansas (KU) Biofuels "Feedstock to Tailpipe (FTT)" Initiative is working to produce next-generation liquid transportation fuels and higher value co-products from multiple oil feedstocks in an economical and environmentally sustainable system. Waste vegetable oil (WVO) would not need to be the only feedstock for the processing plants. However, WVO is the most readily-available feedstock on campus and thus is a natural immediate choice for biodiesel feedstock. In particular, KU Dining Service purchases approximately 23,450 kg of cooking oil per year. This could yield approximately 7000 gallons of pure biodiesel per year using a conservative estimate (Golledge, 2009).

The main objectives of the FTT project are to:

1. Establish a facility to produce biodiesel from WVO and other sources at the University of Kansas, Lawrence campus.

2. Integrate existing and future research on technologies at all stages, feedstock to tailpipe, into the proposed production facility to study various innovations in processing and quality of renewable fuels.

3. Obtain the equipment and experience necessary to perform American Society for Testing and Materials (ASTM) testing of biodiesel produced at the University of Kansas facility and provide a testing service to the broader community.

I.3 Objectives

The current literature has limited data available on how the biodiesel feedstocks affect emissions and performance of non-road diesel engines. Further assessment of the health and environmental impacts associated with biodiesel blends emissions is therefore required. This research focused on the broad study of how biodiesel composition affects the emissions from several off-road diesel engines and on developing methods in order to assess the environmental benefits of biodiesel. This work involved completion of the following tasks:

Objective 1: Review existing data on biodiesel combustion emissions.

Previous work on the effects of biodiesel on emissions is reviewed, including both methodology and results. This review summarizes current understandings of how diesel engines work, what biodiesel is, and how it affects emissions. It also provides a context for the actions taken in the remaining tasks.

Objective 2: Develop analytical methods in order to examine biodiesel composition effects on combustion emissions.

A gas chromatograph-mass spectrometry (GC-MS) method for quantifying the fatty acid composition of biodiesel was developed. The first step in this process was the review of literature analyzing the composition of biodiesel during the biodiesel production process. For each method, the precision, detection limits, and linear range were evaluated. The resulting method was then applied on the GC-MS and used to assess the composition of KU WCO based biodiesel.

A data collection methodology was developed for monitoring gas-phase diesel

emissions. The method used a state-of-the-art onboard vehicle emissions monitoring system, the Semtech-DS, developed by Sensors Inc.; it can provide accurate second-by-second measurements of CO, CO_2, NO_X, and THC for diesel vehicles.

Waste cooking oil (WCO) biodiesel produced by the KU Initiative was used to power two off-road engines- a lawn mower and a generator. Exhaust emissions data were collected for different biodiesel blends to assess the biodiesel composition effects on emissions. The results were evaluated as a function of biodiesel content, ambient temperature, exhaust temperature, absolute humidity and the engine itself. Statistical techniques were used to compare and evaluate the results.

Objective 3: Evaluate biodiesel performance in a switching locomotive.

Up to 20% of soy- and tallow-based biodiesel fuel was used to evaluate the emission profile and long-term performance of biodiesel in a switching locomotive owned by the Iowa Interstate Railroad. Each fuel was used exclusively in the locomotive for a 90-day period during normal operation. Emissions monitoring was performed at the beginning and end of the testing period to determine emissions of regulated pollutants from the different fuel blends. The results of these tests were analyzed to determine emissions patterns for the different fuel blends.

Objective 4: Analyze the particulate elemental composition.

A method using laser ablation inductively coupled plasma mass spectroscopy (LA-ICP-MS) was developed to directly analyze the trace metal content in diesel exhaust particulates. Trace metals have commonly been measured by pretreating particles using acid digestion and analyzing the solution using inductively coupled

plasma mass spectroscopy (ICP-MS) or graphite furnace atomic absorption spectrometry (GF-AAS). This procedure may require large sample sizes, use of potentially hazardous reagents such as hydrofluoric acid (HF) and also risks contamination by reagent impurities and loss of elements through volatilization. Due to the ultraclean sample preparation as well as the significant improvement of the analytical methods, a new LA-ICP-MS method, was used to analyze the metal content in particles. Particles were collected in-line and fractionated by size using a 13-stage Dekati Impactor.

Chapter II. Literature Review

II.1 Diesel Combustion

The first diesel-powered engine appeared in 1898, and since then, diesel engines have become widely used as power sources for transportation, power generation and industrial activities. The primary difference between diesel and spark-ignited gasoline engines occurs in their fuel ignition process. The gasoline engine ignition is triggered by a spark from a spark plug, while diesel engine ignition is caused by spontaneous compression ignition: the pressure and temperature rise during compression provides the appropriate conditions for fuel to be injected, atomized, vaporized, and subsequently burnt.

Diesel engines are also known for their increased fuel efficiency and low emissions of carbon monoxide (CO) and unburned hydrocarbons (HC). In the diesel engine, air is compressed with a compression ratio typically between 14 and 20 (Heywood, 1988). This higher compression ratio promotes more fuel efficient combustion due to a longer effective expansion stroke. In addition, diesel engines run lean overall except at full power, with air-fuel ratios as high as 65:1 (Heywood, 1988). Engine speed and power is controlled by changing the amount of fuel in each injection instead of throttling the intake air, which gives diesel engines a high thermal efficiency. Due to their lower fuel consumption and CO and HC emissions, diesel engines are used in many trucks, almost all railroad engines, ships, and some small electric power plants in the United States. The number of diesel trucks increased from 3,713,200 in 1992 to 4,913,300 in 1997 (Economic Census, 1999). The diesel engine

is also widely used in other countries, especially in Europe due to the high price of gasoline.

II.1.1 Early diesel engine history.

The diesel engine has a long history that is intertwined closely with economic and fuel factors. The initial compression ignition concept dates back to Schmidt in 1861, but the main contribution was achieved by Rudolph Diesel. Diesel devised a pressure-ignited heat engine in 1897 (Ferguson & Kirkpatrick, 2001; Heywood, 1988; Stone, 1992). Peanut oil was injected into the cylinder through a high pressure air blast then spontaneously ignited at high temperature and pressure, doubling the engine efficiency compared to other internal combustion engines at that time. However, the air blast required a costly high-pressure air pump and storage vessel, which made the early diesel engines large and heavy. The size of the fuel injection pump restricted the use of diesel engines to stationary applications until the 1920s.

The 1920s brought a new injection pump design, allowing the metering of fuel as it entered the engine without the need of pressurized air (Stone, 1992). This made a small and compact diesel engine design possible and widened the application of diesel engines. However, the fuel pump and injectors on early diesels were completely mechanical. The working pressure of the fuel system did not sufficiently provide a steady and well-defined fuel spray pattern. Changes in fuel sources also had a great impact on diesel engine development. During the early 1920s, diesel fuel injection systems were altered in order to utilize the lower viscosity fossil fuel residues rather than a biomass-based fuel (Stone, 1992). This was because the petroleum industry

was growing and establishing itself and could support diesel engine development.

Mercedes Benz began to build diesel driven automobiles in the mid-1930s, and by 1974, over a million diesel-engine cars had rolled off its production line. The first diesel truck engines with direct-injection arrived by 1964. The huge torque and long life of the engine was a distinct advantage, as was the better fuel economy (The History of Diesel, 2009). Diesels were popular in the United States during the energy crisis of the 70s; unfortunately they received criticism because the fuel injection technology and the engine design were not optimal. They were noisy, smoky, smelled bad, and hard to start on cold days.

II.1.2 Current diesel engines.

There are two main types of diesel engines: two-stroke and four-stroke. Four stroke engines produce one power stroke for every two-piston strokes, respectively an intake, compression, expansion, and exhaust stroke. Most modern four stroke engines are turbocharged and intercooled in order to increase the power output per unit weight. In addition, these engines have sophisticated electronic controls, which are capable of varying the fuel injection timing and other engine parameters to minimize emissions (Heywood, 1988).

Two-stroke engines use the beginning of the compression stroke and the end of the combustion stroke to simultaneously perform the intake and exhaust functions, which eliminates the separate induction and exhaust stroke and produces more power for every piston stroke. Given a certain size engine, the two-stroke engine will be more powerful than a four-stroke engine since it has twice as many power strokes per

unit time. However, two undesirable features of the two-stroke engine are the mixing of the incoming charge with the exhaust residuals and the passage of the charge directly into the exhaust system. Some of the air is blown through the cylinder with both intake and exhaust valves open in order to purge the cylinder of exhaust gases. This results in a lower exhaust temperature than four-stroke engines which affects the performance of the turbocharger and exhaust catalysts (Heywood, 1988; Stone, 1992). Oil droplets may be blown out during this scavenging portion of the two-stroke cycle. Lubrication oil losses to the exhaust are thus much higher for two-stroke engines, resulting in excessive particulate and HC emissions.

Modern technology leads to quiet, clean, and high-speed diesels, which are more economical and reliable. The maximum diesel engine power available is controlled by the amount of fuel that can be burned efficiently inside the cylinder. For example, Glikin (1985) described an new electronic control injector. The optimum injection timing and fuel quantity are controlled by the microprocessor in response to driver demand, engine speed, turbocharger boost pressure, air inlet temperature and engine coolant temperature. The electronic injector can reach high fuel pressure, up to 1000 bar; however, it was not widely used due to the high cost.

A variable geometric turbocharger (VGT) with intercooler boosts the inlet air density using a compressor and turbine on a single shaft, which increases the injected fuel and engine power. Enhanced turbulence or air flow structures also promote better mixing.

The most recent development was the invention of the common rail injection

system at the beginning of the 1990s. Diesel fuel injectors used in common rail systems operate differently from mechanical fuel injectors, where plungers are controlled by the camshaft position and speed. Common rail fuel injection systems first store fuel under high pressure in a central accumulator rail and then deliver it to the separate electronically controlled injector. This means the fuel pump can charge the fuel rail at a pressure up to 25,000 psi without discharging the fuel. The more precisely controlled quantity of atomized fuel increases fuel economy and reduce exhaust emissions and diesel noise (Gable & Gable, 2010).

The future diesel engine will be influenced by three factors: cost, emission regulations, and the availability of suitable fuel.

II.1.3 Diesel combustion.

There are two types of diesel combustion systems: direct-injection (DI) engine and indirect-injection (IDI) engine. For the DI engine, fuel is injected into a single open combustion chamber. IDI engines have a divided combustion chamber; fuel is injected at a lower injection pressure into the prechamber where combustion starts. The pressure rise associated with combustion forces fuel back into the main chamber where the jet issuing from the nozzle entrains and mixes with the main chamber air. The purposes of a divided combustion chamber are to provide adequate fuel-air mixing and speed up the combustion process. IDI combustion systems are only used with small engine sizes.

A basic understanding of the combustion process of the diesel engine demonstrates how various engine and fuel-related factors affect diesel exhaust

formation and emissions. A low-volatility fuel is introduced into the cylinder by the fuel-injection system at a large pressure towards the end of the compression stroke (Heywood, 1988; Stone, 1992). The cold liquid fuel is atomized to produce fine fuel droplets, which vaporize and mix with air at high temperature and pressure. This leads to autoignition; however, combustion does not occur immediately but is delayed for a few crank angle degrees. This time (or crank angle) interval between the start of fuel injection and the start of combustion is called ignition delay. The initial rapid combustion due to the initial high rate of pressure rise produces diesel knock. When there is a longer ignition lag, a considerable portion of the injected fuel will be permitted to spontaneously ignite, which produces the characteristic knock at the initiation of combustion. One way of reducing diesel knock is to decrease the quantity of mixture during the delay period and to shorten this period.

Once regions of vapor-air mixture around the fluid are at or above the autoignition temperature, a flame rapidly spreads and the fuel spontaneously ignites (Heywood, 1988; Stone, 1992). This period of combustion is called premixed burn. During this phase, the temperature and pressure are relatively high and the heat-release rate reaches a peak. The high temperature and better mixing produce more NO_X and less soot. This is because once the premixed fuel and air during the ignition delay have been consumed; the burning rate is then limited by the mixing rate of the remaining fuel and air mixture. This is called the mixing-controlled or diffusion burn phase. The heat-release reaches a second peak in this phase and decreases as the phase continues. When the piston stroke expands the working volume, the

temperature of the cylinder gases decrease. A fraction of the fuel energy can still be released by the oxidation of soot and fuel-rich combustion products in the mixing air, and heat release continues at a lower rate. This period is called late oxidation.

Of importance, there is a trade-off between NO_X and particulate emissions for diesel engines (Cardone, et al., 2002). The high temperature favors NO_X formation, decreasing the temperature of mixing-controlled combustion will decrease the NO_X formation. When the injection timing is delayed, both the amount of premixed burning and peak in-cylinder combustion temperature are reduced, and NO_X decreases, but the particulates increase due to the slow oxidation rates. The inverse relation between NO_X and PM formation poses the primary challenge in lowering diesel engine emissions.

II.1.4 Diesel emissions.

Mobile emissions continue to be a major source of criteria air pollutants both in the United States and on a global scale. Based on 2002 estimates (Bishop & Stedman, 2008), on-road mobile vehicle sources are the largest supplier of carbon monoxide (CO), volatile organic compounds (VOCs), and nitrogen oxides (NO_X) to the national emission inventory. In particular, on-road vehicle sources contribute 82% of the CO, 45% of VOCs, and up to 56% of all nitrogen oxides. More recent assessments suggest that on-road diesel emissions account for as much NO_X emission as gasoline mobile sources (Shorter et al., 2005). Besides criteria pollutants, transportation accounts for 40% of the total carbon dioxide increase since 1990 (Samaras & Meisterling, 2008).

Diesel engines power most commercial goods transportation vehicles including

trucks, freight locomotives, and marine vessels (U.S. Department of Transportation, 1999). Diesel engine exhaust emissions are a mixture of gases, liquid aerosols, and particulate substances. They contain the products of fuel combustion: carbon, nitrogen, water, carbon monoxide, nitric oxide, sulfur dioxide, aldehydes, and polycyclic aromatic hydrocarbons (Health and Satety Executive, 1999). Diesel exhaust emissions vary greatly in chemical composition between different engine types, engine operation conditions, and fuel types. After being emitted from the tailpipe of the engine, diesel emissions can also undergo dilution and chemical and physical transformation during transport in the atmosphere, resulting in growing health-related and environmentally related concerns. Of all the emissions, NO_X and PM are the most significant ones from a regulatory standpoint.

II.1.4.1 NO_X formation.

It is helpful to have an understanding of the chemical and kinetic pathways by which NO_X is formed during combustion. Nitrogen oxides are formed in the chamber during the combustion process due to the reaction of oxygen and nitrogen present in the intake air. The formation of NO_X is a complex process which takes place in the pre-combustion, combustion, and post-flame regions. It involves the reactive combination of nitrogen found within the combustion air and natural or organically bound nitrogen within the fuel itself and oxygen in high temperature burned gases. Three reaction mechanisms that produce NO are the thermal or Zeldovich mechanism, the Fenimore or prompt mechanism, and the fuel NO_X mechanism (Fernando, et al., 2005).

II.1.4.1.1 Thermal NOx formation.

Thermal NO_X is produced by the reaction of atmospheric oxygen and nitrogen at elevated temperatures, and is the major source of NO_X when the fuel contains little or no inherent nitrogen. It is formed at the conditions of highest temperature during the combustion process. The chain reactions are described by the thermal (Zeldovich) mechanism as follows (Turns, 1995):

$$N_2 + O \xrightarrow{k_1} NO + N \qquad (1)$$

$$N + O_2 \xrightarrow{k_2} NO + O \qquad (2)$$

$$N + OH \xrightarrow{k_3} NO + H \qquad (3)$$

The first step is rate limiting, and due to its high activation energy (314 KJ/mol) requires high temperatures to proceed (Turns, 1995). For lean burning diesel engines, reaction (3) can be neglected because the $[O_2]$ is relatively higher than [OH] (Fernando, et al., 2005), this is due to the equation (4).

$$k_2 [O_2]_{eq} >> k_3[OH]_{eq} \qquad (4)$$

In diesel engines, NO_X forms throughout the high temperature burned gases behind the flame front. The fuel is injected into the cylinder immediately prior to combustion, so non-uniform temperatures and burned gas composition occur due to the uneven fuel distribution. The air-fuel mixture early in the combustion process is especially important since it is compressed to a higher temperature, which increases the NO formation rate. As combustion proceeds past the time of peak pressure, the mixture temperature decreases as the cylinder gases expand. The decreasing temperature freezes NO formation and decomposition of NO to NO_2 can occur.

NO formed in the flame zone can be rapidly converted to NO_2 through reaction (5). NO_2 is formed on the periphery of the flame front due to the relatively low temperature. NO_2 can be 10 to 30% of total nitrogen oxide emissions in diesel engines (Hilliard & Wheeler, 1979). NO_2 can also be converted back to NO through reaction (6) under fuel rich conditions:

$$NO + HO_2 \longrightarrow NO_2 + OH \qquad (5)$$

$$NO_2 + O \longrightarrow NO + O_2 \qquad (6)$$

The sum of NO and NO_2 present is generally considered to be the total NO_X concentration. As NO_X is a thermally produced gas, its reduction is largely dependent on the control of species concentrations, in-cylinder flame temperature, and residence time of the in-cylinder mixture at high temperature. NO_X are formed in significant quantities starting above 1500°C and formation increases rapidly as the temperature increases (Fluent Inc., 2001). Reducing the temperature inside the engine cylinder is the key to lowering thermal NO_X formation.

II.1.4.1.2 Prompt NO_X formation.

Prompt NO_X is formed by the reaction of hydrocarbon radicals with atmospheric nitrogen to produce hydrogen cyanide (HCN), and hence NO_X via a complex series of gas phase reactions. These nitrogen-containing fragments then react with atmospheric nitrogen. The path is shown by the following reactions (Fernando, et al., 2005) .

$$CH + N_2 \longrightarrow HCN + N \qquad (7)$$

$$CH_2 + N_2 \longrightarrow HCN + NH \qquad (8)$$

$$CH_2 + N_2 \longrightarrow H_2CN + N \qquad (9)$$

$$N + O_2 \longrightarrow NO + O \quad (10)$$

$$HCN + OH \longrightarrow CN + H_2O \quad (11)$$

$$CN + O_2 \longrightarrow NO + CO \quad (12)$$

$$C + N_2 \longrightarrow CN + C \quad (13)$$

Prompt-NO formation involves three separate kinetic issues (Fernando, et al., 2005):

(1) The CH concentration and formation process. The mechanism of CH formation depends somewhat on the fuel.

(2) The rate of molecular nitrogen fixation.

(3) The rate of interconversion among fixed nitrogen fragments.

The two largest contributors to prompt NO_X formation are CH and CH_2 (Fernando, et al., 2005). The formation of prompt NO_X is proportional to the number of carbon atoms in each unit volume, but is independent of the parent hydrocarbons. The amount of HCN created increases as the concentration of hydrocarbon radicals increases. The amount of hydrocarbon radicals increases with an increasing equivalence ratio and then reaches a peak and decreases because of a shortage of oxygen. Prompt NO_X formation is only prevalent in fuel-rich combustion, so it might not be significant in most diesel engines.

II.1.4.1.3 Fuel NO_X formation.

Fuel NO_X arises from the reaction of organically-bound nitrogen in the fuel with excess oxygen during the combustion process. This type of NO_X formation is only a problem with fuel containing chemically-bound nitrogen (Heywood, 1988). The

fuel-bound nitrogen species undergo some thermal decomposition to form NO precursors, such as NH_3 and HCN, prior to entering the combustion zone.

The process is complex but can be simply expressed as follows (Heywood, 1988):

(1) Volatile fuel nitrogen is evolved mainly as HCN (and NH_3) during the processes.

(2) The HCN reacts with various free radical species (O, OH) to form intermediates, such as CN, NCO, HNCO, that ultimately react with H to produce NH, NH_2.

High fuel NO_X yields are obtained for lean and stoichiometric air-fuel mixtures and are only weakly dependent on temperature. It can be most effectively minimized by burning the fuel by staged combustion, which implies delayed mixing between the fuel gas and air. This path might be a potential issue in biodiesel fuels, which may contain significant amounts of nitrogen.

II.1.4.1.4 Health and environmental related effects of NO_X.

Most emitted NO converts to NO_2 in the atmosphere. When NO_X and volatile organic compounds (VOCs) react in the presence of sunlight, ground-level ozone is formed. O_3 is the major constituent of smog. Automobile exhaust and other industrial sources can emit NO_X and VOCs to facilitate O_3 formation. Once formed, smog can be transported by wind currents and cause health impacts far from original sources. With low level exposure for only a few months, smog can destroy many forms of synthetic materials and vegetation, and reduce crop yields (EnviroTools, 2002; Fernando, et al., 2005). Exposure to ground-level ozone can cause various diseases

including chest pain, cough, asthma, and lung disfunction (U.S. Environmental Protection Agency, 2010).

Studies on human populations indicate that long-term exposure to high NO_2 levels may decrease lung function and increase the risk of respiratory symptoms, such as acute bronchitis, cough, and phlegm (California Environmental Protection Agency, 1998; Lipsett & Campleman, 1999). Children and people with lung diseases such as asthma, and people who work or exercise outside are susceptible to adverse effects, such as damage to lung tissue and reduction in lung function. Even though some studies have shown associations between NO_2 exposure and mortality, present evidence is not sufficient to conclude that effects on mortality can be attributed to long-term exposure to NO_2 itself (Shorter, et al., 2005).

In addition to these health-related effects, NO_X can react with other substances in the air to form acids which fall to earth as rain, fog, snow or dry particles. Some may be carried by wind for hundreds of miles. Acid rain causes deterioration of buildings, and causes lakes and streams to become acidic and unsuitable for many fish. In North America, acid rain has already decimated the populations of numerous fish and many plants in 50% of the high mountain lakes in the Adirondacks (Vallero, 2008). Excess amounts of nutrient addition due to NO_X emissions can also contribute to eutrophication of water bodies and algae blooms, leading to oxygen depletion. Nitrogen deposition also upsets the chemical balance which affects aquatic wildlife. N_2O, which is emitted at lower levels in diesel exhaust, is also a greenhouse gas. It accumulates in the atmosphere with other greenhouse gases causing a gradual rise in

the earth's temperature, resulting in a rise in the sea level and damage to plant and animal habitats (International Carbon Bank and Exchange, 2000).

II.1.4.2 CO/Hydrocarbon (HC) formation.

CO is the consequence of incomplete combustion of the diesel fuel. It appears in the exhaust of rich-running engines since there is not sufficient oxygen to convert all the carbon in the fuel to carbon dioxide. In lean-running diesel engines, the high combustion temperatures promote both the dissociation of the fuel to produce CO and HC and the dissociation of CO_2 to CO under high temperatures. CO is toxic for living organisms through carbon monoxide poisoning; the affinity of hemoglobin for CO is about 200 times stronger than for oxygen, which reduces the ability of the circulation system to transport O_2. The CO-carrying protein is known as carboxyhemoglobin and when sufficiently high it can lead to acute and chronic effects (Wu & Wang, 2005). CO is also a contributing factor in the photochemistry that leads to elevated levels of ozone (O_3) in the troposphere.

HC are also the consequence of incomplete combustion of the diesel fuel, and can be generated by two pathways (Heywood, 1988). In the first case, the fuel-air mixture is excessively too lean to autoignite or to support a propagating flame at the conditions prevailing inside the combustion chamber. In the other case, the fuel-air mixture during the primary combustion process is excessively rich to ignite or support a flame. Hydrocarbons also can remain unconsumed due to incomplete mixing or from quenching of the oxidation process. Mobile sources release two types of regulated HC, speciated hydrocarbons (C_1-C_{22}) and a subset of known or suspected

carcinogenic compounds titled polycyclic aromatic hydrocarbons (PAHs) (Strong et al., 2004). In addition, HC are a precursor of ground-level ozone as they will react with NO_X in sunlight to form smog. Fuel composition has a strong impact on HC formation. Straight chain aliphatic compounds are more easily combusted than aromatic molecules. Biodiesel has more aliphatic compounds than diesel fuel, so it can have more complete combustion and lower HC emissions.

II.1.4.3 Particulate matter formation.

Diesel engines are a major source of particulate matter (PM). These particulate emissions are of increasing concern as they are small, often less than 2.5 μm in size, and consist of a complex mix of engine oils, sulfates, and inorganic materials. These particles have been identified by health experts as contributing to a variety of lung related illnesses including asthma, emphysema, and bronchitis (Diaz-Sanchez et al., 1999). There is also growing evidence that exposure to diesel particulates may increase the risk of cancer in humans (Diaz-Sanchez, 1997).

Particulate matter is born in soot nuclei of the oxygen-deficient core of fuel sprays and grows in size through incorporation of gas phase molecules (Stone, 1992). PM is formed predominantly during the diffusion burning period as the flame propagates towards the core of the fuel spray. After the rapid combustion of the premixed period, the subsequent combustion of fuel is controlled by the rates of air diffusion into this core. At the fuel core, fuel droplets are larger than at the periphery where combustion started and local fuel-air ratios are rich. Carbon particles are formed by the cracking of the large hydrocarbon molecules, which then agglomerate

to form soot. The soot particles can be oxidized when they enter the lean side of the reaction zone. Further oxidation occurs during the expansion stroke, after the end of the diffusion combustion phase (Stone, 1992).

The three major characteristics of particulate matter are the total mass concentration, size distribution, and chemical composition. Diesel particulates are composed of a center core of elemental carbon and adsorbed organic compounds, as well as a small amount of sulfate, nitrate, metals and other trace elements (Wichmann, 2007). Traditionally, the most frequently used definition of particulate matter is PM_{10} (particles with the aerodynamic diameter less than 10 μm), which are referred to as inhalable particles (Charron & Harrison, 2005). The mass of PM_{10} particles includes both fine (particles with the aerodynamic diameter less than 2.5 μm) and coarse (particles with the aerodynamic diameter between 2.5 to 10 μm) fractions of airborne particulate matter. $PM_{2.5}$ consists of the fine particles with the aerodynamic diameter less than 2.5 μm. Both PM_{10} and $PM_{2.5}$ are under tight emission regulations due to the inhalable nature of the particles.

II.1.4.3.1 The effect of particle size and mass.

The size of particles is directly linked to their potential for health effects. Larger particles settle rapidly to the ground while finer particles remain suspended in the air for a longer time and may travel in winds for hundreds of miles. Large particles, when inhaled, get trapped by fine hairs and mucus in the nose, throat and large airways. Thus, they can cause and worsen respiratory, cardiovascular, infectious and allergic diseases. However, smaller particles less than about 10 μm in diameter pose the

greatest problems because they can get deep into the lungs, and may even reach the bloodstream (Mulawa et al., 1997; Pope III et al., 1995). The number of particles reaching the interstitial space of the lungs is directly proportional to the number of particles applied. $PM_{2.5}$ has a relative larger surface area which may lead to a greater interaction with alveolar cells compared to PM_{10}, thereby having the potential to elicit stronger cellular response. On the other hand, a large surface area may have a greater capacity to adsorb chemical substances, allergens, endotoxin, and other biological components (Granum & Løvik, 2002). Due to the combination of small diameters and large surface area of $PM_{2.5}$, it is considered to be more respirable and toxic than PM_{10}.

II.1.4.3.2 The composition of PM.

$PM_{2.5}$ and PM_{10} in the atmosphere contain a wide range of chemical substances, some of which pose a threat to human health (Jones & Harrison, 2004; Pöschl, 2002). Among the hazardous components of air particulate matter are metals and strong acids (e.g. Zn, Cu, Fe and H_2SO_4), as well as numerous organic compounds like polychlorinated biphenyls and dibenzodioxins (PCBs, PCDDs), polycyclic aromatic hydrocarbons (PAHs) and their chemical derivatives and bioaerosols.

II.1.4.3.2.1 The effect of particle-associated inorganic ions.

Both the amount of particulate matter mass and its constituents are used in assessing health effects. Research on the association between ionic composition of fine and course aerosol soluble fraction and peak expiratory flow of asthmatic patients in Sao Paulo city (Bourotte et al., 2007) showed that SO_4^{2-} (48.4%), NO_3^- (19.6%), and NH_4^+ (12.5%) were the predominant species in the fine fraction, whereas NO_3^-

(35.3%), SO_4^{2-} (29.1%), Ca^{2+} (13.1%), and Cl^- (12.5%) were the predominant species in the coarse fraction. Some ionic chemical species, particulately chloride but also other ions (Na^+, Mg^{2+}, and NH_4^+) may exacerbate airway inflammation in asthmatics. The transition metal and other inorganic ion content of PM are considered to be responsible for hydroxyl radical production (Baulig, et al., 2004). These radicals can induce activation of transcription factors and lead to cytokine production by human airway epithelial cells. This effect has been shown with residual oil fly ash (ROFA) metal rich particles. More recent studies have confirmed that the generation of hydroxyl radicals associated with Fe in the PM_{10} and other respirable particulates is the most important toxicological mechanism for adverse health effects in the respitarory system (Donaldson et al., 1997; Ghio et al., 1998). Other health effects have been traced to the presence of specific elements. Exposure to Mn and Fe have been linked to Parkinsonism, Cr has been linked to increased cancer risk, Pb has been linked to adverse effects in the nervous system, and Ba may lead to paralysis (Chillrud et al., 2005; Department of Health and Human Services, 2007). Zn, Cu and Fe may release free radicals in lung fluid through Fenton's reaction and cause cellular inflammation (Donaldson et al., 1997).

II.1.4.3.2.2 The effect of particle-associated organic ions.

Organic material associated with diesel particles originates from unburned fuel, engine lubrication oil, and small quantities of partial combustion and pyrolysis products (Heywood, 1988). This is frequently quantified as the soluble organic fraction (SOF). Fine particles emitted from diesel engines are coated with a mixture of

nitroaromatics, benzene dioxins, and other toxic substances that irritate the respiratory system and can cause or exacerbate various respiratory conditions and lead to premature death (Lloyd & Cackette, 2001; Pöschl, 2002). Over the past 20 years, numerous researchers have reported that variations in the organic composition of gaseous and particulate emissions are attributable to differences in test cycles, fuel composition, engine model year and type, and sampling methodology, but only limited studies have investigated PAH emissions of biodiesel (Durbin et al., 2000; Yang et al., 2005; Yang, et al., 2007). Due to the mutagenic carcinogenic and endocrine disrupting effects of some PAHs (Ohura et al., 2004), the knowledge of the fate of those compounds, particularly in the atmospheric environment, prompts increasing interest. Moreover, they are soluble in fatty and lipid-rich tissues, where they are accumulated.

The higher molecular weight PAHs are more likely to be associated with the particulate phase (Wu. et al., 2010). This is not simply a result of condensation; in practice, the majority of PAHs are generally found to be present in the particulate phase, some almost exclusively, despite the saturation vapor concentration rarely being exceeded. This results from either the adsorption of the PAHs onto particle surfaces, or the absorption (i.e. dissolution) of the PAHs into the bulk aerosol. The importance of these processes depends on temperature, humidity and the composition and abundance of the atmospheric aerosol, and some variability in the gas-particle partitioning is observed on a temporal and geographical basis (Borrás & Tortajada-Genaro, 2007). In general, PAHs containing 5 or more rings, including

benzo[a]pyrene (BaP), are found predominantly in the particulate phase (Zhang et al., 2004); those containing 2 or 3 rings are almost entirely present in the vapor. The observed variability relates mainly to 4-ring PAHs, such as fluoranthene, pyrene, benz[a]anthracene, and chrysene. A study on adverse health effects of airborne $PM_{2.5}$ showed that short-term exposure to PAH coated onto $PM_{2.5}$ induced oxidative stress and inflammation in human lung epithelial cells (L132) (Dagher et al., 2006). PM exposure induces apoptosis by activating not only the tumor necrosis factor-alpha-induced pathway, but also the mitochondrial pathway. Together with the changes in the transcription rates of DNA, fragmentation in PM-exposed proliferating L132 cells revealed short-term exposure to $PM_{2.5}$ induced apoptosis in L132 cell (Dagher, et al., 2006) .

II.1.4.3.3 The environmental effect of particulate matter.

Airborne particulate matter also has a major impact on air quality by reducing visibility, damaging materials, and soiling monuments and other architectural structures (Gillies et al., 2001). These particles can also travel long distances and function as vehicles for transporting chemical contaminants to bodies of water and soil. Acid deposition, for example, can be influenced by particle associated ions (Arimoto, 1989). Dry particles enter ecosystems and potentially reduce the pH of receiving waters, while other particles are washed out of the atmosphere and, in the process, lower the pH of the rain. The same transport and deposition mechanisms can also lead to exposure to persistent organic contaminants like dioxins and organochlorine pesticides, and heavy metals like mercury that have absorbed in or on

particles (Ottley & Harrison, 1991).

II.1.4.4 SO_X formation.

SO_X is generated from the sulfur present in diesel fuel. Reducing the fuel sulfur content can also effectively lower PM emissions because sulfur atoms in diesel fuels provide the nuclei for PM formation (U.S. Environmenal Protection Agency 2001). Most biodiesel fuels have naturally low sulfur content, equivalent to or lower than ultra-low sulfur diesel. The concentration of SO_2 in the exhaust gas depends on the sulfur content of the fuel. Ultra-low-sulfur fuel which contains less than 0.05% sulfur is used for most diesel engine applications throughout the USA and Canada (Faiz et al., 1996). Most sulfur in the fuel burns to SO_2, which is released to the atmosphere in diesel exhaust, making diesel vehicles a significant SO_2 contributor in some areas. The remaining sulfur in the diesel fuel is converted to metal sulfates during or immediately after the combustion process. Oxidation of sulfur dioxide produces sulfur trioxide which is the precursor of sulfuric acid which, in turn, is responsible for the sulfate particulate matter. Sulfur oxides have a profound impact on the environment, being the major cause of acid rain.

II.1.5 Emissions regulations.

The 1990 Clean Air Act Amendments set standards for criteria pollutants in ambient air, which are shown in Table 1 (Vallero, 2008). The primary standards are to protect public health, and the secondary standards are to protect public welfare. Based on the review of air quality and previous standards, U.S. EPA proposed new standards in 2010 to tighten $PM_{2.5}$ 24-hour ambient air levels to 35 μg m^{-3} from 66 μg m^{-3}. The

$PM_{2.5}$ annual average standard would remain unchanged at 15 µg m^{-3}. For particles sized between 2.5 to 10 µm, the 24-hour emission threshold would be established at 70 µg m^{-3} with the intent to better control anthropogenic urban emissions (U.S. Environmental Protection Agency, 2010).

Table 1: National Ambient Air Quality Standards (U.S. Environmental Protection Agency, 2010)

POLLUTANT	AVERAGING PERIOD[A]	PRIMARY STANDARDS[B]	SECONDARY STANDARDS[C]
Ozone	1h	125ppb	125ppb
	8h	85ppb	85ppb
Carbon monoxide	1h	35.5ppm	35.5ppm
	8h	9.5ppm	9.5ppm
Sulfur dioxide	3h	na	550ppb
	24h	145ppb	na
	Annual	35ppb	na
Nitrogen dioxide	Annual	54ppb	54ppb
Respirable PM (aerodynamic diameters ≤ 10µm =PM_{10}).	24h	150 µg m^{-3}	150 µg m^{-3}
	Annual	51 µg m^{-3}	51 µg m^{-3}
Respirable PM (aerodynamic diameters ≤ 2.5µm =$PM_{2.5}$).	24h	35 µg m^{-3}	35 µg m^{-3}
	Annual	15.1 µg m^{-3}	15.1 µg m^{-3}
Lead	Quarter	1.55 µg m^{-3}	1.55 µg m^{-3}

[a] Integrated time used to calculate the standard. For example, for particulates, the filter will collect material for 24h and then it will be analyzed. The annual integration will be an integration of the daily values.

b Primary NAAQS are the levels of air quality that the EPA considers to be needed, with an adequate margin of safety, to protect the public health.

[c] Secondary NAAQS are the levels of air quality that the EPA judges necessary to protect the public welfare from any known or anticipated adverse effects.

The U.S. EPA is currently tightening the PM and NO_X emission standards regarding light-duty diesel vehicles and trucks, heavy-duty diesel vehicles and

engines, and non-road diesel engines and vehicles in order to improve ambient air quality. The current final rule establishes standards for on-road diesel engines and fuels that are modeled on the recently adopted Tier 2 program for cars and light trucks, and the 2007 highway diesel program for on-highway diesel engines (DieselNet, 2007). This regulatory initiative addresses the problem of particulate matter (PM) and nitrogen oxides (NO_X) emissions by setting stricter emission standards. For truck and bus engines, the particulate standard was reduced from 0.6 g/bhp-hr in 1988 to 0.1 g/bhp-hr in 1994. For urban bus engines, the particulate standard was reduced in 1994 to 0.07g/bhp-hr and again in 1996 to 0.05 g/bhp-hr. The NO_x standard was reduced to 4.0 g/bhp-hr in 1998 for all on-road diesel engines (DieselNet, 2007)

In addition, EPA is adopting new emission standards for non-road diesel engines by integrating engine and fuel controls as a system in order to gain the greatest emission reductions (U.S. Environmental Protection Agency, 2009). The requirements will result in substantial benefits to public health and welfare through significant reductions in emissions of nitrogen oxides and particulate matter, as well as nonmethane hydrocarbons, carbon monoxide, sulfur oxides, and air toxics. Exhaust emissions from these engines will decrease by more than 90 percent. It is projected that by 2030, this program will reduce annual emissions of nitrogen oxides and particulate matter by 738,000 and 129,000 tons, respectively.

Estimates show that heavy-duty engines, such as locomotives and marine engines will contribute 27% of the total NO_X emissions and 45% the total $PM_{2.5}$ emissions from all mobile sources combined without new controls (McKenna et al., 2008). In

2008, EPA also published new emission rules for diesel locomotives of all types (line-haul, switching and passenger) based on their year of manufacture (Table 2 (U.S. Environmental Protection Agency, 2008)). The EPA estimates this final rule will result in PM reductions of about 90 percent and NO_X reductions of about 80 percent from engines meeting these standards through 2015.

Table 2. Tier regulations for locomotives (g/bhp*hr) (U.S. Environmental Protection Agency, 2008)

	Tier 0		Tier 1		Tier 2		Tier 3		Tier 4	
Year	1973-1992		1993-2004		2005-2011		2012-2014		2015+	
	Line	Switch	Line	Switch	Line	Switch	Line[a]	Switch	Line	Switch
CO	5.0	8.0	2.2	2.5	1.5	2.4	1.5	1.5	1.5	2.4
HC	1.0	2.1	0.55	1.2	0.3	0.6	0.3	0.3	0.14[b]	0.3[c]
NOx	8.0	11.8	7.4	11.0	5.5	8.1	5.5	5.5	1.3[b]	1.3[c]
PM	0.22	0.26	0.22	0.26	0.13[d]	0.13[e]	0.10	0.10	0.03	0.03

a- Must also meet Tier 2 switch standards
b- Can also choose NOx + HC standard of 1.3 g/bhp*hr
c- Can also choose NOx + HC standard of 1.3 g/bhp*hr
d- 0.22 g/bhp*hr until January 1, 2013
e- 0.24 g/bhp*hr until January 1, 2013

II.1.5.1 Exhaust gas recirculation.

Exhaust gas recirculation (EGR) is one of the most effective methods currently used in diesel engines to reduce NO_X emissions. NO_X emissions are mainly

influenced by the available oxygen and combustion temperature. This system takes a portion (about 10-30%) of the exhaust gas and circulates it back into the intake. The exhaust gas acts as a diluent in the fuel-air mixture, which lowers the flame temperature and the oxygen concentration of the working fluid in the combustion chamber. The exhaust gas is essentially inert and, therefore, does not react in the combustion chamber but only absorbs heat which lowers NO_X emissions. This, however, results in poorer specific fuel consumption and particulate emissions.

The performance of EGR is affected by both the engine load and EGR ratio (Abd-Alla, 2002). The oxygen concentration in the exhaust decreases with increasing engine loading, which results in higher specific heat due to the increase in the combustion product CO_2. When operating at a lower load, diesel engines generally tolerate higher EGR ratio because the exhaust contains a high concentration of O_2 and low concentrations of combustion products CO_2 and H_2O. At a higher load, however, the exhaust oxygen becomes limited and the engines tend to generate more particulates. Increasing the EGR ratio causes the heat release rates during the premixed burn to be suppressed significantly. Higher injection pressures and cooling EGR help reduce the NO_X emissions without affecting soot generation. Better mixing allows for more EGR tolerance and less soot production. The combined EGR and turbocharging can achieve an approximately 50% NO_X reduction at a 20% EGR ratio without affecting smoke and unburned HC emission (Uchida et al., 1993).

II.1.5.2 Aftertreatment modifications.

There are several after-treatment modifications for minimizing diesel exhaust

emissions including catalytic converters (oxidizing catalysts for HC, CO and NO_X), lean NO_X trap (LNT) or selective catalytic reduction (SCR) for NO_X, traps or filters for particulates, and the improvement of post-injection techniques. The disadvantages of the above methods are expense and complexity. In order to meet the more stringent diesel engine emission requirements, it is urgent to develop more feasible and economical methods. Clean-burning fuels such as biodiesel or biodiesel blends could help in the production of fuels with lower emissions per gallon burned. However, NO_X levels are a significant issue for biodiesel.

II.2 Biodiesel Basics

An alternative fuel for petrol diesel must be technically feasible, economically competitive, environmentally acceptable, and easily available. Biodiesel, an oxygenated fuel, is increasingly examined as a potential substitute for conventional petroleum based fuels because it is a biodegradable, non-toxic, and clean-burning fuel. Biodiesel is generated from natural and renewable sources, such as algae, vegetable oils, animal fats, and recycled restaurant greases (Graboski & McCormick, 1998). By weight, biodiesel contains less carbon, sulfur, and water, and more oxygen than fossil diesels (Graboski & McCormick, 1998; Lapuerta, et al., 2008). The reduced carbon content decreases tailpipe emissions of carbon monoxide, carbon dioxide, and soot; the lower sulfur content of biodiesel is important because biodiesel produces little or no emission of sulfur dioxide and reduced PM. Biodiesel is simple to use in compression-ignition diesel engines with few or no modifications. In addition, it can be blended at any level with petroleum diesel to create a biodiesel blend. This section

will provide a basic understanding of biodiesel, including what biodiesel is, how it is produced, what its principal properties are, how these properties affect exhaust emissions, and a review of the use of biodiesel or biodiesel blends in diesel engines.

II.2.1 Background.

Vegetable peanut oil was first used in a diesel engine by Rudolf Diesel when he exhibited his new diesel engine invention to the public at the 1900 Paris World's Fair (Peterson, 1986). Vegetable oil has been used as a diesel fuel in the 1930s and 1940s, but generally only in emergency conditions, such as World War II (Knothe, 2001). Most studies have concluded that vegetable oils can be burned for short periods of time in a diesel engine (McCormick et al., 2001; Murayama et al., 2000; Reed et al., 1992; Wang et al., 2000). However, due to the high viscosities, low volatilities, and the presence of highly unsaturated fatty acids, using fresh vegetable oils and waste cooking oils in a diesel engine for extended periods may result in severe engine deposits, piston-ring sticking, injector coking, and thickening of the lubrication oil. In addition, the high viscosity of vegetable oils and waste cooking oil reduces fuel atomization, increases fuel spray penetration, and produces higher smoke emissions (AltIn et al., 2001; Pugazhvadivu & Jeyachandran, 2005; Usta, 2005; Yahya & Marley, 1994). These problems worsen in modern diesel engines, which have direct injection fuel systems that are more susceptible to fuel quality and atomization issues than indirect injection systems.

Transesterification is an ester conversion process that splits up the triglycerides, replacing the glycerol of the triglyceride with the alkyl radical of the alcohol used.

Transesterification modifies the relevant properties of vegetable oils and waste cooking oil so that they meet the requirements for modern diesel engines (Nwafor, 2004). The process of transesterification significantly reduces viscosity and enhances biodiesel's physical properties. Esterification transforms the structure of plant oil by substituting glycerol with methanol or ethanol, while the fatty acids remain unaltered relative to their degree of unsaturation.

Figure 1 shows the transesterification process for biodiesel production, where R_1, R_2, and R_3 are long fatty acid chains (Nwafor, 2004). Through transesterification, the viscosity is reduced to a value close to diesel. The heating value is the amount of energy released during the combustion process and is measured on a gravimetric or volumetric basis. For biodiesel production, different studies have used different feedstocks, alcohols (methanol, ethanol, butanol) and catalysts. There are two kinds of catalysts used in transesterification: homogeneous ones, such as sodium hydroxide, potassium hydroxide, sulfuric acid, and supercritical fluids; and heterogeneous ones, such as lipases (Marchetti et al., 2007). At present, homogeneous catalysts, particularly the alkaline catalysts, are most commonly preferred, since they react more quickly and a lower catalyst amount is sufficient to carry out the reaction when compared to lipase (Freedman et al., 1986; Liu, 1994; Schwab et al., 1987).

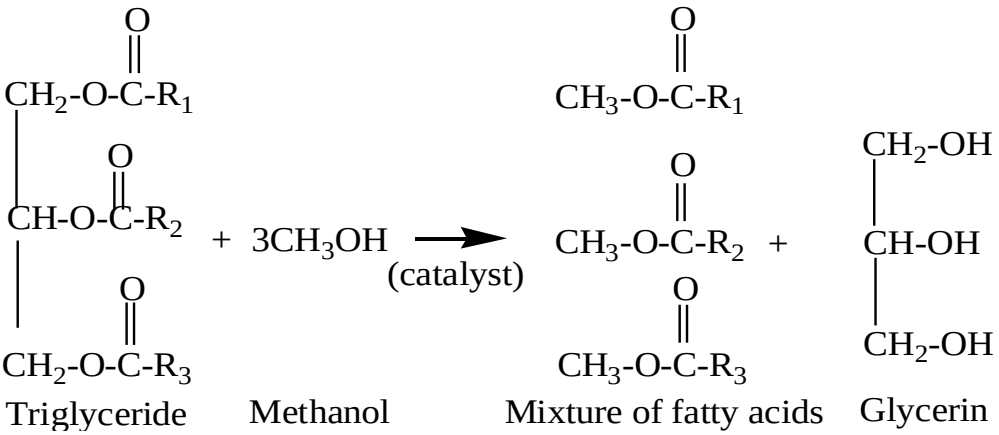

Figure 1: Transesterification process (Nwafor, 2004)

Figure 2 shows a schematic diagram of the biodiesel production process. For this process, alcohol, catalyst, and oil are combined in a reactor and agitated for approximately 1h at 60ºC (Gerpen, 2005). Following conversion of oils and fats to methyl esters through the transesterification process, the by-product, glycerin, is removed from the methyl esters through settling or centrifugation, as it has a much higher density than biodiesel and is soluble in water. The excess methanol has to be removed from the glycerol and methyl esters because methanol can slow the separation process. After separation from the glycerol, the methyl esters enter a neutralization step and then pass through a methanol stripper. The washing step removes salts, remaining catalyst, soap, methanol and free glycerol from the biodiesel.

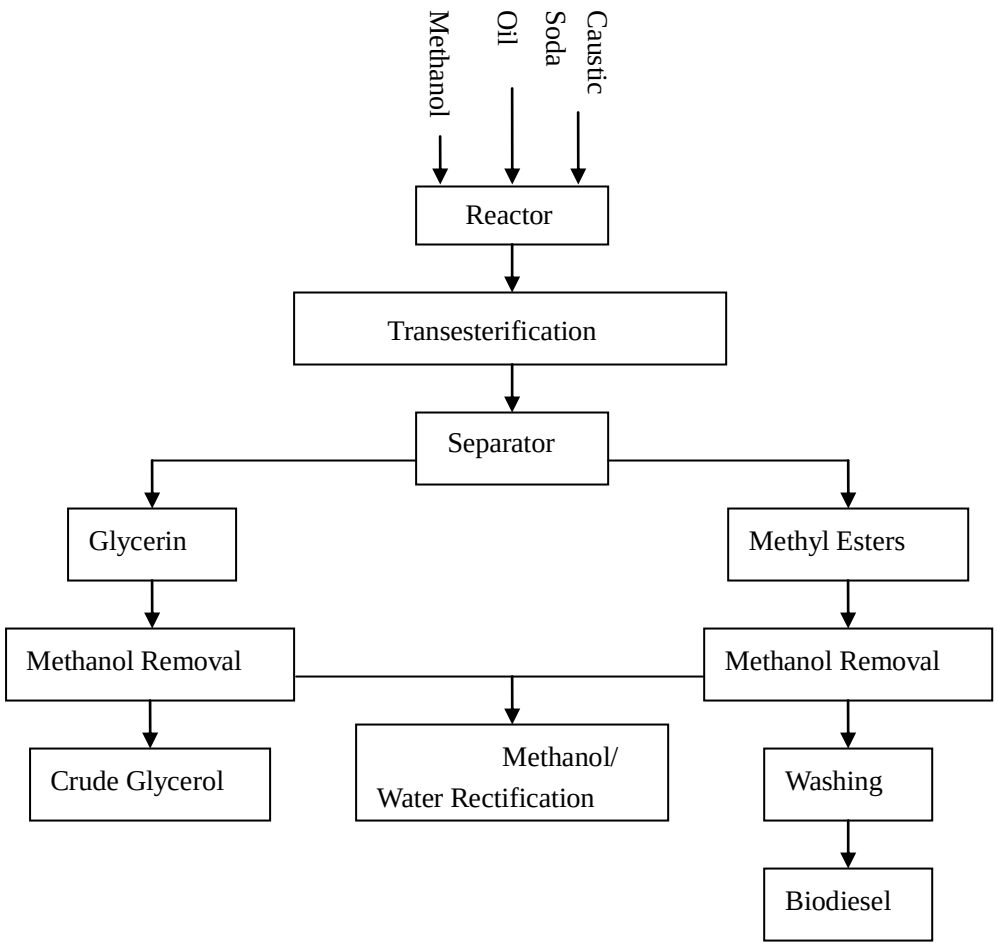

Figure 2: Schematic flow chart for the biodiesel production process

II.2.2 Biodiesel properties.

The chemical composition and properties of biodiesel depend on the length and degree of unsaturation of the fatty acid alkyl chains. The higher molecular weight and number of double bonds, lack of aromatic compounds, and presence of oxygen in the esters all affect combustion properties relative to diesel fuel. Table 3 shows ASTM D 6751, the specifications used to standardize the quality of biodiesel fuel in the United States (ASTM international) .

Table 3: American standard specification for biodiesel ASTM D 6751 (ASTM international, 2008)

Property	Test Method	Limits	Units

Kinematic viscosity (at 40ºC)	D445	1.9-6.0	mm^2/s
Cetane number	D613	47 min	-
Flash point (closed cup)	D93	130.0 min	ºC
Cloud point	D2500	Report	ºC
Water and sediment	D2709	0.050 max	Volume (%)
Sulfated ash	D874	0.020 max	Mass (%)
Sulfur	D5453	0.05 max	Mass (%)
Copper strip corrosion	D130	No. 3 max	-
Carbon residue (100% sample)	D4530	0.050 max	Mass (%)
Acid number	D664	0.80 max	Mg KOH/g
Free glycerol	D6584	0.020 max	Mass (%)
Total glycerol	D6584	0.240 max	Mass (%)
Phosphorus content	D4951	0.001 max	Mass (%)
Distillation temperature (90% recovered)	D1160	360 max	ºC

II.2.2.1 Cetane number.

Cetane number is one of the prime indicators of the quality of diesel fuel. It can be defined as the measure of knock tendency of a diesel fuel (Freedman & Bagby, 1990). It relates to the ignition delay time of a fuel upon injection into the combustion chamber. With a higher cetane number, the engine would experience shorter ignition delay. This will produce lower premixed combustion temperature and pressure, which are beneficial to lowering HC emissions. However, the advance in timing tends to promote higher NO_X formation.

Cetane number depends primarily on fuel structure (straight-chain or branched-chain), molecular weight, volatility, and the number of double bonds (Freedman & Bagby, 1990). Biodiesel typically has a longer carbon chain and a

higher degree of unsaturation, so it has a higher cetane number and a shorter ignition time.

II.2.2.2 Viscosity.

Viscosity is another important property of biodiesel since it affects the operation of fuel injection equipment, particularly at low temperatures where the high viscosity affects the fluidity of the fuel, mixture formation, and combustion process. High viscosity leads to poorer atomization of the fuel spray and less accurate operation of the fuel injectors. Viscosity increases with increasing chain length and fewer double bonds (Goering et al., 1981; Graboski & McCormick, 1998; Szybist et al., 2007). Biodiesel has a higher viscosity than conventional diesel fuel.

II.2.2.3 Density.

The density of fuel influences the efficiency of fuel atomization. No. 2 diesel has a specific gravity of about 0.85, while the values for biodiesel range between 0.87 and 0.89 (Prakash, 1998). Fuel injection equipment operates on a volume metering system, so a higher density for biodiesel results in the delivery of a slightly greater mass of fuel. However, biodiesels have lower energy content on both volumetric and mass basis. Therefore, although the injection system delivers a larger mass of biodiesel fuel, the actual energy delivered is less than for No. 2 diesel (Prakash, 1998).

II.2.2.4 Flash point.

The flash point is the temperature at which the fuel starts to burn when it comes in contact with fire. The combination of high viscosity and low volatility of a fuel causes poor cold engine start up, misfire, and ignition delay (Szybist, et al., 2007). A

fuel with a low flash point may also cause carbon deposits in the combustion chamber. The flash point of biodiesel is far above diesel fuel (Table 4), reflecting the less volatile nature of the fuel. So carbon deposits are not usually a problem because biodiesel acts as a solvent because it has better lubricating properties.

II.2.2.5 Oxygen content.

The oxygen content in biodiesel is typically 9-11% by weight (Graboski & McCormick, 1998; Mittelbach & Gangl, 2001). The presence of oxygen in the fuel lowers the local fuel/air ratio and may contribute to the observed reductions in PM emissions and other products of incomplete combustion, such as CO and HC. Diesel engines always operate under overall fuel-lean conditions, but the fuel-rich core of the spray where the solid carbon is formed may burn leaner if the oxygen provided by the fuel is available for combustion (Chang et al., 1996).

II.2.3 Biodiesel feedstocks.

Table 4: Biodiesel properties from different feedstocks (Graboski et al., 1998)

Property	No.2 diesel	Soybean Methyl	Rapeseed Methyl	Soybean Ethyl	Rapeseed Ethyl	Tallow Methyl	Frying oil
Cetane number	40-52	50.9	52.9	48.2	64.9	58.8	61.0
Flash point, ºC	60-72	131	170	160	185	117	124
Specific density, g/cm^3	0.85	0.885	0.883	0.881	0.876	0.876	0.872
Lower heating value, MJ/kg	43.4	37.0	37.3	36.7	37.4	-	37.2
Higher heating value, MJ/kg	44.9	40.4	40.7	40.0	40.5	40.2	40.5
Cloud point, ºC	-15 to 5	-0.5	-4.0	-1.0	-2.0	13.9	9.0

Pour Point, ºC	-35 to -15	-3.8	-10.8	-4.0	-15.0	9.0	9.0
Viscosity at 40ºC, cSt	2.6	4.08	4.83	4.41	6.17	4.8	5.78
Iodine number	8.60	133.20	97.4	123.00	99.70	-	-

The end cost of the biodiesel mainly depends on the price of feedstock. The high cost of the food-grade oils causes the price of biodiesel to increase and prevents its use. Currently, biodiesel unit prices are 1.5-3.0 times higher than that of petroleum-derived diesel fuel, depending on feedstock (Demirbas, 2007; Zhang et al., 2003). To become an economically viable alternative fuel and to survive in the market, biodiesel must compete economically with diesel fuel.

In selecting a feedstock, the cost of raw materials, the processing cost, and the quality of biodiesel and other byproducts all need careful assessment. An option for reducing the cost of biodiesel is to look to other sources of fats and oils that have less competition, so biodiesel could reign as the primary consumer. For example, the use of waste frying oils can substantially reduce the cost of raw materials, although it may increase the processing cost. Waste cooking oil is often hydrogenated oil with a higher pour point, which may present a problem for making biodiesel. More recently, researchers have begun looking into applying waste cooking oil, which is the waste product of the vegetable oils used to cook a variety of foods. Huge quantities of surplus waste cooking oil are available throughout the world. In the United States, the Energy Information Administration estimates 100 million gallons are produced per day (Radich, 2004), of which only a small amount is retained for industrial use. While some is used in manufacturing soap or as an additive in fodder production, large amounts of waste cooking oil are dumped into rivers and landfills illegally, causing

environmental degradation (Pugazhvadivu & Jeyachandran, 2005). This waste cooking oil could be a cheaper alternative to both diesel and edible vegetable oil (Usta, 2005). However, there can also be problems with the relatively high free fatty acid content in waste oils, which make it more difficult to properly separate the glycerol and esters obtained from the transesterification process.

Another important aspect of using waste cooking oil as biodiesel feedstock is the per capita oil consumption in the United States, which is almost 3 gallons per person per day. There were 290,809,777 persons in 2003 (U.S. Energy Information Administration, 2003). This number continues to increase, while the waste cooking oil supply remains steadily at 100 million gallons per day. Unfortunately, biodiesel from waste cooking oil and vegetation cannot provide even a small fraction of the fuel demand. However, waste cooking oil based biodiesel can be used as an additive to blend with fossil diesel or other feedstock-based biodiesel fuel.

The other promising feedstock for biodiesel is microalgae, which have the potential to accumulate lipids with very high actual photosynthetic yields. Unlike other feedstock, microalgae grow very fast and the oil content in the biomass is much higher. These advantages result in a much higher biodiesel yield. It is the only alternative fuel with the potential capacity to replace diesel fuel. However, production of microalgae biomass is generally more expensive than growing crops; more economical and feasible production of microalgae based biodiesel is needed to make it competitive with fossil diesel (Chisti, 2007).

II.2.4 Biodiesel impacts on emissions.

The United States Environmental Protection Agency conducted a comprehensive analysis of the emission impacts of biodiesel based on data collected on heavy-duty engines (U.S. Environmental Protection Agency, 2002). Statistical analysis was used to correlate the regulated emissions and the biodiesel percentage in the test fuels. The average effects are shown in Figure 3. Emissions of all pollutants except NO_X decreased with increasing biodiesel percentage, while NO_X emissions of biodiesel blends increased slightly when compared with fossil diesel.

Cardone et al. (2002) compared the performance of *brassica carinata* oil-derived biodiesel, rapeseed oil-derived biodiesel, and petroleum diesel in terms of engine performance, and regulated and unregulated exhaust emissions. The results showed that both biofuels lowered the particulate matter and carcinogenic potential of emissions compared with fossil diesel. However, higher levels of NO_x were produced due to advanced combustion.

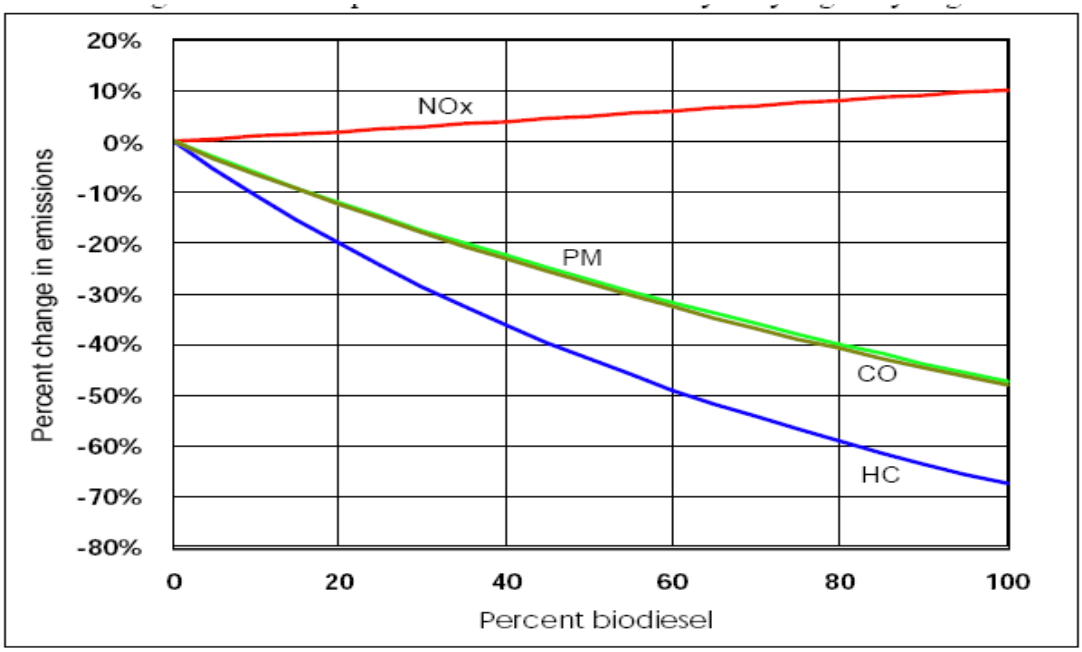

Figure 3: Average emission impacts of biodiesel for heavy-duty highway engines

(U.S. Environmental Protection Agency, 2002)

Graboski et al. (1998) tested ethyl soyester and diesel-soy ester blends in a four-stoke engine, and the PM emissions decreased by 26%. PM is made of carbon and soot, a soluble organic fraction and sulfate. Biodiesel caused a reduction in the soot fraction of PM. Gomez et al. (2000) investigated the emission difference between esterified waste cooking oil and mineral diesel fuel in a 2 liter Toyota diesel van. The results showed power values were comparable for both fuels; esterified waste cooking oil had a significantly lower smoke opacity and reduced CO, CO_2 and SO_2 emissions. However, NO_2 and NO levels were higher compared to mineral diesel.

The studies cited above clearly indicate that a substantial reduction in particulate emissions can be obtained through the addition of oxygenated additives. Because diesel particulate matter is essentially smaller than 1μm, the addition of oxygenates could have significant public health benefits. The reductions in PM emissions generally are more effective with lower biodiesel concentration in the blending. Haas and coworkers found 20% reduction in B20, while only 50% reduction with pure biodiesel (Haas et al., 2001). Lapuerta et al. (2008) found higher relative reduction of PM occurred with B20 than with B50, B75 or B100.

Generally, biodiesel and biodiesel blends from a range of feedstocks are considered to have lower emissions of CO, THC and PM than standard diesel fuel due to the oxygen content, higher cetane number, advanced injection, and combustion of the biodiesel, all of which result in a more complete combustion (Lapuerta, et al., 2008). However, biodiesel generates slightly higher levels of NO_X. Nitrogen oxides

can be a limiting reactant for ozone formation in some areas and are an important source of fine secondary particulates. The perceived NO_X penalty associated with biodiesel threatens to limit their widespread acceptance since engine manufacturers and environmental agencies alike continue to struggle with NO_X emissions from mobile diesel sources.

The causes of increased NO_X emissions with biodiesel are uncertain. Most researchers propose that the advance in engine injection timing is derived from the physical properties of biodiesel (viscosity, density, compressibility, speed of sound) (Cardone, et al., 2002). For example, McCormick et al. (2001) reported that NO_X emissions increased with increased fuel density or a lower fuel cetane number. However, pure biodiesel or biodiesel blends have a lower aromatic content and a higher cetane number compared to fossil diesel. On this basis, biodiesel or biodiesel blends should improve combustion and lower NO_X emissions. Other physical properties such as viscosity and bulk modulus impact the injection and combustion behavior as well. Biodiesel has a higher bulk modulus, which results in a higher NO_X production. The bulk modulus of a substance measures the substance's resistance to uniform compression. McCormick et al. (1997) speculated on other possible causes for increased NO_X during biodiesel combustion. First, the flame temperatures in either the premixed or burn regimes are increased. Although biodiesel has a higher adiabatic flame temperature, carbonaceous PM or soot particles are very effective heat radiators. Therefore, the net result of the PM reduction caused by supplying oxygen to the fuel pyrolysis zone may increase flame temperature because of the loss of radiant heat

transfer, which then increases NO_X. An electronic advance in the injection pump might be another reason for increased NO_X emissions in more modern engines (Lapuerta, et al., 2008). The advance of injection timing caused by the rapid transfer of the pressure wave from the fuel injection pump to the fuel injector causes it to open early.

There are two other reasons for increased NO_X emissions provided by other researchers. One is the ignition delay (Monyem & H. Van Gerpen, 2001). Ignition delay within an engine using biodiesel can be a function of both the fuel used and fuel spray properties. At the start, the oxygen/nitrogen mixture is under high pressure and is relatively hot. If there is a delay in the ignition timing, a large amount of accumulated fuel suddenly ignites, resulting in a very hot flame front, which could create a large amount of NO_X. The other is the higher oxygen availability in the combustion chamber; the heat loss from soot is reduced, which could promote NO formation (McCormick, et al., 1997).

Chapter III.

Waste Cooking Oil Biodiesel Use in Two Off-road Diesel Engines

III.1 Introduction

The development of biologically based fuels from multiple feedstocks has attracted increased attention for both environmental and energy reasons. This chapter examines the use of biodiesel produced from waste cooking oil (WCO) from both a fuel property and an emission perspective. The physical and chemical properties of different fuel batches produced from waste oil used in dining-hall fryers were examined to determine their composition and batch-to-batch variability. Emissions of carbon monoxide (CO), total hydrocarbons (THC) and nitrogen oxides (NO_X) from combustion of 5-100% biodiesel blends were then monitored using two off-road engines: a 2005 Yanmar diesel generator and a 1993 John Deere front mower.

Several comprehensive reviews of the existing literature have concluded that biodiesel typically reduces the emissions of particulate matter, total hydrocarbons, and carbon monoxide in a range of diesel engines (Lapuerta, et al., 2008; U.S. Environmental Protection Agency, 2002). Published results from experiments using WCO biodiesel are generally in line with these trends (Dorado et al., 2003; Gomez, et al., 2000; Kocak et al., 2007; Utlu & Kocak, 2008). Di et al. (2009) observed a decrease in THC emissions in blends of WCO biodiesel with ultra-low sulfur diesel (ULSD), with the greatest reductions (50%) achieved with pure biodiesel. Lin et al. (2007), however, found that a B20 blend of waste cooking oil and conventional diesel produced lower CO emissions than either pure fuel.

The effects of WCO biodiesel on NO_X emissions are less predictable. Several studies have reported reductions in total NO_X emissions for pure WCO biodiesel compared to #2 diesel (Kocak, et al., 2007; Utlu & Kocak, 2008), while others have reported increases (Gomez, et al., 2000) or no substantial effect (Leung, 2001). Di et al. (2009) and Lin et al. (2007) observed increases in NO_X emissions when WCO biodiesel fuels were blended with ultra-low sulfur diesel and premium diesel, respectively. Dorado et al. (2003) observed different results based on NO_X speciation, with NO concentrations decreasing by 37%, but NO_2 concentration increasing by up to 81%. Much of this variation between studies may be due to the greater sensitivity of NO_x emissions to engine combustion conditions (Lee et al., 2005).

The current study uses biodiesel produced from waste cooking oil feedstocks at the University of Kansas. Multiple batches of WCO biodiesel were analyzed to determine physical and chemical properties and to assess elemental composition and hydrocarbon content. One batch of the WCO biodiesel was then blended with #2 diesel to create fuels with 5-100 percent biodiesel by volume. These fuels were used to power two off-road diesel engines. Exhaust emissions from both engines were analyzed to determine concentrations of CO_2, CO, nitrogen oxides, and total hydrocarbons. The results are used to evaluate the suitability of WCO biodiesel blends for related off-road applications and to assess the relative importance of fuel makeup and engine operations on pollutant emissions.

III.2 Gas-phase Emission Monitoring System

Table 5: Measurement ranges and accuracies for the Semtech-DS emission system

Pollutant	Method	Range	Resolution	Accuracy
CO_2	NDIR	0-20%	0.01%	± 0.1% or ± 3% of rdg
CO	NDIR	0-8%	10 ppm	50 ppm or ± 3% of rdg
		0-8%	0.00%	± 3% or ± 0.02% of rdg
THC	FID	0-100 ppm	0.1 ppm	2 ppm or ± 1% of rdg
		1-1000 ppm	1 ppm	5 ppm or ± 1% of rdg
		1-10,000 ppm	1 ppm	10 ppm or ± 1% of rdg
NO	NDUV	0-2,500 ppm	1 ppm	15 ppm or ± 3% of rdg
NO_2	NDUV	0-500 ppm	1 ppm	10 ppm or ± 3% of rdg

Gas-phase emissions from two different diesel engines were collected using a Semtech-DS emission analyzer, which is designed and manufactured by Sensors, Incorporated (Saline, Michigan). The Semtech-DS is the only commercially available on-board vehicle emission monitoring system developed in conjunction with EPA, and it is the only on-board system capable of providing continuous, real-time laboratory-quality measurements of carbon monoxide (CO), carbon dioxide (CO_2), nitric oxide (NO), nitrogen dioxide (NO_2), and total hydrocarbons (THC) in vehicle emissions. CO_2 and CO are measured using non-dispersive infrared spectroscopy (NDIR), NO and NO_2 are measured by non-dispersive ultraviolet spectroscopy (NDUV), and THC is measured by a heated flame ionization detector (FID). In addition to these pollutants, an electrochemical sensor provides oxygen (O_2) measurement. Table 5 shows the measurement ranges and accuracies for the

Semtech-DS emission analyzer.

III.3 Test Engines

Table 6: Specification of the generator and lawnmower

Manufacturer	Yanmar	Yanmar
Year	1993	2007
Model	3TN75RJ	YDG L100V6-GY
Cylinder No.	3	1
Displacement, L	0.994	0.435
Bore, mm	75	86
Stroke, mm	75	75
Rated power hp	24	9.1
Compression ratio	17.8:1	21.2:1

A 2005 year Yanmar YDG L100V6-GY generator was used to test both the gas- and particle-phase emissions of different biodiesel blends. It was located in a test cell under controlled conditions, with an ambient temperature between 23.0 and 24.5 ºC during all tests. Five different biodiesel blends at 0%, 5%, 20%, 50%, and 100% biodiesel (petroleum diesel, B5, B20, B50 and B100) were tested in a rotating order each day for six days, ensuring that each fuel was in each position once. During the final two experiments, a sixth blend of 75% biodiesel (B75) was also tested. Between each test, the gas tank was completely drained and rinsed several times with the fuel for the next test. During each test, the engine was fully warmed up for 30 minutes prior to the beginning of data collection. Emissions were then monitored for 30 minutes. All experiments were performed with the generator at zero-added loading. All gas-phase measurements collected by the Semtech-DS were corrected for the

density and hydrogen-carbon ratios of each biodiesel blend. Fuel consumption was measured by the volume difference of the test fuel before and after the test. Particulate matter analysis is described in Chapter V.

The emission results from a 3-cylinder lawn mower (2.95- stroke Yanmar Model 3TN75RJ installed in a 1993 F1145 John Deere Front Mower were compared with those from the generator. This mower had been consistently operated on a 5% biodiesel fuel prior to these tests. Exhaust sampling experiments with the John Deere Front Mower were performed in the west bay parking lot of Learned Hall at the University of Kansas. Ambient temperatures during the test period varied from 13.5 ºC to 28.0 ºC. The variation within a given day was between 3-4 ºC and 10 ºC. Four different biodiesel blends were used in these tests: B5, B20, B50 and B100. Since the mower had been operating on a B5 mixture for more than a year before the beginning of the experiment, no tests were performed using only the petroleum diesel fuel. Daily testing followed the same procedure as described above for the generator tests, except that not all fuels were tested on each day. The engine was set to idle throughout each experiment. Direct measurement of fuel consumption was difficult to determine due to the recirculating nature of the fuel system. The generator uses a mechanical pump line nozzle fuel injection system, while the front mower uses a mechanical unit injector system. Table 6 shows the specifications of the two test engines.

III.4 Test Procedure

The exhaust pipe from each engine was attached to a high-speed exhaust flow meter (EFM-HS; Sensors, Inc.) using one foot of metal tubing with seven-foot-long

silicon hose connectors as illustrated in Figure 4. Eight L/min of heated exhaust was pulled from the flow meter and transferred by heated line to the emission analyzer. The heated line maintained the exhaust at 192 ºC to prevent water and total hydrocarbon condensation. Ambient temperature, relative humidity and exhaust temperature were continuously monitored and recorded via an external weather probe for user reference and humidity corrections. In order to get accurate data, the Semtech-DS was calibrated and audited at the beginning and end of each test. The span function checked and calibrated each analyzer to the high end of the sampling range, and the audit function served as a mid-range check for each analyzer. Ambient air was used as the reference zero for each analyzer prior to the calibration.

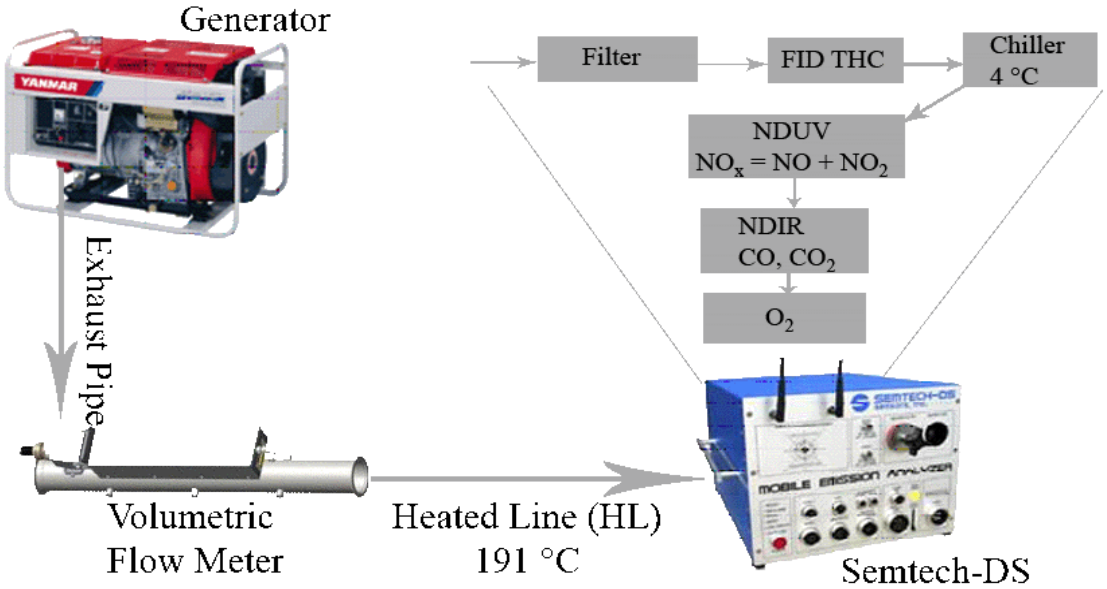

Figure 4: Configuration of the Semtech setup

III.5 Data Collection

The second-by-second data collected by the Semtech-DS were processed using the post-processing software provided by Sensors. In order to calculate the mass fuel consumption during the test period, the chemical and physical fuel properties and fuel

consumption were measured for all the test fuels. Table 7 gives the standard densities for each pollutant at 20ºC and one atmosphere (Calculations; exhaust emissions, 1986). Note that the mass rate of NO_X was computed using the density of NO_2 and the mass rate of HC was computed using the density for the average molar H/C ratio of the test fuel. Equations (1), (2), and (3) show the computation.

Table 7: Standard densities used in instantaneous mass emission calculation

Constituent	Standard Density (g/ft^3)	Standard Density (g/l)
CO_2	51.81	1.830
CO	32.97	1.164
No.1 Diesel HC (CH1.80)	16.27	0.5746
No.1 Diesel HC (CH1.93)	16.42	0.5800
Gasoline HC (CH1.85)	16.33	0.5768
NO_X (as NO_2)	54.16	1.913

Instantaneous mass emissions (g/s) are determined by multiplying the wet gas concentration by the density of the constituent (ρ_x) and also by the standard volumetric exhaust flow rate (V_{std}), which is shown in Equation 1. X is the name of the constituent, $[X]_{wet}$ is the concentration of the constituent.

$$X(g/s) = [X]_{wet} * V_{std} * \rho_x \quad (1)$$

V_{std} is computed by dividing the mass flow rate by the density of the exhaust at standard temperature and pressure in equation 2.

$$V_{std} = m / \rho_{std} \quad (2)$$

The standard density is then determined by weighting the CO_2, N_2, O_2 and water vapor by their respective wet concentrations, which yields the following equation.

$$MW_{exhaust} = 1/100 \sum \{[CO_2] * 44.01 + [O_2] *32.0 + [N_2] *28.013 + [H_2O] *18.01\} \quad (3)$$

The fuel specific mass emissions are converted from raw data using the Semtech analytical software. This is accomplished by composing an overall carbon balance in the exhaust, which reflects moles of fuel consumed per mole of exhaust. The calculation for the fuel-specific emissions is shown below for NO (Sensors Inc., 2006).

$$NO_{fs} = \left(\frac{[NO]}{[CO]+[HC]+[CO_2]_{adj}} \right) * \left(\frac{MW_{NO}}{MW_{fuel}} \right) \quad (4)$$

where NO_{fs} is the fuel- specific NO concentration (g/g fuel), $[CO_2]_{adj}$ is the measured CO_2 concentration minus the ambient CO_2 concentration determined during calibration, MW_{NO} and MW_{fuel} are the molecular weights of NO and the fuel, respectively, and all concentrations are in parts per million (ppm). The fuel MW and carbon content of the exhaust hydrocarbons are based on the user-entered H: C ratios for each fuel. The above equation is suitable for fossil diesel but ignores any potential oxygen content. Therefore, the molecular weight used in our calculations for biodiesel blends was adjusted for the oxygen content of the fuel to give the final fuel specific emissions rate. The WCO biodiesel contained 10.5% oxygen by weight (Table 9). The molecular formula is therefore $CH_{1.87}O_{0.105}$ and the correction factor is 0.895. The biodiesel blends' correction factors are calculated according to the biodiesel content in the test fuel (These correction factors are shown in Appendix A).

IV.6 Data Analysis

An Analysis of Variance (ANOVA) was performed to estimate the effects of

biodiesel content and other factors on the fuel specific emissions. ANOVA decomposes the variability in the response variable amongst the different factors (He et al., 2007). A general linear model, with biodiesel percentage and the test order of the different blends as the fixed effects, was used. Ambient temperature, exhaust temperature (measured at the exhaust flow meter, and used as a surrogate for engine temperature during combustion), and absolute humidity were chosen as covariates. All statistical analyses were performed using MiniTab and all variables were tested at the 95% confidence interval.

III.7 GC-MS Method for Fatty Acids

The KU biodiesel initiative produces biodiesel from a variety of used cooking oil obtained from the University of Kansas dining halls. This used oil is processed to biodiesel in an on-campus pilot scale facility by conversion of the triglyceride fats to fatty acid methyl esters via base-catalyzed transesterification. Each batch of fuel produced is tested for compliance with ASTM standards for density, viscosity, and flash point. Samples from six biodiesel batches produced in 2009 and 2010 were analyzed to determine their hydrocarbon composition. For the emissions experiments, one batch of WCO biodiesel was blended with petroleum No. 2 diesel fuel. The fuels were mixed by hand to create 5 gallons of each blend. The blended fuels were used in the engine tests within 10 days after mixing.

The biodiesel used in this study was produced by alcoholysis of triglycerides in the waste cooking oil. The resulting product typically consists of C_{10} through C_{26} methyl esters (Freedman, et al., 1986). The actual chemical composition and

properties of each batch depends on the length and degree of unsaturation of the fatty acid alkyl chains. The waste cooking fuel composition was determined by a GC/MS technique developed for this study.

An Agilent 6890A gas chromatograph coupled with an Agilent 5973N mass spectrometer was used to analyze the composition of the biodiesel and biodiesel blends. The chromatographic column was an HP-INNOWax Polyethylene Glycol column of 15m length ×0.25mm i.d. ×0.5μm film thickness. Data collection and analysis were performed with HP Chemstation software. A certified fatty acid methyl ester (FAME) standard and ethyl stearate used as a chromatographic internal standard were supplied by SUPELCO.

Samples were prepared for analysis by adding 0.1mL biodiesel samples to 100mL of n-hexane. About 2mL of this mixture was put into GC auto sampler vials. One microliter of the sample was injected into the GC, which was programmed at 120°C for 1 min, then ramped at 6°C/min to 180°C, 1.5°C/min to 198°C, 5°C/min to 228°C and held at 228°C for 5min. The total running time was 34 min. The injection port and transfer line were held at 250°C. Samples were injected in splitless mode with helium as the carrier gas with a flow through the column of 1.4 mL/min.

Electron ionization (EI) at 70eV was used in the analysis. The ion source temperature was 230°C and the quadrupole temperature was 150°C. The electron multiplier operated at 1482V (the number increases with age and condition of the electron multiplier) and the solvent delay was 2.5 min. The instrument operated in the scan mode.

The GC-MS method described previously was used to quantify fatty acids in biodiesel samples. Six FAME standards, 0, 0.5, 1, 2, 5, and 10 µg/ml, were injected into the GC-MS to obtain the calibration curve; the internal standard concentration was 2 µg/ml. The response factor (RF) values for each target compound were calculated by the following equation. The response factors of different fatty acids in the standard are shown in Appendix B.

$$RF = \frac{A_s \times C_{is}}{A_{is} \times C_s} \quad (1)$$

where:

A_s = peak area of the analyte or surrogate

A_{is}= peak area of the internal standard

C_s= concentration of the analyte or surrogate, in µg/L

C_{is}= concentration of the internal standard, in µg/L

If the relative standard deviation (RSD) of the response factors is less than or equal to 20% over the calibration range, then linearity through the origin may be assumed, and the response factor may be used to determine sample concentration.

The concentration of different fatty acids in the biodiesel sample is calculated using the average response factor from the initial calibration by the equation shown below.

$$Concentration(\mu g / L) = \frac{(A_s)(C_{is})(D)(V_i)}{(A_{is})(\overline{RF})(V_s)1000} \quad (2)$$

Where D = dilution factor

V_s = volume of aqueous sample extracted in mL

V_i = volume of the extract injected µL

$\overline{RF}$ = average response factor

III.8 Results

III.8.1 The composition and properties of the test fuel.

In addition to the source materials used to make the cooking oil, variations in frying temperatures and times could also affect the distribution of fatty acid compounds in biodiesel product. Several studies of WCO biodiesel have identified oleic and linoleic acid as the predominant compounds present {Chhetri, 2008 #237;Mittelbach, 2001 #28;Issariyakul, 2007 #244}. However, in a study of used cooking oils, Knothe and Steidley (2009) observed high variability in composition from different restaurants and between batches at the same location, which could result in similar variability in the final fuel.

Figure 5 shows a representative GC-MS plot used for analysis; peaks are displayed for (1) methyl palmitate, (2) methyl stearate, (3) methyl oleate, (4) ethyl stearate, (5) methyl linoleate, and (6) methyl linolenate. The detection limit was 0.44×10^{-3} ng, and the mean relative standard deviation (RSD) of the response factors was less than 6%.

The fuels consisted primarily of C_{16} to C_{20} esters, with oleic and linoleic acids accounting for at least 75% of the total mass of each sample (Table 8). This makeup is consistent with previously published analyses of WCO biodiesel composition {Mittelbach, 2001 #28;Chhetri, 2008 #237}. The two samples from 2009 (WCO1 and WCO2) had higher concentrations of more saturated compounds, particularly palmitic

acid, while the 2010 samples (WCO 3-6) had relatively higher concentrations of more unsaturated compounds. The uncharacterizable fraction was less than 6% of the total carbon for all samples.

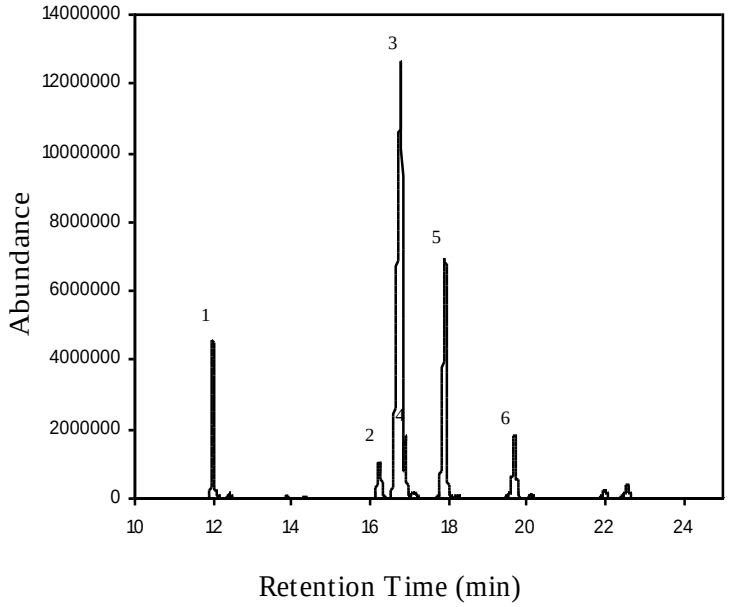

Figure 5: Chromatogram of 0.1% of biodiesel in hexane (the peaks from 1 to 6 are respectively methyl palmitate, methyl stearate, methyl oleate, methyl linolenate, methyl linoleanate, and methyl arachidate)

The GC-MS compositional data predicted identical H: C ratios and oxygen contents for all six of the WCO biodiesel fuels (Table 9). Elemental analysis of WCO 3-6 also produced very similar values between each of the fuels, with the exception of WCO3, which has a lower H: C ratio. This was also the only fuel for which the variation between the measured and actual values was outside of the estimate of uncertainty. The measured oxygen content was slightly lower than the predicted value for all four samples, but also within the error of the measurement technique. Thus, the GC-MS analysis appears to be a reasonably accurate predictor of the elemental composition of the WCO biodiesel fuels. There was very little variation in the density

of the six fuels, with values ranging from 873-886 g/L and an average of 881 ± 1.73 g/L (an RSD of 0.5%). The kinematic viscosity showed slightly more variation, ranging from 4.55 - 5.03 mm^2/s, with an average of 4.73 ± 0.092 mm^2/s (RSD = 4.8%). There was no apparent correlation between fuel composition and variations in either the density or viscosity. All flash point values exceeded 140 °C.

Table 8: Composition (as % weight) for six waste cooking oil biodiesel samples

Sample	Palmitic (C16:0)	Palmitolic (C16:1)	Stearic (18:0)	Oleic (C18:1)	Linoleic (C18:2)	Linolenic (C18:3)	Arachidic (C20:0)	Behenic (C22:0)	Others
WCO1	12.9	na	2.4	54.3	21.4	5.3	0.7	na	3.1
WCO2	14.4	na	4.8	51.6	21.6	3.5	n.a.	na	4.1
WCO3	7.08	0.4	2.99	45.24	25.92	11.45	0.75	0.43	5.74
WCO4	7.02	0.4	3.27	45.96	26.45	12.39	0.86	0.56	2.64
WCO5	7.18	0.39	3.29	46.42	26.22	12.22	0.94	0.56	2.77
WCO6	7.38	0.33	2.97	46.3	23.4	12.7	0.78	0.47	5.68

Table 9. Measured and estimated H:C ratios and oxygen contents

H: C Ratio		Oxygen Content (% weight)	
Measured [a]	Predicted	Measured [a]	Predicted
1.82	1.85	10.5	10.6
1.86	1.85	10.5	10.6
1.86	1.85	10.5	10.6
1.86	1.85	10.5	10.6

a. Uncertainties in the measured H:C ratio and oxygen content are ± 0.02 and 0.1%, respectively.

III.8.2 Emission analysis.

A single batch of the waste cooking oil biodiesel (WCO1) was used in all of the emissions experiments, in order to minimize any effects due to fuel quality variations.

Table 10 lists specific properties of this fuel, as well as of the B5-B75 blends created through mixing with petroleum diesel. The H: C ratio for each blend is estimated from a linear combination of the B100 fuel (as determined by compositional analysis) and the #2 diesel. Similarly, the oxygen content is a mixture of the two end member fuels, with the B100 assumed to have 10.5% oxygen based on the measured values for the 2010 fuels and the #2 diesel was assumed to have no oxygen. Other properties were measured individually for each fuel blend.

Table 10: Fuel properties of biodiesel blends used in the emissions study

Fuel type	H: C	Oxygen (% wt)	Density (g/L)	Flash point (°C)	Viscosity (@40°C)
B100	1.87	10.5	881	158	4.99 cST/s
B75	1.85	7.9	870	98	4.17 cST/s
B50	1.84	5.3	859	75	3.47 cST/s
B20	1.81	2.1	847	65	2.81 cST/s
B5	1.80	0.5	840	62	2.61 cST/s
B0 (# 2 diesel)	1.80	0	825	23	2.17 cST/s

III.8.2.1 Engine comparison.

Raw CO_2 exhaust concentrations did not vary significantly for either engine as a function of biodiesel content. The observed decrease in fuel-specific emissions shown in Figure 6 is due to the increased oxygen content in the biodiesel fuels, which results in a higher MW_{fuel} value for higher biodiesel blends. However, this decrease would be offset by the lower energy content of the biodiesel fuel, which will result in greater fuel consumption for the same power output. In general, biodiesel fuels are not typically expected to have a significant effect on exhaust CO_2 emissions. Biodiesel may, however, be more carbon neutral overall because of the source of the carbon

(biological versus fossil carbon). Determining the actual net CO_2 emissions difference due to biodiesel blending requires a lifecycle emissions analysis for the specific fuel that is beyond the scope of this work.

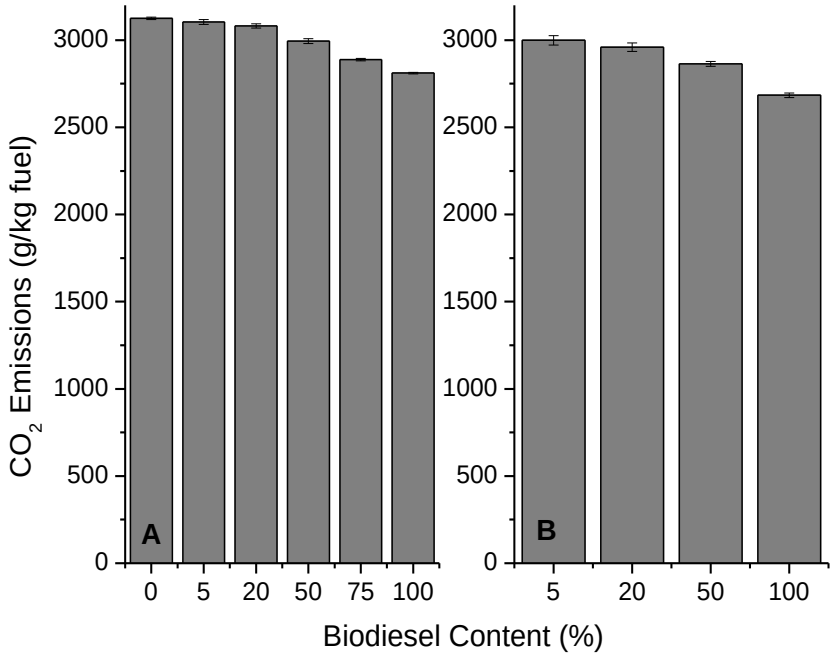

Figure 6: Fuel-specific CO_2 emissions from (A) generator and (B) front mower for biodiesel blends

Fuel specific emissions for all pollutant compounds except for CO were much higher from the front mower than from the generator (Figures 9 and 10, Appendix C and D) at all biodiesel contents. Most notably, total NO_X concentrations were 4-5 times higher (70 g/kg fuel at 5% biodiesel content, compared to 15 g/kg fuel from the generator), with the majority of this difference due to higher NO formation. The generator and front mower used in this experiment represent two very different systems, both in age and in engine design. In particular, they are different injection systems, with a mechanical pump line nozzle fuel injection system for the generator and a mechanical unit injector system for the mower. The age of the front mower

means that its engine was designed and built prior to implementation of any U.S. EPA emission regulations for off-road mobile diesel sources of its type. The generator, built in 2007, was required to meet EPA certification for NO_X and particulate matter. Engines built prior to more restrictive NO_X emissions standards are more likely to have fuel injection timing optimized for performance at the expense of emissions control.

III.8.2.2 Biodiesel effects on generator emissions.

The higher bulk modulus of compressibility of biodiesel fuels can result in advanced fuel injection timing of as much as one to two crank angle degrees (Boehman et al., 2004; McCormick et al., 2006). Additionally, changes in the spray and mixing behavior from oxygen content and fuel stoichiometry can increase the local temperature and heat release in the autoignition zone of the flame {Mueller, 2009 #42}. Both of these factors will result in a hotter combustion process as the biodiesel content of the fuel increases. In turn, this should result in more complete combustion, and a corresponding decrease in carbon monoxide and total hydrocarbon emissions. While NO_x emissions typically increase with increasing biodiesel content, the reasons are more complex, and may be due to a combination of several different mechanisms {Ban-Weiss, 2007 #43;Mueller, 2009 #42;McCormick, 2001 #255}.

Figure 7 shows that the average emissions rates for criteria pollutants from the Yanmar generator followed this pattern. Carbon monoxide and total hydrocarbon emissions decreased by 46 and 68%, respectively, between the #2 diesel and B100 fuels. The majority of this decrease occurred between 0 and 20% biodiesel content,

while further increasing the biodiesel content had a noticeably smaller incremental effect on emissions for both compounds. This suggests that the largest impact on emission is achieved at relatively low oxygen concentrations. Total nitrogen oxides, on the other hand, generally increased with increased biodiesel content. As with the partial combustion products, most of the change in exhaust concentrations occurred at biodiesel contents $\leq$ 20%. Observed changes in NO_X emissions with different blends were due primarily to variations in NO, as NO_2 emissions showed no consistent trend with biodiesel content.

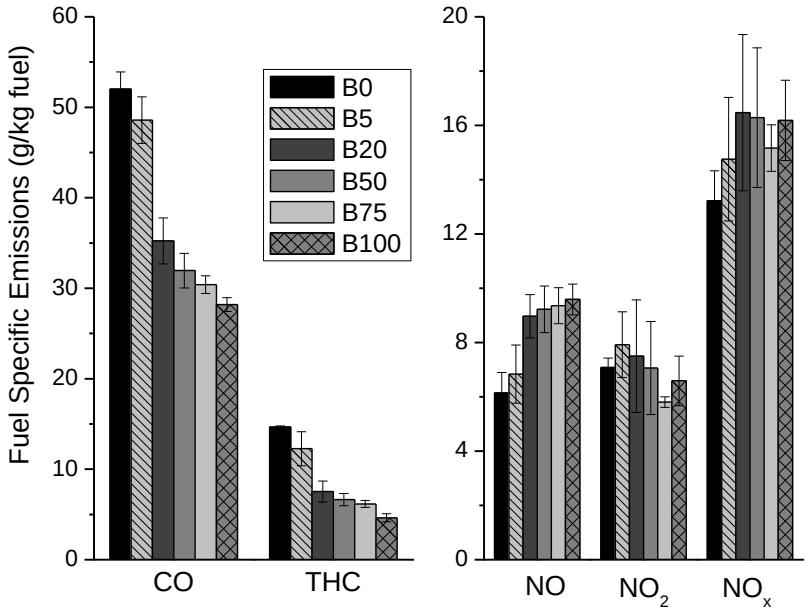

Figure 7: Gas-phase pollutant emissions from the Yanmar generator (error bar indicate one standard deviation of the uncertainty)

Results from the ANOVA analysis of the generator emissions data are shown in Table 11 and Appendix E. The biodiesel content was significantly correlated to changes in all compounds except for NO_2. Nitrogen dioxide is both quickly formed and rapidly destroyed during the combustion process, with the relative extents of

these two processes are affected by multiple factors. In this case, it appears that the complexity of this process outweighs any consistent effect due to the presence of biodiesel in the fuel. Variations in ambient temperature and humidity in the test cell were small during these tests, with temperatures ranging from 22-24 °C and humidity from 55-60 grains/lb dry air, and there was no apparent effect of these changes on the exhaust composition. The measured exhaust temperature did decrease with higher biodiesel content, with a high of 106°C with #2 diesel to a low of 98°C with the B100 fuel. This change is directly related to the advanced injection timing. When fuel injection timing is advanced, the resulting hotter combustion will produce more NO_X, as their formation is highly temperature dependent. Since combustion now occurs earlier in the expansion stroke of the engine, the working fluid is given more crank angles (volume) for expansion and more time for heat transfer. Therefore, as combustion is completed closer to top dead center, more work can be done by the engine before the exhaust valve opens and the cylinder walls see a larger temperature gradient for a longer time, promoting convective heat transfer. As a result, the exhaust temperature will decrease even though the peak combustion temperature is higher.

Table 11. ANOVA results (P value) for generator test data

Influence Factor	CO_2	CO	NO	NO_2	THC
Biodiesel Content	**0.000**	**0.000**	**0.000**	0.647	**0.000**
Exhaust Temperature	**0.052**	0.090	0.130	0.674	0.335
Ambient Temperature	0.594	0.949	0.704	0.685	0.769
Ambient Humidity	0.423	0.563	0.869	0.748	0.564

Statistically significant effects at the 5% confidence level in bold

III.8.2.3 Biodiesel effects on mower emissions.

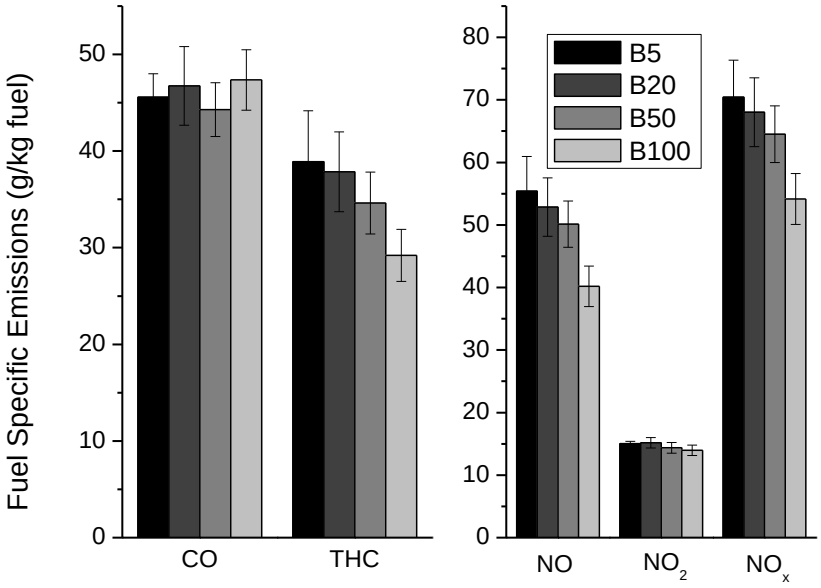

Figure 8: Gas-phase pollutant emissions from the front mower (error bar indicate one standard deviation of the uncertainty)

The emission patterns for CO, THC, and NO_X as a function of biodiesel content are substantially different for the front mower exhaust (Figure 8). While total hydrocarbon emissions did decrease with increasing biodiesel content, the change was not significant except for the B100 fuel. The maximum reduction of 25% from the B5 to the B100 fuel was also much smaller than the 52% reduction between the same two fuels in the generator studies. CO emissions showed no consistent pattern as biodiesel content increased, despite the typical linkage between these two partial combustion products. NO_X emissions, by contrast, declined with increasing biodiesel content, with the greatest change between 50% and 100% biodiesel. This trend was very similar to that observed for total hydrocarbon emissions. NO was also a substantially higher fraction of total NO_X emissions from the mower, accounting for > 75% of recorded

NO_X, compared to 46-52% from the generator. This difference is also likely related to differences in fuel injection control between the two engines.

As the mower engine was designed prior to EPA emission standards for off-road engines, it is postulated that the injection timing was set to prime conditions for performance. Combustion in newer engines happens more in the expansion stroke in a relatively "cooler" environment because the engine manufacturers retard the injection timing to reduce NO_X emissions for regulatory reasons. NO_2 is formed quickly from NO in a hot environment and can be destroyed just as quickly, as long as the mixture temperature remains hot. When injection timing is retarded, the conditions outside the flame are cooler, resulting in greater quenching of the flame. Under these conditions, the NO_2 formation process happens as rapidly as before, but the flame quenches more easily, removing the necessary energy to convert NO_2 back to NO. Since combustion for the generator happens later in the expansion stroke (due to an attempt to minimize emissions generation), there is a more extensive flame quenching, which promotes NO_2 formation over NO.

The ANOVA results for the mower study (Table 12) indicate that changes in fuel biodiesel content are significantly correlated with changes in emissions of all measured compounds, including NO_2, although the absolute changes in NO_2 emissions are very small. The overall range of exhaust temperatures was smaller in the mower studies, with a maximum of 84° C during the B5 tests and a minimum of 81° C with B100. However, both NO and total hydrocarbons show some correlation with this parameter. Ambient conditions also varied more during the front mower

tests, which were conducted outdoors. Temperatures during these tests ranged from 13-27 °C, and humidity from 23-73 grains/lb dry air. Even so, ANOVA indicated no significant effect for ambient temperature on emission results.

Table 12. ANOVA results (P value) for front mower test data.

Influence Factor	CO_2	CO	NO	NO_2	THC
Biodiesel Content	**0.000**	0.067	**0.000**	**0.000**	**0.000**
Exhaust Temperature	**0.000**	0.491	**0.000**	0.838	**0.000**
Ambient Temperature	0.139	0.153	0.258	0.825	0.460
Ambient Humidity	**0.011**	**0.001**	**0.005**	**0.005**	0.068

Statistically significant effects at the 5% confidence level in bold

Humidity is correlated with CO_2 CO and NO_2 results. Increased humidity in the intake air has been shown to decrease total NO_X production in published studies (Brown et al., 1970; Krause, 1971; Manos et al., 1972). The correction factors available for naturally aspirated off-road diesel engines (Dodge et al., 2003) was used to adjust NO_X results for the effects of humidity by calculating a reference NO_X value for each biodiesel content that was independent of ambient conditions. These adjusted data produced a similar trend in total NO_X emissions to the uncorrected results. So, humidity had little effect on the NO_X emissions for this case. The relationship between CO emissions and humidity may be related to humidity- induced changes in fuel viscosity, which can affect fuel injection timing and duration, thereby influencing the combustion process (efficiency and pre-mixed versus diffusion burn amounts).

The increase in biodiesel content should result in an accelerated fuel injection sequence in both the generator and front mower as discussed previously. The change

in injection timing may have a much less significant effect on the combustion profile for an older engine designed and optimized prior to emission regulations. For later model year engines, changing a few crank angle degrees for combustion can have a large effect on results, as pressures and temperatures are changing dramatically during the expansion stroke. The piston accelerates from top dead center to the middle of the expansion stroke. When fuel injection timing is optimized for performance, heat release is maximized closer to top dead center when the piston is moving relatively slowly. Hence, a few changes in crank angle degrees will have a much less dramatic effect on conditions within the cylinder. In this case, the energy content of biodiesel may play a more important role in determining the generation of exhaust products than combustion phasing. Reducing the overall in-cylinder temperature could result in the decrease in NO_X reductions observed in the front mower. Under this scenario, the reduction in total hydrocarbon emissions at higher biodiesel content would be due almost entirely to differences in the chemical composition of the WCO fuel, which produces more complete fuel combustion even at the reduced temperatures, while CO is more strongly affected by combustion conditions and does not decline. Further examination of this postulate would require collection of in-cylinder pressure and temperature data, which was beyond the scope of this effort.

III.8.3 B100 emissions at different loadings.

WCO biodiesel and ultra low sulfur diesel (ULSD) were used to power the Yanmar generator in order to investigate the emission differences between different loadings. The engine experimental setup was the same as before but engine

performance data were recorded. Criteria pollutant emissions were evaluated under five different diesel engine loadings. The engine load was changed by employing a NorthStar electric heater coupled to the crankshaft (Table 13). Resistance heaters supplied variable electrical loading. Selection of the specific power of these heaters was a function of the generator capacity to offer 0 to 100% loading which is approximately 80.6% of engine load rating. Figure 9 showed that fuel specific CO_2 emissions remain constant. CO, NO_2, and THC decreased with increasing loading, while NO emissions increased when the loading increased to 50%, then kept constant in the range of 50% to 100% loading. NO and NO_2 trends depend mostly on engine temperature, which is a direct function of engine power output. As the engine loading increases the combustion gas temperature increases, which in turn increases the formation of NO.

Table 13: The specification of NorthStar electric heater.

Manufacture and model	NorthStar 5500BDG
Maximum output rated	5500 W
Continuous output rated	5000 W
Voltage	120V/240V
Phase	Single-phase (4-wire)
Frequency	59.0-62.0 Hz
Power factor	100%
Allowable current (120V/240V)	2@20 Amp/ 1@20 Amp

Brake-specific fuel comsumption (BSFC) is the ratio between mass fuel consumption and brake effective power, and it is inversely proportional to thermal

efficiency. BSFC is used to relate the fuel consumed by any engine size to the work performed in order to standardize fuel economy (Heywood, 1988). As biodiesel has a lower heating value, the BSFC of biodiesel is expected to increase by around 14% compared with diesel (Lapuerta, et al., 2008). In order to maintain 3600 rpm and the energy required by the resistance heaters, the BSFC with pure WCO biodiesel from 0 to 100% loading was 14 to 18% higher than diesel fuel, with the greatest difference at idle condition (Figure 10). At low load conditions, the fuel flow is relatively low, so torque fluctuates in non-ideal combustion conditions. The combustion efficiency increases with increasing loading, and the BSFC was lower at higher load. However, there was no loss of generator output power with biodiesel.

Brake specific emissions (BSE) can be used to normalize the production of gaseous emissions from any engine size. A lower BSE means less emissions for the same amount of work produced and illustrates a cleaner engine (Heywood, 1988). All brake-specific emissions decreased with increasing loading (Figure 11). The highest decrease happened from 0-50 percent loading, with little change when loading increased from 50% to 100%. This is because diesel engines operate lean with excess air. Combustion efficiency increases with load due to hotter combustion and is typically near 100% at 50% load or higher (Cecrle et al., Submitted). Biodiesel had a lower BSE of HC and CO at all loadings compared with diesel due to higher oxygen content. Meanwhile, NO_x and NO increased, but NO_2 was lower for biodiesel. The causes of increased NO_X emissions with biodiesel may be the advance in engine injection timing derived from the physical properties of biodiesel (viscosity, density,

compressibility, sound velocity) {Cardone, 2002 #9}

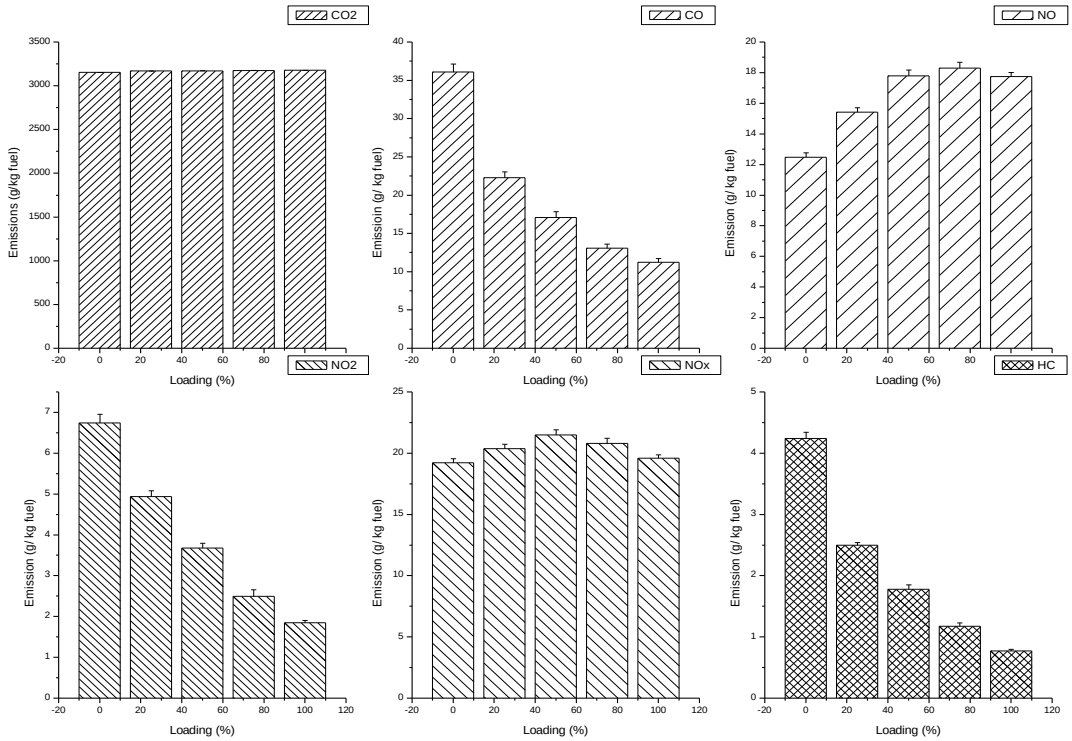

Figure 9: Criteria pollutant emissions at different engine loadings for 100% waste cooking oil (Error bar indicate one standard deviation of the uncertainty)

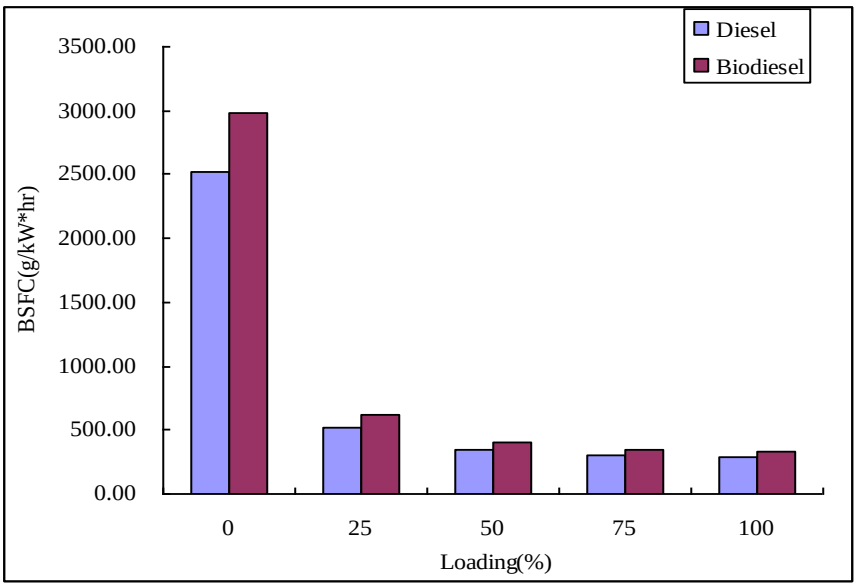

Figure 10: Brake specific fuel consumption of diesel and pure biodiesel at different loadings

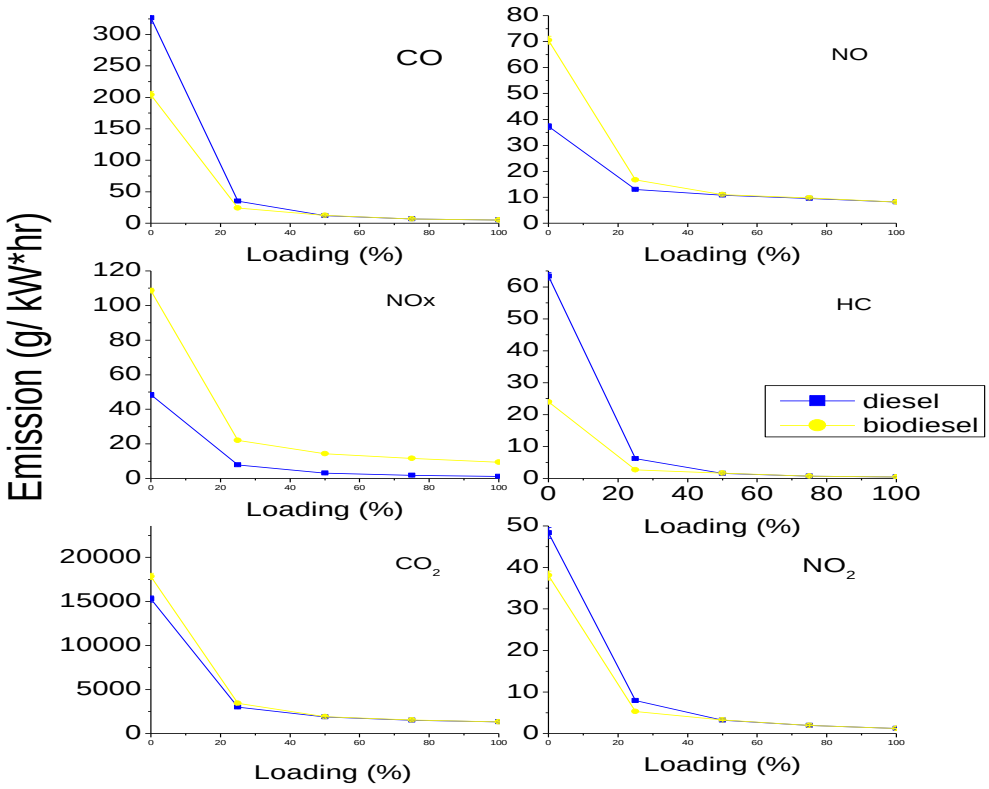

Figure 11: Criteria pollutant emissions at different engine loadings for 100% waste cooking oil and ULSD

III.9 Conclusions

A GC-MS method was developed to analyze the composition of WCO biodiesel. The physical properties of the six WCO biodiesel batches produced by the KU Biodiesel Initiative showed very little variation. While there was some change in chemical composition from batch-to-batch, H: C ratios and oxygen contents were very similar, and could be estimated from GC-MS analysis. Increased blending of biodiesel from waste cooking oil into the B5 fuel currently used by KU produced lower emissions of total hydrocarbons in both engines. These decreases are consistent with similar results from other studies of waste cooking oil biodiesel, and most likely related to the observed differences in fuel composition, particularly the higher oxygen

level and lower aromatic content. The relationship between biodiesel content and both CO and NO_X emissions, by contrast, vary substantially between the two engines. The generator results follow typical patterns for biodiesel, with decreased CO and increased NO_X production. In the front mower, increased biodiesel content resulted in decreased NO_X emissions and had no measurable effect on CO. This difference is likely related to differences in fuel injection strategies between the two engines that resulted from changes in emissions regulation for off-road engines implemented over the last two decades. Brake specific emissions of six pollutants from WCO biodiesel and ULSD decreased with increasing engine loading. Biodiesel had a lower BSE of HC and CO at all loadings compared with diesel due to higher oxygen content. Meanwhile, NO_X and NO increases, but NO_2 is lower for biodiesel.

These results indicate that the effects of biodiesel use in non-road engines on emission profiles may depend greatly on the fuel injection strategy used, which in turn will be related to the age of the engine. In the United States, comprehensive emissions regulations for most mobile off-road sources (including portable generators) were put in place between 1994 and 2001. Vehicles and equipment less than 10-15 years old (depending on the specific engine class) would thus be expected to employ delayed fuel injection timing to control NO_X emissions, and may see increased NO_X and reduced hydrocarbon emissions due to biodiesel use. Stationary engines, however, have been required to meet these same emissions standards only for new engines built since 2007. Exhaust emissions from existing stationary engines, as well as older mobile off-road sources, may thus be less affected by the introduction of biodiesel

fuels based on waste cooking oil.

Chapter IV.

Impact of Biodiesel Blends on Emissions from a Switching Locomotive

The U.S. EPA Renewable Fuel Standard program is designed to increase the use of renewable fuels in the transportation industry. Under the terms of the Energy Independence and Security Act of 2007 (EISA), this program has been expanded to include diesel fuels and to increase the volume of transportation fuel that must be supplied from renewable sources to 36 billion gallons by 2022 (U.S. Environmental Protection Agency, 2010). For diesel locomotive engines, the only commercially-significant renewable fuel source currently available is biodiesel. In the United States, the majority of available biodiesel is produced from soybean oil and contains primarily C_{16} and C_{18} esters (Pinto et al., 2005). Biodiesel can be used directly in existing diesel engines, both as a pure fuel and as a blend with petroleum diesel, and is therefore the most promising short-term way for railroads to increase their use of renewable fuels over the next few years. There are outstanding questions, regarding biodiesel's impact on locomotive performance, particularly with respect to engine compatibility and exhaust emissions.

The major impetus for increasing renewable fuel use under EISA is the reduction of greenhouse gas emissions, in particular net carbon dioxide (CO_2). However, there are also other potential impacts of biodiesel use on locomotive exhaust emissions that must be considered. Currently, the U.S. EPA regulates four categories of hazardous air pollutants in locomotive emissions: carbon monoxide (CO), nitrogen oxides (NO_X),

total hydrocarbons (THC), and particulate matter (PM). A 2005 study estimated that freight rail accounts for 15% and 12%, respectively, of total NO_X and PM emissions resulting from freight transportation (Ang-Olson & Ostria, 2005). To reduce these emissions and improve local and regional air quality, the EPA published new rules for emissions from diesel locomotives of all types (line-haul, switching and passenger) in 2008 {U.S. Environmental Protection Agency, 2008 #13}. These rules require that newly manufactured or re-manufactured locomotive engines meet increasingly stringent standards for NO_X and PM that will be implemented in stages through 2015. As meeting these requirements will involve substantial challenges for locomotive manufacturers and railroads, any alternative fuels introduced during this period will be much more widely accepted if they have reduced emission profiles for these regulated pollutants. At a minimum, the fuels should not significantly increase NO_X or PM emissions compared to the baseline fuels already in use.

Existing emissions studies typically show substantial reductions in particulate matter, CO, and THC resulting from the blending or substitution of biodiesel for petroleum diesel fuels. Unfortunately, existing data on biodiesel use in locomotive engines is sparse. A study conducted for the National Renewable Energy Laboratory compared a 20% biodiesel blend (B20) to several other fuels in an EMD GP38-2 locomotive using various duty cycles (Fritz, 2004). Biodiesel use resulted in a 4% to 6% increase in NO_X emissions compared to baseline EPA certification fuel, and minimal changes in other regulated constituents (including PM). The reduction of CO and THC were respectively 17% and 5%. More recently, McKenna et al. (2008)

presented preliminary results from a study of passenger locomotives belonging to the New Jersey Transit that were tested with multiple different fuels. In static testing of a GP40FH-2 locomotive, B20 blends reduced opacity compared to both #2 diesel and ULSD summer fuel blends. NO_X exhaust concentrations were comparable for B20 and #2 diesel, although brake-specific horsepower values increased 2.2%. Total hydrocarbon emissions were comparable for all fuels. A recent study was also conducted using ULSD, B50 and B100 in a 1994 Alco S2 switch locomotive moving cargo at the Port of San Francisco (Gavrich et al., 2008). Nitrogen oxides increased by 21 and 48% while HC and PM significantly decreased, over 50% with B50 and B100. There was no change of CO emissions with B50 and 19% reduction with B100 compared with ULSD.

Biodiesel can be produced from various food-grade vegetable oils, including soybean, palm, and sunflower. Soybean oil is of primary interest as a biodiesel source in the United States. The high cost of the food-grade oils causes the price of biodiesel to increase and prevents its usage. Currently, biodiesel unit prices are 1.5-3.0 times higher than that of petroleum derived diesel fuel, depending on feedstock (Demirbas, 2007). Researchers are looking for other sources of biodiesel, such as tallow, waste cooking oil, and algae.

One reason for slow adaptation of biodiesel in locomotives lies in a lack of knowledge about the effects of biodiesel on engine emissions. Second, biodiesel has a higher solvent characteristics than conventional diesel fuels, which could affect degradation of materials or the plugging of filters, depending mainly on their

degradability and glycerol content (Waynick, 2005). The third major issue with biodiesel usage is cold start during winter times. Diesel engine start depends on self-ignition quality, cetane number, viscosity, fuel freezing and cloud temperature (Marissiu & Varga, 2010). Biodiesel has a much higher cloud point than diesel, which may cause problems relating to flow through the injection pump, clogging filters and supply lines.

If biodiesel is to play a greater role in the railroad industry in the future, it is important to determine whether it can meet railroad needs for performance, reliability and emissions. Given the minimal data and inconsistent results currently available for biodiesel emissions data in locomotive engines, it is particularly crucial that additional data be obtained to better estimate the effects of biodiesel amendment on locomotive exhaust emissions, particularly for NO_X. In the current study, two biodiesels, one soy and one tallow, were blended with ULSD to create 10% (B10) and 20% (B20) biodiesel blends. These blends were then tested in a switching locomotive owned by the Iowa Interstate Railroad. The soy biodiesel blends were used exclusively in the locomotive for a 90-day period during normal operation. Emissions monitoring was performed at the beginning and end of the testing period to determine emissions of regulated pollutants from the different fuel blends. The results of the operations and emissions tests are used to assess the suitability of biodiesel as a “drop in” replacement for petroleum diesel from both a performance and air quality standpoint.

IV.1 Test Engine

A 4-axle EMD GP38 switching locomotive (Figure 12, Table 14) owned by the Iowa Interstate Railroad was used to test biodiesel performance. This locomotive is equipped with a 645E 16-cylinder engine. The engine is a 2-stroke, 45° V-engine with a twin-roots blower and a 2000-hp rating. It has four exhaust stacks located in the center of the locomotive. The tested locomotive was originally manufactured in 1966, but the engine has undergone multiple rebuilds since that time, most recently in June, 2006.

Table 14: Locomotive specification

Locomotive	EMD GP-38
Year Mfgd.	October 1966
# of axles	4
Function	Switch only
Engine	EMD 645E
Type	2 stroke, 45 ° V
# of cylinders	16
Displacement per Cylinder	645 in^3
Rated hp	2000
Compression ratio	16:1
Turbocharged	No – 2 Roots Blowers
Last rebuild	2009
# of stacks	4

All engine operations and static load tests were performed at the Iowa Interstate rail yards in Council Bluffs, IA in 2009 and 2010. Static load tests were conducted using a custom-built load box (Figure 13). This load box takes electrical power generated by the locomotive, passes it through a set of resistor banks, and then expels

excess heat to the atmosphere. Both voltage and amps from the main electrical generator are measured during the load tests, and horsepower is then calculated using the following equation (Toliyat & Kliman, 2004):

Horsepower = Voltage * Shunt ratio * Amps/700

Figure 12: EMD GP38 switching locomotive

Figure 13: Load box

Table 15: Fuel used in static load tests

Test Date	6/22/2009	9/20/2009	5/11/2010	10/19/2011
Test #1 (Used Fuel)	ULSD	B10 (soybean)	B20 (soybean)	ULSD
Test #2 (Fresh Fuel)	B10 (soybean)	B20 (soybean)	ULSD	B20 (tallow)

Locomotive operation tests using two biodiesel blends were conducted between June, 2009 and January, 2010 (Table 15). The procedure followed for each 90-day test was similar. First, a static load test was conducted on the locomotive using the current fuel. Following this test, the locomotive underwent routine maintenance and the fuel tank was drained and refilled with the next fuel. After an extended idling period to clean out the fuel lines, a second static load test was performed. The locomotive then

returned to regular operation for at least 90 days, during which time it was supplied exclusively with the respective biodiesel blend. At the end of this period, the testing and fuel change-over process was repeated. In the first test, from June-September 2009, the locomotive was operated on B10. In September, the B10 was removed and replaced with B20. Due to an unrelated transformer problem that occurred in mid-November, B20 use was extended to late January, 2010 to provide for a full 90 days of operation. At the end of the B20 test, the locomotive resumed operation with ULSD fuel.

Figure 14: Diesel locomotive experiment configuration

Emission tests were conducted during the static load tests, using the procedure described below. No emission tests were conducted in January 2010 due to adverse weather conditions. To obtain emissions data from the locomotive after extended operation with B20, the locomotive was re-fueled with B20 in late April, 2010. After two weeks operation with the B20 fuel, a final set of load tests was performed with

the B20 fuel and then with the ULSD. Figure 14 shows the configuration of the experiment setup.

In October of 2010, tests were conducted using a tallow-based biodiesel in the same switching locomotive. The set of load tests was performed with ULSD first and then B20 fuel. The ambient temperature was around 13°C which is below the cloud point of the tallow biodiesel, so it was not possible to be assured to completely mix with fossil diesel before the test.

IV.2.1 Test fuel.

All biodiesel fuel for locomotive tests was supplied by Renewable Energy Group (Ames, IA). The B100 fuel (REG-9000 biodiesel) used for blending from June 2009 to May 2010 was made from soybean oil with an animal fat component of 10% or less and a density of 884 g/L (at 60℉), kinematic viscosity of 4.03 mm^2/s (at 40°C), cloud point of 2°C, and flash point of 131°C. The sulfur content of the B100 was 2.5ppm. The B100 biodiesel was blended on-site with commercially-available ultra-low sulfur diesel (density = 800-850 g/L, viscosity = 1.3-2.1 mm^2/s at 50°C) to produce the B10 (10% biodiesel) and B20 (20% biodiesel) fuels used in this study. There was little variation of the test fuel before and after use.

Tallow biodiesel used in October 2010 has a density of 876 g/L (at 60℉), kinematic viscosity of 4.8 mm^2/s (at 40°C), cloud point of 13.9°C, and flash point of 117°C. The B100 biodiesel was blended on-site with commercially-available ultra-low sulfur diesel (density = 800-850 g/L, viscosity = 1.3-2.1 mm^2/s at 50°C) to make B20 fuel for the test.

IV.2.2 Static load test.

For each load test, the locomotive was connected to the load box, started, and left to idle for 10 to 15 minutes. The locomotive was then put to full throttle, producing maximum electrical power, for 30 minutes. Power readings were taken when the engine was first put to full throttle, and every five minutes thereafter during the test. Flow meters on the fuel supply and return line were reset at time zero. Final readings on both lines were read at 30 minutes, and the return reading subtracted from the supply reading to determine total fuel consumption during the load test. During the September, 2009 load tests, a calibration error in the fuel flow meters meant that absolute fuel quantities used for the two load tests on that date could not be obtained.

During each of the static load tests, an in-line sample probe was placed in the rearmost of the engine's four stacks to collect engine exhaust. This probe collected exhaust continuously throughout the load test at a rate of eight liters per minute. A heated sample line was used to transfer the collected exhaust to the emissions analyzer while maintaining a temperature of 192 ºC to prevent water and total hydrocarbon condensation. The exhaust temperature at the point of collection was also recorded for each test using an auxiliary temperature probe.

Gas-phase exhaust constituents were measured using a Semtech-DS portable emissions analyzer (Sensors Inc., 2006). For the ULSD and B20 tests conducted in May and October 2010, the soot content of the exhaust from the rearmost exhaust stack was determined using a 415S G002 Variable Sampling Smoke Meter (AVL). The smoke meter draws a fixed volume of exhaust through a probe mounted directly

in the stack exhaust stream. The sample passes through a filter paper, and an optical reflectometer is used to determine the extent of filter darkening due to soot deposition. For these tests, the sampler was mounted in the rearmost exhaust stack adjacent to the emission analyzer probe. Exhaust was collected for six seconds every three minutes during the static load tests at a rate of 10 L/min, for a total sample size of one liter of exhaust. The extent of filter blackening was used to calculate a Filter Smoke Number (FSN) and soot concentration (in mg/m^3) according to ISO 10054 (International Organization for Standardization, 1998). Ambient air checks showed no significant background soot concentrations either before or after the load tests for each fuel.

IV.2.3 Data analysis.

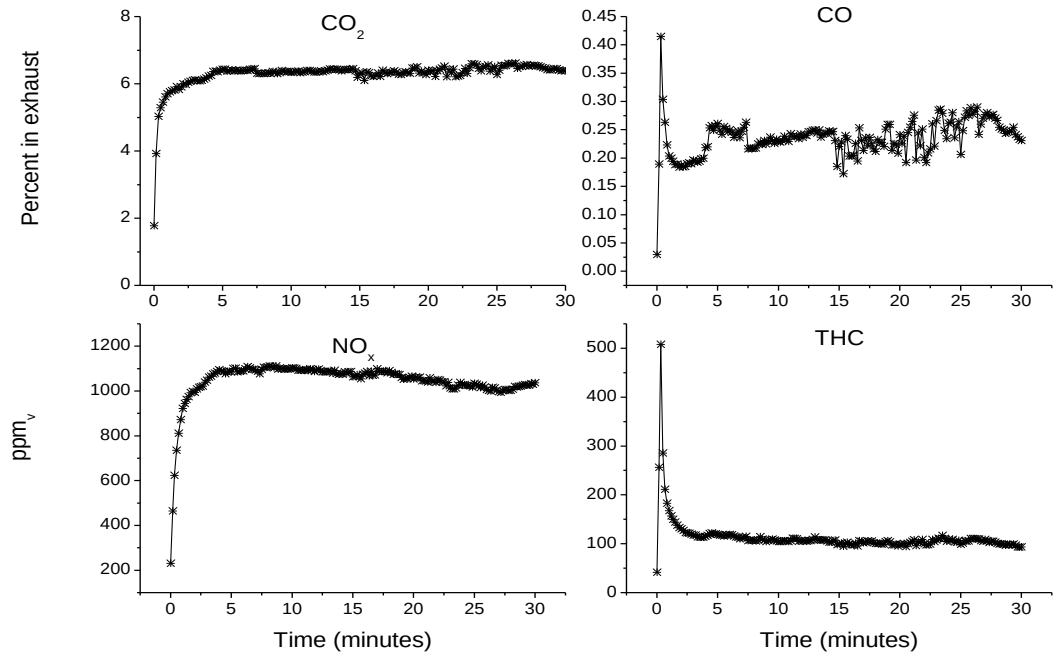

Figure 15: Exhaust emission profiles for CO_2, CO, NO_X and THC from B10 test in June, 2009

The Semtech analyzer collects data continuously during operation, with a time resolution of one second. For these experiments, the raw data output file was averaged

over 10s intervals to reduce the effects of random noise, creating 181 data points for each 30-minute load test. Figure 15 shows a typical emission profile for the four gas-phase pollutants monitored during the tests. Concentrations of all constituents displayed significantly greater variability during the initial portion of each test, as the engine and stack heated up. For this reason, analysis of the gas-phase emission results was broken into two portions. Transient-phase results were averaged over the first five minutes of operation, while steady-state results were taken from the remaining portion of the load test data (minutes 5-30), the steady-state was determined by the standard deviation of the exhaust temperature was less than five percent. For the most part, pollutant concentrations did not display any consistent increases or decreases during the steady-state portion of the test, except as described below for total hydrocarbons.

For both the transient and steady-state results, raw concentrations were converted to fuel specific mass emissions using the Semtech analytical software. This is accomplished by composing an overall carbon balance in the exhaust, which reflects the moles of fuel consumed per mole exhaust. The fuel MW is based on the C: H ratio, which we assumed to be 1.8 for the ULSD and 1.87 for the pure soy biodiesel, based on our measurements for the generator studies. This approach does not account for the oxygen content of the biodiesel fuel (approximately 10% by weight in the B100), which increases the overall molecular weight of the biodiesel relative to a standard diesel fuel with the same C:H ratio. The initial results were therefore adjusted to account for the actual molecular weight of the biodiesel fuel. This adjustment resulted in a 1% and 2% decrease in the reported fuel-specific emissions for the B10 and B20

fuels, respectively. Brake specific emissions (BSE) results were calculated from the fuel specific emission and the average fuel consumption and horsepower results over the 30 mins test for each run.

IV.3.1 Locomotive operation.

The operational tests with the B10 and B20 fuels were conducted from June 2009 to January, 2010. During this time, the maximum temperatures during the study period ranged from 28 to -5 °C, while the low temperatures ranged from 17 to -12 °C. No changes in the operation of the switching locomotive were noted during operation with B10 or B20. During the quarterly maintenance, fuel filters are routinely changed out. The filters used for the B10 and B20 tests did not show any additional clogging when removed after 90 days. The only maintenance performed on the locomotive, outside of the standard quarterly maintenance period, was replacement of the main generator and an electric motor in November, 2009, an event unrelated to biodiesel use.

IV.3.2 Brake specific fuel consumption (BSFC).

Due to the incorrectly fuel flow rate calibration on September 2009 test, only three test were compared for their BSFC. Figure 16 shows the BSFC emissions of the two test fuels during the static load tests on the same day. The average BSFC was somewhat higher on each day for the fuel containing a higher percentage of biodiesel. The greatest difference of the REG-9000 biodiesel, of 3.67%, was observed between the B0 and the B20 fuels tested in May, 2010. This is because biodiesel has around 9% lower heating value in volume than conventional diesel fuel (Lapuerta, et al.,

2008). In order to obtain the same engine power, the fuel consumption of biodiesel should be proportionally higher. For the September, 2009 tests, the fuel meters were incorrectly calibrated, so absolute fuel consumption values cannot be compared for all six tests, but the results also followed the same trend. Comparing the results from 20% of soybean and tallow biodiesels with the same day diesel results, soybean biodiesel has a higher BSFC because the heating value of the tallow biodiesel is slighter higher than that of soybean biodiesel. A t-test was used to compare the BSFC of the two fuels on the same day and the differences were not statistically significant. Overall, however, differences in measured fuel consumption between test days outweigh differences due to biodiesel content.

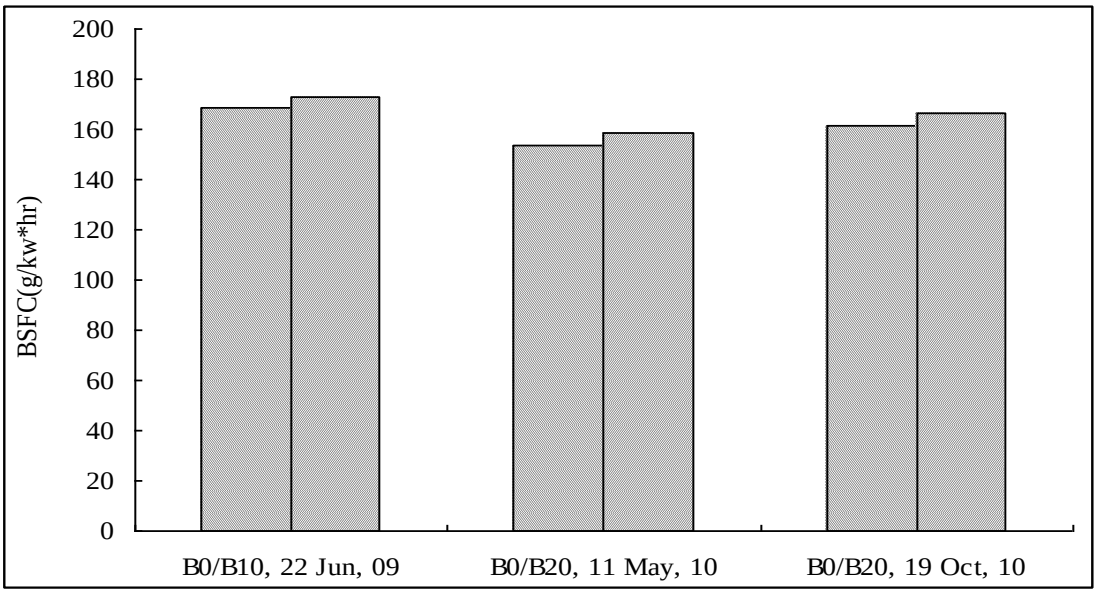

Figure 16: Same day brake specific fuel consumption for different fuel biodiesel levels.

IV.3.3 Emission results.

Table 16 presents the operating conditions and average concentration of measured constituents in the stack exhaust for each static load test. While biodiesel exhaust

temperatures are often slightly hotter than petroleum diesel, any differences in these tests were obscured by the large variations in ambient temperatures between test days. Differences between average emission values for the same fuel on different test dates were assessed using a two-tailed t-test and were found to be significant at the 95% confidence level. Thus, each test was treated as an independent data point for the subsequent analysis. NO comprised more than 95% of the total NO_X emissions during all tests, and trends in total NO_X emissions therefore mirrored those in NO. For this reason, only overall NO_X results are discussed in subsequent sections.

Table 16. Average raw emission results from all load tests

Date	6/22/09	6/22/09	9/24/09	9/24/09	5/11/10	5/11/10	10/19/10	10/19/10
Fuel	B0	B10	B10	B20	B20	B0	B0	B20
Humidity (%)	47.5	43.9	39.0	35.8	31.9	32.0	34	33
Ambient Temperature (° C)	33.6	38.2	20.4	28.0	17.6	16.0	21	22
Exhaust Temperature (° C)	519.3	524.3	486.6	465.8	398.3	403.7	436	431
CO_2 (%)	6.151	6.093	5.228	5.462	5.94	6.209	6.33	6.34
CO (%)	0.210	0.228	0.109	0.108	0.127	0.095	0.16	0.14
NO (ppm)	943	1006	909	1004	1102	981	1177.50	1234.97
NO_2 (ppm)	9.740	2.847	51.284	1.342	<1	6.82	27.40	46.27
NO_X (ppm)	952.62	1008.50	960.52	1004.88	1102	987.48	1204.90	1281.24
HC (ppm)	279.22	127.32	240.75	84.85	90.7	176.44	192.95	91.44
O_2 (%)	10.99	11.18	12.60	12.32	11.5	11.47	11.48	11.55

IV.3.3.1 Steady state emissions from REG-9000 biodiesel.

Steady-state CO_2 concentrations in the exhaust ranged from 52,000-63,400 ppm. While raw CO_2 concentrations were highest in the two ULSD tests, the fuel-weighted

emissions values showed no trend with increasing biodiesel content (Figure 17). Biodiesel is not typically expected to have a significant effect on CO_2 emission rates because exhaust CO_2 emissions are determined by fuel consumption. Rather, the impact of biodiesel use on net CO_2 emissions derives from the source of carbon in the exhaust (i.e., biological carbon versus fossil carbon). Determination of the net CO_2 emissions of a fuel requires a lifecycle emissions analysis that is beyond the scope of this work. However, the U.S. EPA has recently ruled that, based on their life cycle analysis, soybean oil and animal fat derived biodiesels will meet the EISA requirement of a life cycle greenhouse gas reduction of 50% compared to the baseline 2005 conventional petroleum diesel fuel (U.S. Environmental Protection Agency, 2010).

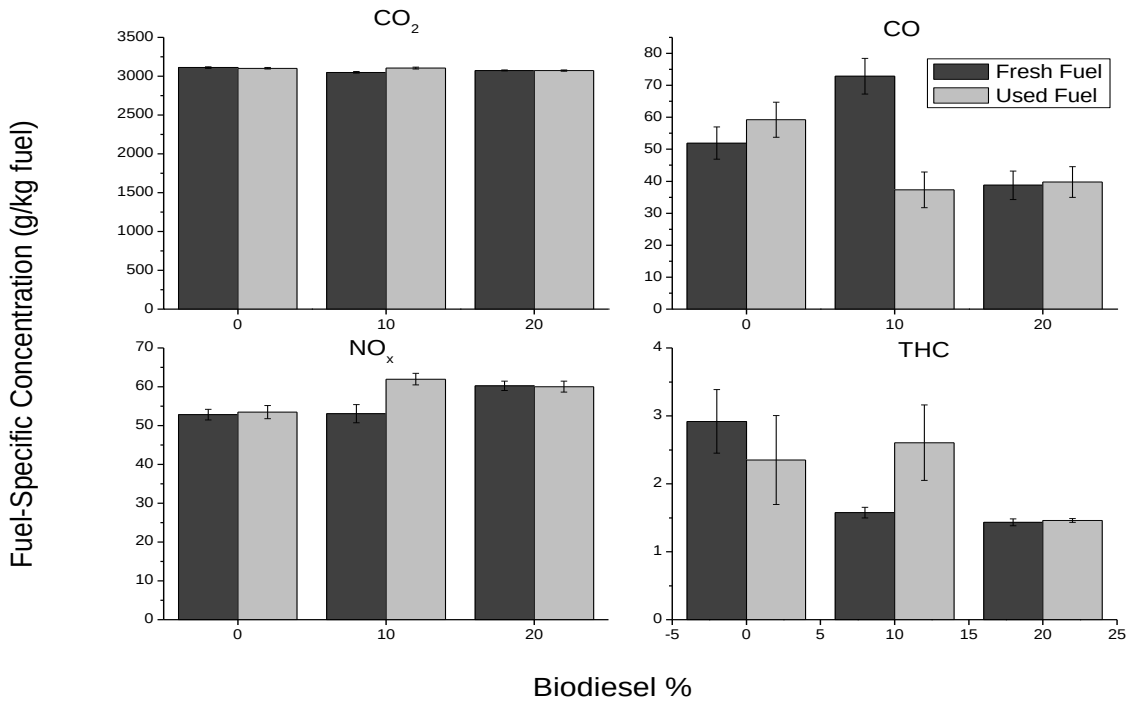

Figure 17: Average steady-state fuel-specific emissions of soybean biodiesel blends before and after the three months use. Error bars represent standard deviations around the average.

No consistent difference in pollutant emissions was observed between soybean biodiesel blends tested fresh and after use in the locomotive from June 2009 to May 2010. Both tests with the B20 fuels show increases in NO_X emissions compared to the base diesel fuel. The B10 results, however, are split, with the June, 2009 test showing no increase and the September test showing the same levels of NO_X emissions (on a fuel-specific basis) as the B20 data. The higher NO_X emission level corresponds to higher adiabatic flame temperature of the biodiesel, which is counter to most studies showing a relationship between increased NO_X production and higher combustion temperature. The chemistry of nitrogen oxide formation in the combustion chamber is a complicated, multi-step process that can be influenced by a number of engine variables. Overall, however, it appears that biodiesel addition may result in increased NO_X emission from this locomotive, although the extent is difficult to quantify due to the small number of data points and variation in the B10 data.

The results for incomplete combustion products (CO and THC) both showed lower fuel-specific emissions for the B20 blends than for the ULSD. This would suggest that biodiesel, which contains a higher proportion of straight-chain aliphatic molecules than most petroleum diesel, generally combusts more completely. However, the B10 results show the same type of internal variation observed for NO_X. The correspondence of higher CO values with lower NO_X in the June test would be consistent with a cooler combustion process, although, as mentioned above, it is not consistent with the measured exhaust temperatures from the two tests. Total hydrocarbon emissions, however, followed an opposite pattern, suggesting that a

different factor is at play.

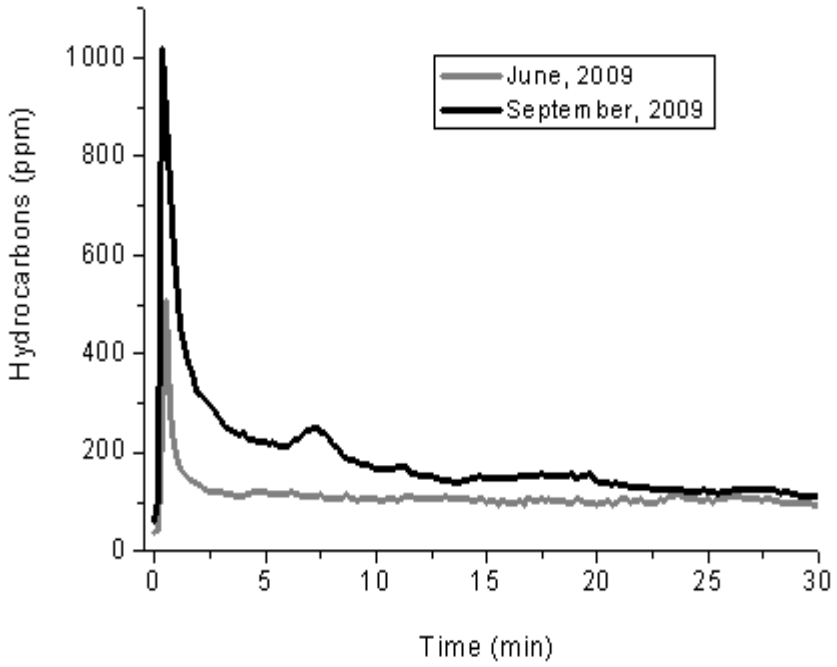

Figure 18: Time dependent total hydrocarbon data from the two B10 load tests.

Figure 18 shows the overall trend of hydrocarbon emissions during the two B10 load tests. While the steady-state results are relatively constant throughout the June test, the September data show both a higher average concentration and much greater variation throughout the test interval, in particular between five and 10 minutes. The September B10 test was the first of the day and was conducted under colder ambient conditions than the June tests. Unburned hydrocarbon emissions are typically greater under cold start conditions, and decrease as the combustion temperature increases. In the September load test, the data suggest that THC emissions did not reach a steady state condition, accounting for the higher overall emission rate. Based on concentrations from the latter part of the test, it appears that extending the test time would have resulted in THC emission levels similar to those for the June test. These

results suggest that hydrocarbon emissions are particularly sensitive to both ambient temperature conditions and the order of fuel testing. The lack of a similar effect in the B20 test from May, 2010, which was also the first test of the day, can be explained by the fact that this test had to be re-run due to difficulties with the emissions analyzer during the initial load test (see next section). As a result, the engine had already warmed up prior to the test.

IV.3.3.2 Transient state emissions from REG-9000 biodiesel.

Transient concentrations for CO_2 and NO_X (Figure 19) were very similar to the steady-state values, indicating a rapid approach to steady-state conditions. Both CO and THC experienced a spike in exhaust concentrations in the first two to three minutes of the test, followed by a steep decline. The duration and height of this spike depended not only on the type of fuel used but also on external conditions such as engine temperature. For the ULSD and B10 fuels, the variability in transient emissions was also generally higher for the used fuel than the fresh fuel tests. This difference is likely due to the fact that the used fuel tests were all cold starts, while the fresh fuel tests, as the second test of the day, were conducted on a warmer engine. For the May 2010 B20 test, a droplet of unburned fuel was collected by the emission probe, saturating the Semtech hydrocarbon detector for several minutes and also disrupting the collection of NO_X and CO emissions data. After a two minute idle period, the locomotive was retuned to full throttle for an additional 12 minutes to allow collection of steady-state data only.

These results suggest that pollutant emissions, and especially THC, will be

sensitive to multiple variables beyond the type of fuel used, including the length of time the locomotive is operated and ambient temperature conditions. Given the pattern of THC emissions observed here, the greatest benefit for THC reductions would likely be gained from biodiesel use in line-haul locomotives or other situations where the engine is operated for extended periods.

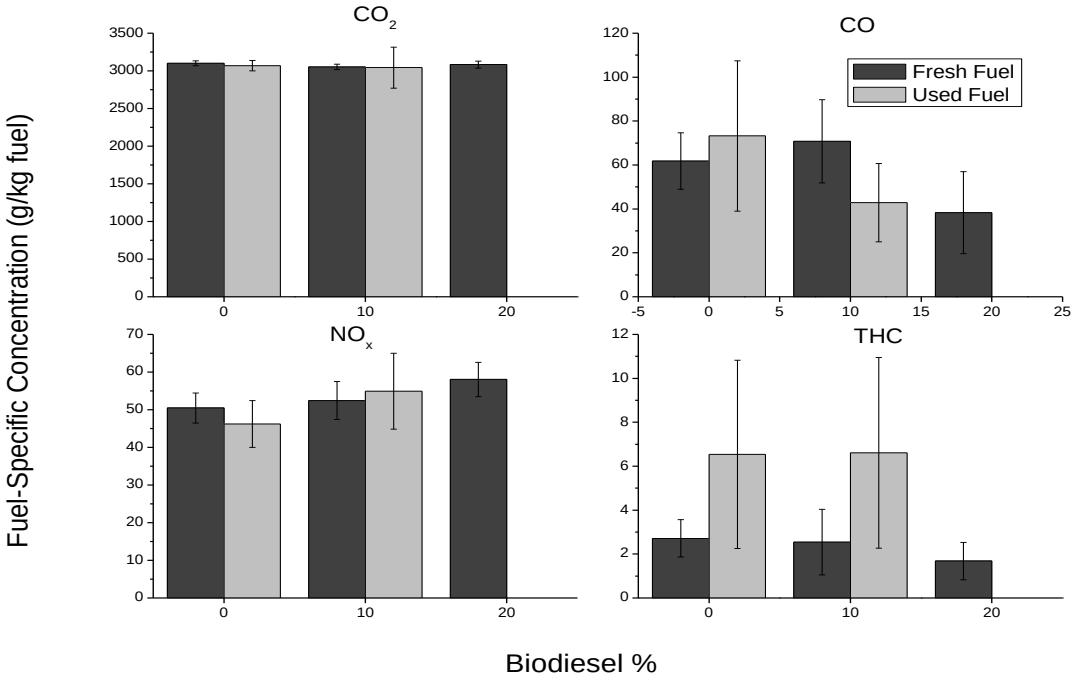

Figure 19: Average transient fuel-specific emissions soybean biodiesel blends before and after the three months use. Error bars represent standard deviations around the average.

IV.3.4 BSE results.

Emissions of all compounds were higher in the October, 2010 test than in the previous experiments (Table 16). The difference may be related to the fuel consumption or the cooler ambient conditions. Adding biodiesel to the ULSD slightly increased BSE CO_2 emissions on the same test date, but the results were not

statistically significant. THC was reduced by 31% when 10% biodiesel was used, and by 50% for both B20 blends. This is because biodiesel favors a more complete combustion as biodiesel has a higher adiabatic flame temperature. The CO emission results were in consistent during the three tests. B10 in 2009 had a higher CO emission due to the high viscosity of the soybean based biodiesel, which can cause poor spray characteristics, forming locally rich air-fuel mixtures during the combustion process leading to CO formation (Pugazhvadivu & Jeyachandran, 2005). When the biodiesel content increased to 20%, the CO emissions decreased for both biodiesels, likely due to the increased oxygen content. Correction factors available for locomotive diesel engines (Dodge, et al., 2003) were used to adjust our NO_X results for the effects of humidity by calculating a reference NO_X value for each test that was independent of ambient conditions. The emission of NO was significantly influenced by the in-cylinder gas temperature and availability of oxygen during combustion. Because of the peak pressures for biodiesel are higher than that for diesel, which is likely to result in a higher combustion temperature that promoted NO formation. With the corrections, NO increased with increasing biodiesel percentage for these two biodiesels, but it increased less for tallow biodiesel than soybean biodiesel. Tallow biodiesel has more saturated fatty acids than soybean biodiesel (Lapuerta, et al., 2008). All the BSE emissions were higher than the Tier 0 locomotive emissions standards (Table 2). However, the engine used, based on its original manufacture date, is not required to meet these emission standards.

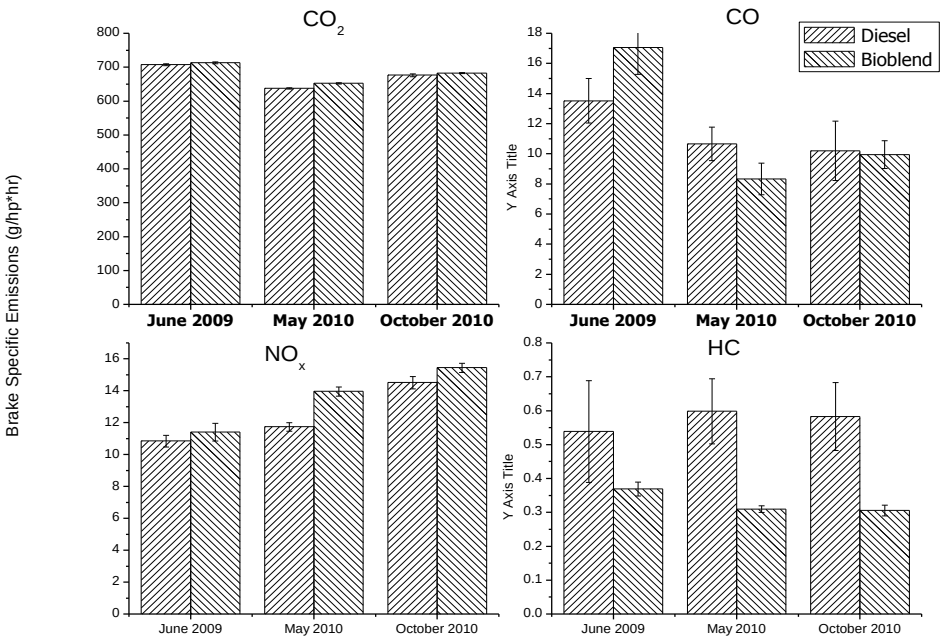

Figure 20. Brake fuel specific emissions. (Error bar indicate one standard deviation of the uncertainty)

IV.3.5 Smoke opacity measurement.

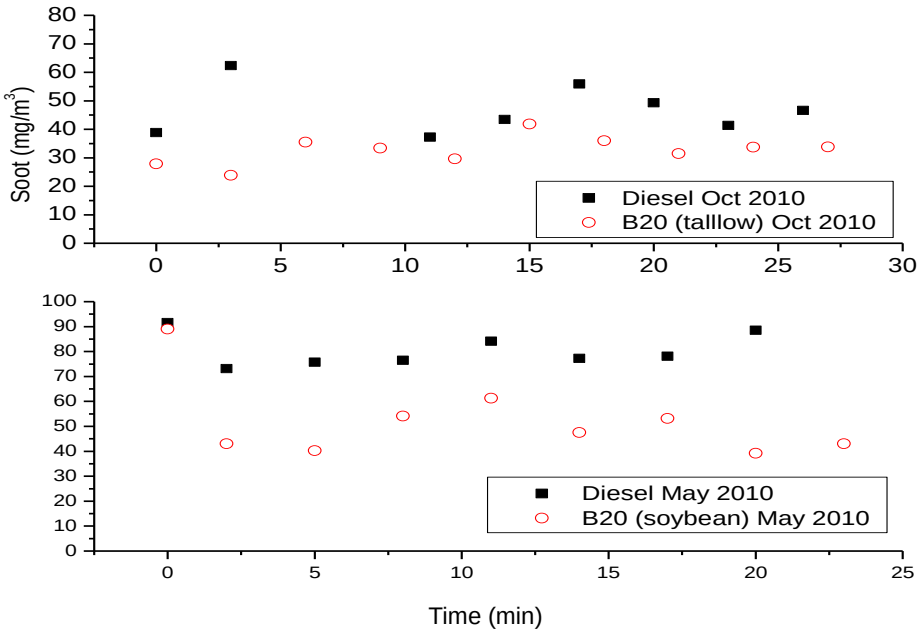

Figure 21. Instantaneous soot concentration data during the May and October, 2010 load tests.

Figure 21 shows the instantaneous soot emissions measured using ULSD and B20 fuels during the May (soy-based) and October (tallow-based), 2010 load tests. For both fuels in the May 2010 test date, soot concentrations were highest at the beginning of the load test and dropped sharply between three and five minutes. The drop was much more pronounced, however, for the B20 fuel. Average soot concentrations during the B20 load test were 52 $\pm$ 5 mg/m^3, compared to 81 $\pm$ 2 mg/m^3 with the ULSD fuel, a difference of 35%. It should be noted that the B20 test was performed first on this testing date, so factors that could increase the extent of combustion, including higher ambient and engine temperatures, would not have favored the B20 fuel. The instantaneous soot emissions measured using ULSD and B20 fuels during the October, 2010 load tests were both lower for the two fuel blends compared with the May tests. For the B20 fuel, average soot concentrations during the B20 load test were 33 $\pm$ 5 mg/m^3, compared to 47 $\pm$ 8 mg/m^3 with the ULSD fuel, a difference of 42%. The observed reduction in particulate emissions in both tests is consistent with the previous literature on biodiesel use, as the higher oxygen content in the biodiesel allows for more complete combustion and limits soot formation (Graboski & McCormick, 1998; Wang, et al., 2000).

IV.4 Conclusion

These tests show that up to B20 blends of soy based biodiesel can be used successfully for extended periods of time in currently-operating locomotives without engine modifications. Both the B10 and B20 blends caused no performance or maintenance issues for the GP38 locomotive under Iowa summer and winter

conditions. The 30-minute static load test results show that biodiesel blends may produce slightly higher BSFC, and more extensive tests are warranted to determine whether this effect is significant on a longer-time scale and under actual operating conditions. From an emission standpoint, the performance of the B10 and B20 fuels used here was in line with the conventional assessment of biodiesel fuels. The biodiesel blends produced lower amounts of combustion byproducts, including soot and total hydrocarbons, but slightly increased the amount of NO_X released. Thus, soy-based biodiesel could aid efforts to meet future regulatory limits for locomotive emissions in unmodified engines, with the probable exception of NO_X. Additional mechanisms for NO_X reductions with biodiesel, such as biodiesel production from other alternative feedstocks, such as beef tallow, and engine injection-timing modifications, should be explored in future studies.

The limited number of tests conducted in this study did not allow for a full assessment of the effects of all relevant variables, such as ambient temperature conditions, on exhaust emissions. Total hydrocarbon emissions, in particular, appear to be strongly sensitive to engine temperature, and possibly to fuel temperature as well. More extensive testing under a broader range of conditions, such as winter operation and different throttle settings, is recommended to obtain a more complete picture of biodiesel effects on locomotive emissions. Additional testing with a greater variety of engine types is also recommended, as engine design parameters could affect the production of NO_X and partial combustion products. The fuel properties of both the ULSD and biodiesel, such as, oxygen content, viscosity and cetane number, all

had effects on the diesel emissions. Based on the results presented here, the use of biodiesel could effectively help meet requirements for increased use of renewable transportation fuels in the railroad industry, so a more complete picture of its effects on exhaust emissions and air quality is highly desirable for planning and regulatory purposes.

Chapter V.

LA-ICP-MS Trace Metal Determination in Particulate Matter

Atmospheric particulate matter can have an adverse impact on human health, including causing or worsening respiratory, cardiovascular, infectious and allergic diseases (Mulawa, et al., 1997). The composition and size of these particles greatly determines their negative health and environmental effects. At a given mass, ultrafine particles (diameter < 0.1 μm) have 10^2 to 10^3 times more surface area than particles with diameters in the 0.1-2.5μm range and approximately 10^5 times more surface area than coarse particles (2.5 to 10μm) (Harrison et al., 2000). Ultrafine particles pose higher health risks due to the increased surface-mass ratio associated with smaller particle size as well as their ability to efficiently reach the alveolar region of the lungs (Lin et al., 2005).

The diesel engine is a major source for air particulates in urban areas. It is very important to accurately characterize the chemical composition of the particles emitted from internal combustion engines. Both the chemical composition and the particle size have adverse effects on the human health. A major factor in the health related impact of these particulates is the emission of heavy metals present in the fuel caused by diesel engines. (Birmili et al., 2006; Weckwerth, 2001). Trace metals significantly contribute to adverse health effects associated with the inhalation of particulate matter. The Hazardous Air Pollutant (HAP) inventory lists the following hazardous metal elements commonly found in airborne particulates: As, Cd, Co, Cr, Hg, Mn, Ni, Pb, Sb and Se. All can have significant health effects. Exposure to Mn and Fe have

been linked to Parkinsons; Cr has been linked to increased cancer risk; Pb has been linked to adverse effects in the nervous system; and Ba may lead to paralysis (Chillrud, et al., 2005; Department of Health and Human Services, 2007). Zn, Cu and Fe may release free radicals in lung fluid through Fenton's reactions, causing cellular inflammation that leads to both acute and chronic lung injuries (Donaldson, et al., 1997; Valavanidis et al., 2000). Besides these allergic reactions, other metals (As, Cd and Hg) are known or suspected carcinogens (Weckwerth, 2001).

Diesel particulate size distribution and trace element composition are greatly affected by a number of factors, including fuel source. Sharma et al. (2005) used a mid-size direct injection Mahindra DI-2500 diesel engine to test the metal content at four different engine loadings. They found that both particulate mass and metal content gradually decreased when the load increased from idle to full load. The metal content in the particulates was correlated with that in diesel fuel. The concentrations of commonly occurring metals (Fe, Mg, Ca) were much higher than those of Cr, Ni, Pb, Zn, Ba and Cd (anthropogenic elements). Dwivedi et al (2006) compared the particulate emission characteristics between biodiesel and diesel by using a medium duty transport diesel engine. Results showed that B20 fuel had a lower particulate mass emission than fossil diesel. Cd, Pb, Na, and Ni were also lower in biodiesel particulate. However, Fe, Cr, Ni, Zn and Mg were higher in B20 exhaust. Wang et al. (2003) evaluated the metal contents of fuel emissions from a non-catalyst turbo-charged diesel engine using the U.S. transient cycle. The top four anthropogenic elements were Zn, Cr, Mo and Ti. The metal content was almost entirely from the

consumption of diesel fuel and increased with increasing engine speed. Lubricant oil could also play an important role in emission of metal contents in engine exhaust, particularly for Ca and Zn. Weckwerth et al. (2001) verified traffic emitted metal components in the ambient air of Cologne, Germany. It was found that the relative abundance of Zn, Mo, Cu and Sb comprised an average of approximately 30% of diesel soot in the fine fraction.

Trace metals in soot and atmospheric particles have commonly been measured by pretreating particles with acid digestion and analyzing the resulting solution using inductively coupled plasma mass spectroscopy (ICP-MS) or graphite furnace atomic absorption spectrometry (GF-AAS). ICP-MS techniques have been largely promoted in recent decades for their rapid and reliable measurements in complex matrices for most elements at g/L to ng/L levels (Lamaison et al., 2009). A number of different digestion agents (e.g., HNO_3, HCl, HF, H_3BO_3 and H_2O_2) at various concentrations have been used to release metal elements from particulate matter prior to analysis (Kulkarni et al., 2007). Total solubilization using a mixture of HNO_3 and HF is generally preferred as it allows the complete digestion of silicon-containing compounds. This procedure may require large sample size, use hazardous reagents, primarily hydrofluoric acid (HF), and risks contamination by reagent impurities and loss of elements through volatilization. Dilution factors may also limit effective limits of metal determination. Metals only constitute an extremely small fraction of total diesel particulate, and only a small $PM_{2.5}$ mass fraction is collected. Digestion

methods may therefore have trouble reaching high sensitivity in trace metal analysis for diesel particulates.

Additional problems with metal analysis can arise due to digestion procedures. In ICP-MS, the formation of polyatomic interferences arising from the plasma gas and the sample matrices is observed especially at masses below 80 (Birmili, et al., 2006; Espinosa et al., 2001; Lüdke et al., 1994). Many of the serious polyatomic ion interferences are only present because of the presence of water and addition of H, O, N, Cl or S from the acids used for dissolution (Jarvis et al., 1995). Different approaches have been employed to reduce these interferences, including separation by electro-thermal volatilization, laser ablation, cold plasma, pre-concentration, solvent or matrix removal, sector-field ICP-MS, and dynamic reaction cell (Jakubowski et al., 1998). The direct analysis of solids can provide equivalent information about elemental composition, and may reduce or eliminate some of the problems associated with solution introduction.

In this experiment, a new method, laser ablation inductively coupled plasma mass spectroscopy (LA-ICP-MS), was used to analyze the metal content in diesel exhaust particulates as a function of particulate size. LA-ICP-MS is one of the most sensitive measuring methods for solid samples. It uses high energy UV or IR photons emitted by a laser to generate fine dense aerosols that are transported by an auxiliary gas stream to an ICP-MS. The primary advantage of the laser ablation method is that it can provide improved detection limits for trace metals without sample pre-treatment. Other advantages are that it enables a multi-elemental analysis with only a little

amount of sample (Ito et al., 2009). Due to these advantages, LA-ICP-MS has been successfully applied in the geochemical analysis of solid samples.

Since the introduction of the first commercial LA-ICP-MS, there have been relatively few publications dealing with air-born particulates, and diesel particles. The coupling of size-segregated sampling techniques and chemical speciation analysis thus constitutes a step forward in the sound identification of trace metals in different size fractions. In this chapter, biodiesel produced from waste cooking oil by the KU Biodiesel Initiative and No.2 diesel were used to power a Yanmar diesel generator. Emitted particulate matter was collected using a Dekati Impactor to separate particulates based on size. The focus of this chapter is on comparative characterization of the metal loading in particulates from these two fuels by the ICP-LA-MS method.

V.1 Sampling Method

The sampling system for particles (Figure 22) consisted of a particle impactor PM_{10} Model supplied by Dekati (Tampere, Finland), equipped with polycarbonate filters with diameters of 25mm. The impactor was powered by a vacuum pump supplied by Vacuumbran (Wertheim, Germany) The Impactor separates the particulate matter into 13 stages (at 50% efficiency) with the following equivalent cutoff diameters (in microns): 0.030-0.060, 0.060-0.108, 0.108-0.17, 0.17-0.26, 0.26-0.40, 0.40-0.65, 0.65-1.0, 1.0-1.6, 1.6-2.5, 2.5-4.4, 4.4-6.8, and 6.8-10 μm. A final filter collects all remaining particulate matter. The sampling flow rate of the Impactor was 10L/min, which was calibrated before each test. Particulate matter

emissions were collected by connecting the Impactor sampling line to the generator exhaust pipe without dilution. Sampling lasted for 2 hours after the engine warm-up that was determined by the maximum particulate matter yield. The generator specifications were described in Chapter 3.

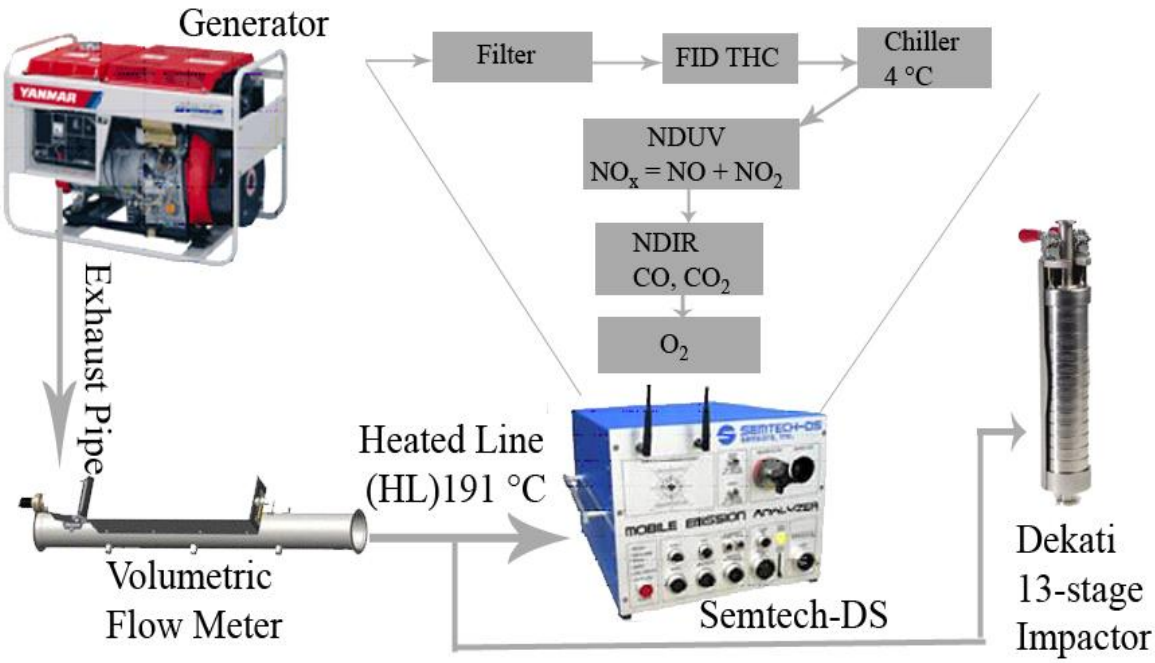

Figure 22: Configuration of Impactor and Semtech setup

The first and second sampling periods were executed during July 2009 and 2010, respectively, at zero and 25% loading. The tests were done in the KU engine test cell, so the temperature and relative humidity remained relatively constant. The aluminum foil or polycarbonate filters were precoated with silicone grease to minimize particle bounce between the different stages of the Impactor during the sampling. The particle mass was determined by gravimetry. Filters were conditioned for 24h at a constant temperature of 25ºC and a relative humidity of 40% prior to being weighed on an electronic microbalance before and after sampling. Field blank samples also were

collected by loading filters into the sampler but prohibiting the flow of exhaust through the filter.

V.2 Test Fuel

The KU Biodiesel Initiative produces biodiesel from a variety of used vegetable oil feedstocks in an on-campus batch facility. Oil is acquired from dining facilities on campus and transported to the processing laboratory, where biodiesel is made by conversion of the triglyceride fats to esters via transesterfication. After the production step the fuel undergoes quality testing to determine fuel properties as defined under ASTM D6751. No. 2 diesel was purchased from the university's Facilities and Operations Department. The physical properties of these two fuels are listed in Table 17.

Table 17: Fuel properties of biodiesel and No. 2 diesel

Fuel type	H: C	Oxygen (% wt)	Density (g/L)	Flash point (°C)	Viscosity (@40°C)
B100	1.87	10.5	881	158	4.99 cST/s
B0 (# 2 diesel)	1.80	0	825	23	2.17 cST/s

V.3 ICP-MS Method

Acid digestion was used to release metal elements from particulate matter prior to ICP-MS analysis in a manner common to existing procedures. The same size particles collected from six experiments using polycarbonate filters were combined in order to get enough sample size. Filter sections of 10 cm^2 in area were transferred into a clean Digi Tube plastic digestion tube, and 10 mL of inverse aqua regia digestion solution (18.9% v/v trace metal grade HCl, 6.6% v/v trace metal grade HNO_3, 74.5% v/v

deionized water) was added into the tube and then vibrated for 10 minutes by using a vortex mixer to guarantee thorough mixing. The acidified sample was heated to 65ºC with a Digi PREP MS heating block (SCP Science) for one hour. The operational temperature was then increased to 95ºC for 4 hours to ensure the complete digestion of particles collected on the filters. Finally, the digested sample was filtered and diluted with high purity Milli-Q water to produce a solution with 2-5% acid content. All acid digestion samples were transferred to clean centrifuge tubes to be analyzed. To minimize contamination, all digestion tubes and vessels were cleaned before use by soaking in an 8N nitric acid bath for at least 24 h, followed by thorough rinsing with high-purity water. In addition to samples and field blanks, lab control blanks were prepared and analyzed. All sample concentrations were corrected for their respective field and lab control blank concentrations.

Trace metal concentrations in the acid-digested samples were determined using a VG PQII+XS model ICP-MS (Waltham, MA) in peak-jumping mode with ion lenses tuned for maximum sensitivity using ^{115}In (Beary & Paulsen, 1993). The isotopes monitored as proxies for total elemental concentration are ^{51}V, ^{59}Co, ^{60}Ni, ^{65}Cu, ^{66}Zn, ^{88}Sr, ^{95}Mo, ^{114}Cd, ^{120}Sn, ^{121}Sb, ^{138}Ba, ^{182}W, ^{208}Pb and ^{238}U. Details on instrumental operating condition are given in Table 18. Calibration standards were prepared by dilution of certified multi-element standards (Spex Certiprep) to 1, 10 and 100 ppb using DI water and distilled nitric acid, to a final acid concentration of 2% by volume. A 10 ppb standard solution was analyzed at regular intervals to adjust for instrument drift.

Table 18: Instrumental operating condition and measurement parameters for ICP-MS

Parameters	
Forward RF power	1.35kW
Reflected RF power	0-3 watts
Frequency	40MHz
Spry Chamber	Scott double pass spray chamber with extra cooling jacket
Nebuliser	Microflow
Coolant gas flow	13.8 min^{-1} Argon
Carrier gas flow	1.1 min^{-1} Argon
Auxiliary gas flow	0.8 min^{-1} Argon
Sampling cone	1mm orifice
Skimmer cone	0.7mm orifice
Ions lens setting	Adjusted to obtain maximum signal intensity
Acquisition mode	Pulse jumping
Total measurement points/peak	3

V.4 LA-ICP-MS Method

A VG PQII+XS Model ICP-MS (inductively-coupled plasma mass spectrometer) with a laser ablation microprobe (LA: Merchanteck LUV266X Laser Ablation Station) was used to analyze the metal content on the filters having the most particles, which were the stages of 0.030-0.060, 0.060-0.108, 0.108-0.17, 0.17-0.26, 0.26-0.40, and 0.40-0.65μm.

It is difficult to analyze powder samples for LA-ICP-MS because the powder may explode during the ablation process, which may cause an unstable MS signal and

possibly damage the equipment. There are two methods to increase the hardiness of the powder samples. One is to fuse the sample with lithium borate flux by heating the sample to over 1000 °C (Eggins, 2003; Spandler et al., 2007). Certain elements may be selectively volatilized in this way. The other method is to make a pellet by compressing the powder (Stokes et al., 2003). For the particulate samples in this experiment, the first method will destroy the sample, and there are not enough particles to make the pellet. Since neither method will work for these samples, the filters were directly mounted to the sample holder to be analyzed by LA-ICP-MS.

The LA system uses a frequency-quadrupled (266nm) Nd:YAG laser; blanks were measured to correct the sample ion intensities for background signal. It is essential that the ICP-MS instrument be correctly optimized in order to achieve accurate and precise analysis. The LA-ICP-MS was tuned using ^{139}La in National Institute of Standards and Technology Standard Reference Material (NIST SRM) 610, which contains trace metals in alumino-silicate glass. Thirty metal isotopes that have the least interference and highest abundance were selected for analyses. The element menu is shown in Appendix F. Average concentrations were obtained by moving the sample underneath the laser beam over four lines randomly distributed on the particle area. The scan speed was 7μm/s; a laser line with a width of 50 μm was produced at an energy density of 3.1 or 5 J/cm^2 using a repetition rate of 4 Hz for samples, or 4.5 J/cm^2 using a repetition rate of 10 Hz for calibration standards and reference samples. The typical operating parameters are listed in Table 19. Each analysis includes approximately 60 seconds of background acquisition (gas blank with laser on but

blocked from ablating the sample) and 60 seconds of data acquisition from ablation of samples. All analyses were processed using CONVERT and LAMTRACE software with calculations following published methods (Longerich et al., 1996).

Table 19: Operating conditions and data collection for the LA-ICP-MS

ICP-MS conditions	
Forward RF power	1.35kW
Reflected RF power	0-3 watts
Carrier Gas	Argon
Coolant gas flow	13.8 min^{-1} Argon
Carrier gas flow	1.1 L min^{-1} Argon
Auxiliary gas flow	0.8 min^{-1} Argon
Sampling cone	1mm orifice
Skimmer cone	0.7mm orifice
Laser operating parameters	
Laser type	Nd:YAG
Fundamental wavelength	1064 nm
Operating wavelength	266 nm
Laser mode	pulsed
Maximum output	4 mJ
Data collection parameters	
Site pattern for each analysis	Line
Ablation diameter	50μm
Laser energy	0.21 or 0.39 mJ per pulse
Repetition rate	4 Hz for sample; 10Hz for standards
Scan speed	7μm/s
Data process software	CONVERT and LAMTRACE
Number sweeps averaged	3 sweeps

In LA-ICP-MS, the sensitivity from one analysis to another may vary considerably between samples and within a single sample due to the removal and transport of different masses of material during each analysis. Elemental particle analysis used NIST SRM 1648 (urban particulate matter) for calibration and JA-1 (The Geological Survey of Japan andesite) to verify method accuracy (Appendix G). These standards most closely match the concentration range and matrix of the trace metals collected in the diesel particulates. Both reference standard powders were pressed with powdered Teflon to make a pellet, which was used to estimate the analytical reproducibility and to validate the whole analytical procedure. Every 12 samples were followed by two analyses of JA-1 and NIST SRM1648 in order to correct the time-dependent drift of sensitivity and mass discrimination.

In the initial experiments, ^{66}Zn was selected to compensate for differential sampling because it was present in all the samples analyzed as well as the calibration and reference standards. The total Zn concentration in each stage was independently determined by acid digestion followed by ICP-MS analysis. However, there were questions about the accuracy and reproducibility of this extraction-determined concentration.

To address these issues, ^{13}C was selected as the internal standard for the second run. A CM 5015 CO_2 Coulometer (UIC, Inc) was used to determine the total carbon content in the diesel and biodiesel sample using direct combustion (UIC Inc., 2008). Particulate matter was initially weighed into a platinum or porcelain “boat”. The boat was then placed into a quartz ladle that was introduced into a high temperature

oxygen atmosphere (typically 950 C) within the sample combustion zone. In that environment, all carbon within the sample is rapidly oxidized to CO_2. The resulting carbon dioxide is then swept into CM5015 CO_2 Coulometer where it is automatically measured using absolute coulometric titration. Interfering reaction products (including sulfur oxides, halides, water and nitrous oxides) were removed by the post-combustion scrubbers. This method achieves more complete removal of the measured element, and provides better sensitivity, as carbon account for up to 70% of the particulate matter.

V.5 Results and Discussion

V.5.1 Filter selection.

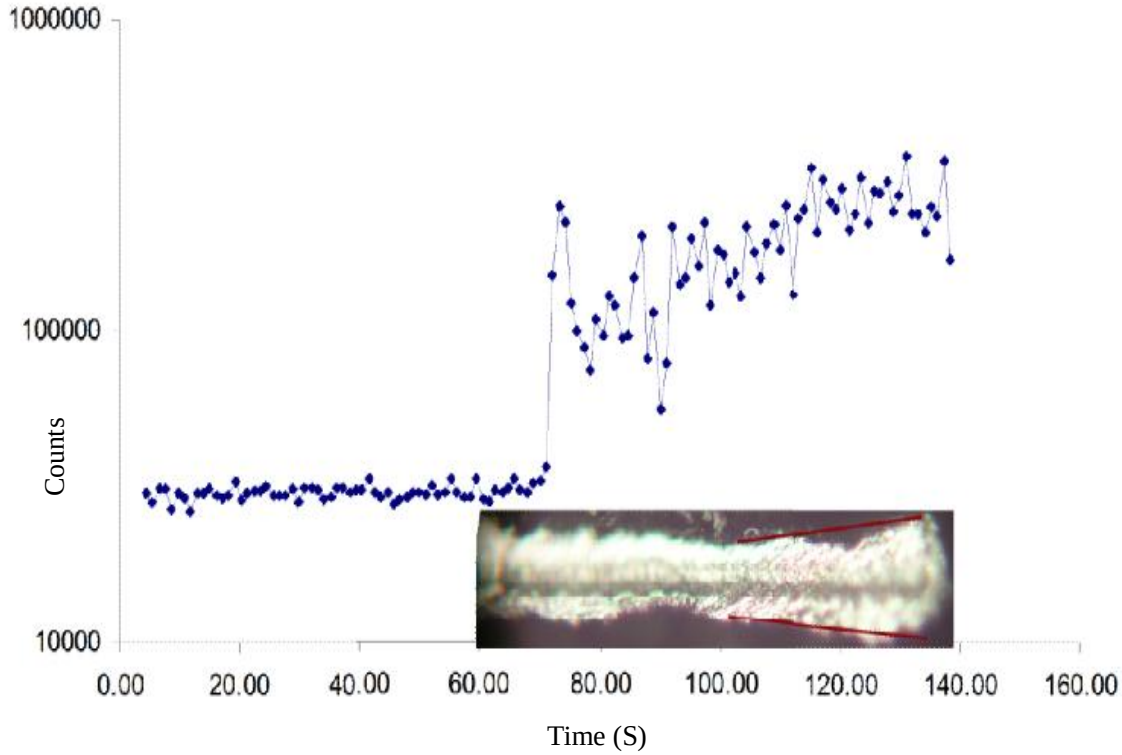

Figure 23: Aluminum counts with depth penetration of laser ablation

To begin the analysis, it is necessary to select the most appropriate support to trap the diesel particulates in the Impactor. In initial experiments, aluminum foil filters

were chosen for the substrate, but these did not show satisfying results during LA-ICP-MS analysis because of the high aluminum concentration and the high degree of absorption of laser radiation by the aluminum foil filter (Figure 23 and 24). Polycarbonate filters with low trace element contents were selected for further experiments.

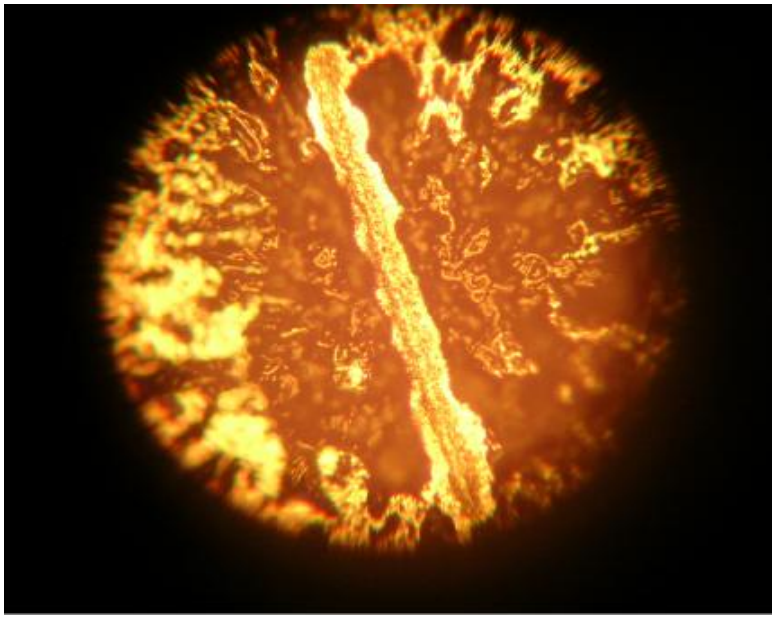

Figure 24: Photomicrograph of laser penetration on aluminum foil filter

V.5.2 Particle size and mass distribution at two different diesel engine loadings.

The majority of particles emitted from the generator were < 1 μm in size. In a test experiment, the smallest six size fractions (0.03 to 0.4 μm nominal diameter) accounted for 91% and 96% of the total No 2 diesel and biodiesel particulate mass, respectively, at zero engine loading (Figure 25, Table 20). These six fractions were therefore chosen for analysis by the LA-ICP-MS system. Overall, the particulate mass in the exhaust from the waste cooking-oil biodiesel (B100) was 34% higher than from the No. 2 diesel. Idle is very rough for the single cylinder engine. This result is

inconsistent with the general trends described previously, although few of those results were from small stationary engines such as this generator. When the engine load increased to 25%, the smallest six size fractions (0.03 to 0.4 μm nominal diameters) accounted for 87% and 93% of the total No 2 diesel and biodiesel particulate mass respectively. Overall, the particulate mass in the exhaust from the waste cooking-oil biodiesel was 20% lower than from the No. 2 diesel at 25% load. Because the emission concentrations of particulate matter from diesel engines are inversely related to the specified engine speeds, the higher driving speed will relate to higher fractions of metal elements in diesel particles. Compared to diesel particles, the large particulate matter mass decreased and the small particulate matter mass increased when biodiesel was used.

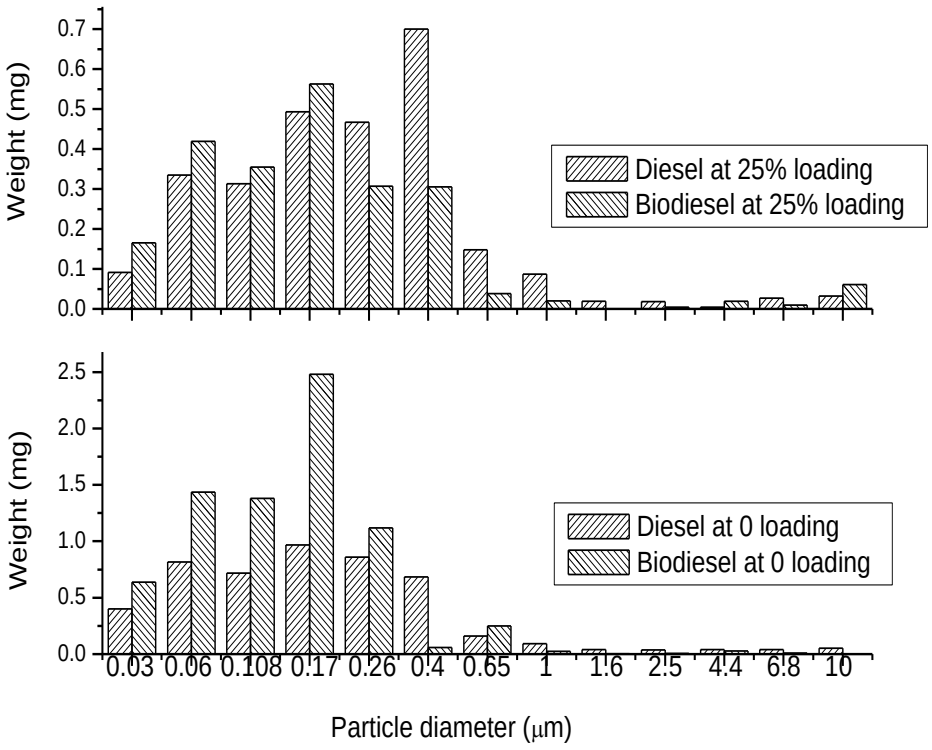

Figure 25: Size distribution of the total diesel and biodiesel particles for zero loading

Table 20. The mass of ultra-fine, fine, and coarse fraction of diesel and biodiesel particulates.

Cut size (μm)	0 loading		25% loading	
	Diesel (mg)	Biodiesel (mg)	Diesel (mg)	Biodiesel (mg)
$PM_{1.0}$	4.698	7.381	2.634	2.172
$PM_{2.5}$	4.775	7.39	2.671	2.176
PM_{10}	4.905	7.426	2.734	2.266

V.5.3 Internal standard determination.

For LA-ICP-MS analysis, the absolute amount of material ablated during each run varies from one sample to another due to the differences in the sample matrix and the related absorption behavior of the wavelength used for the ablation; therefore internal correction is crucial to obtain accurate data (Hemmerlin & Mermet, 1996; Longerich, et al., 1996). The element selected for this correction must be present either at a constant concentration or at a known concentration in each sample and calibrations standard prior to the LA-ICP-MS analysis.

The acid digestion method was used to determine the internal standard concentrations for the LA-ICP-MS analysis. To obtain a sufficient quantity of particulate material for this analysis, filters of each size fraction from four separate tests were combined, cut into small pieces, and extracted with inverse *aqua regia* as described above. The resulting solution was diluted before analysis to produce a solution with 2% acid content.

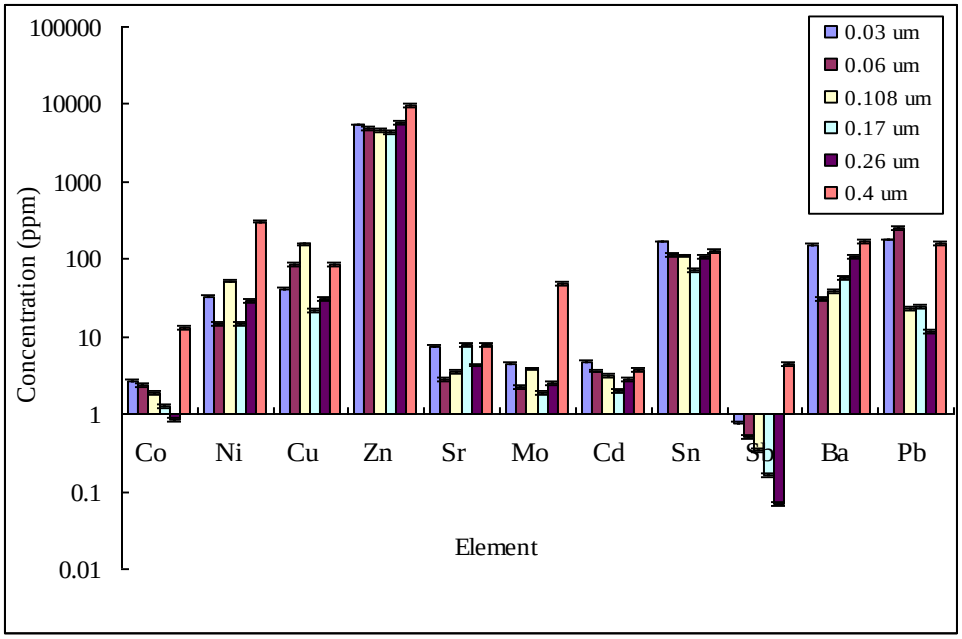

Figure 26: The metal content in diesel samples (Error bar indicate one standard deviation of the uncertainty)

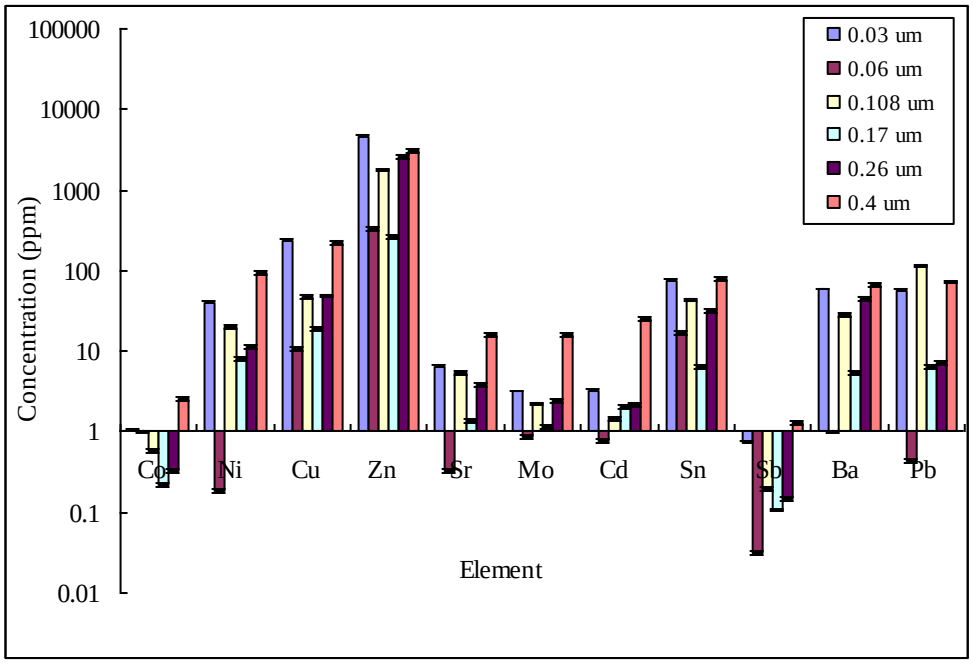

Figure 27: The metal content in biodiesel samples (Error bar indicate one standard deviation of the uncertainty)

The detection limits were calculated to be two times the absolute value of the relative standard deviation of the blanks times the absolute value of the y-intercept of

the calibration curve (Corley, 2002; Woods & Fryer, 2007). The values are showed in Appendix H. The recovery rates of the standards are in the range of 89%-115%.

Figure 26 and 27 show the common metals existing in both diesel and biodiesel particulates, which are Co, Ni, Cu, Zn, Sr, Mo, Cd, Sn, Sb, Ba and Pb. Zn was the most abundant metal present in both diesel and biodiesel samples at different size ranges, so Zn was chosen as the internal standard. The internal standard concentrations are listed in Table 21 and Appendix I.

Table 21. Zn concentration for different size particles

Particle size (μm)	Biodiesel Zn (ppm)	Diesel Zn (ppm)
Dp<0.03 μm	4529	5325
Dp<0.06 μm	337	4968
Dp<0.108 μm	1778	1312
Dp<0.17 μm	259	4579
Dp<0.26 μm	2624	5889
Dp<0.40 μm	3109	9777

Table 22. ^{13}C concentration for different samples

Sample	**^{13}C(ppm)**
NIST 1648	4312
Biodiesel	9350
Diesel	9020

Since the siliceous fraction in the PM cannot be fully extracted by this acid digestion, Zn concentration in the extract may not represent the total Zn in the particles, and so may not be the optimum internal standard. Depending on the engine type and driving cycle, diesel engines emit PM with 53 to 78% total carbon (Shah et

al., 2004). ^{13}C was selected as the internal standard since it is prevalent in diesel and biodiesel particles (Hanć et al., 2011; Marshall et al., 1991). The internal standards in the laser samples were determined by combining the residue particles from the previous laser run and analyzing for the total carbon content. The internal standards concentrations are listed in Table 22.

V.5.4 Metal content when Zn used as the internal standard using LA-ICP-MS method.

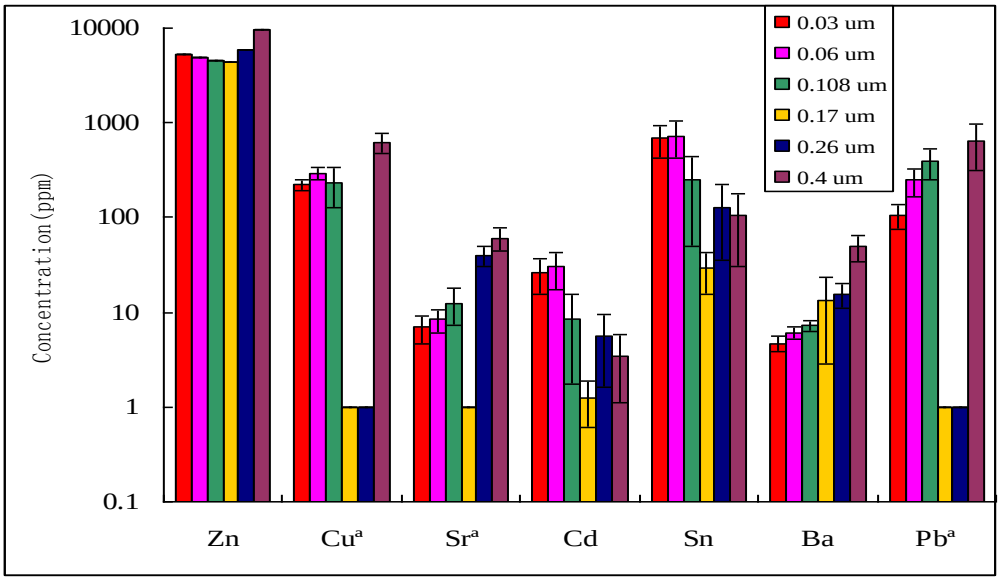

Figure 28: Average metal concentrations (n=4) in ultra-fine particle fractions in diesel particulates. * indicates that concentrations in some size fractions are below the detection limits of 3, 0.2 and 5 μg/g for Cu, Sr and Pb, respectively. (Error bar indicate one standard deviation of the uncertainty)

Figures 28 and 29 show the concentrations of the most common metals found in the particulate exhaust from the two fuels. If a concentration was below the low detection limit (LLD), then half of that value was used in the calculation of averages (Gleit, 1985). In both sets of samples, zinc was by far the most common trace metal

present. In samples of both fuels sent to a commercial lab for trace element analysis, Zn was the only compound present at detectable levels (> 1 μg/g fuel), with 2.4 μg/g in the No. 2 diesel. It was below detection limit in the biodiesel. The No. 2 diesel samples contained a wider range of trace metal elements, with zinc, barium, tin and cadmium present in all six size fractions and copper, lead and strontium present in four or more size fractions at detectable concentrations. These results are consistent with previous studies of diesel particulates (Espinosa, et al., 2001; Lough et al., 2005). By contrast, the biodiesel particles contained detectable concentrations of only two elements, zinc and barium. Zn may be introduced to the biodiesel through the production process. The batch reactors used by the KU Biodiesel Initiative contain a number of brass fittings. Most biodiesels are not compatible with brass, and Zn may have leached from these fittings during fuel production.

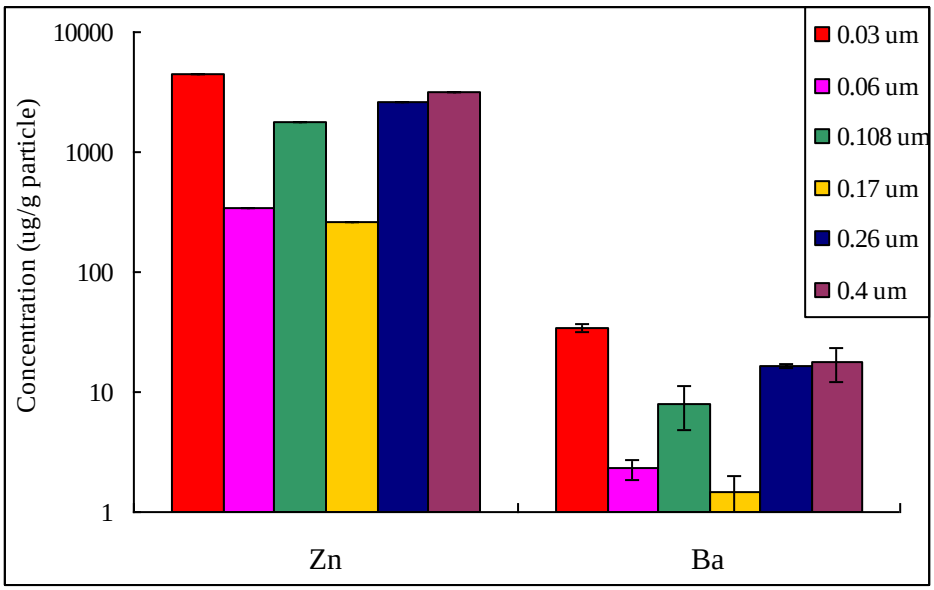

Figure 29: Average metal concentrations (n=4) in ultra-fine particle fractions in biodiesel particulates. (Error bar indicate one standard deviation of the uncertainty)

Zn concentrations in the diesel particulates are relatively consistent in the five smaller size fractions (Figure 30), at 4500-6000 μg/g, but increase to 9777 μg/g in the 0.4 μm particles. Strontium and barium showed a generally increasing trend with increasing particle size, while Cd and Sn displayed the opposite effect. Cu and Pb had wide variations in concentration, with some stages > 100 μg/g and other stages below the detection limits of 3 and 5 μg/g, respectively. For the biodiesel samples, Zn and Ba both showed more variation with particle size (Figure 31), but with no consistent pattern. For Pb and Cu, detection limits in these stages were 40 and 23 μg/g, respectively, while for the other metals present in diesel, they ranged from 3-5 μg/g. For the other stages, detection limits were ~5 times lower, similar to the detection limits in the diesel samples. As none of the other four metals were detected in any of the 6 biodiesel samples, it is unlikely that this increased detection limit had a significant effect on the reported results.

The concentration data determined from the ablation studies (or for Zn, from the acid-digestions) were combined with the total mass of particulates in each stage to determine the total mass of each metal in the < 0.4 μm particles. For metals not detected in a given sample, half of the detection limit was used instead. As shown in Table 23, the estimated total metal loading is lower in the biodiesel particulates for all elements, despite the greater total particulate mass collected in the biodiesel experiments. Based on these results, it appears that the use of biodiesel fuel in this type of engine should result in a lower total metal exposure due to particulate inhalation.

Table 23: Total metal content in ultrafine particles (in μg)

	Zn	**Ba**	**Sr**[a]	**Cu**[a]	**Cd**[a]	**Sn**[a]	**Pb**[a]
Diesel	26	0.072	0.095	0.92	0.049	1.3	0.97
Biodiesel	9.6	0.056	0.011	0.12	0.011	0.015	0.17

a. Estimated maximum concentration for the biodiesel, as metal was below detection limits in one or more fractions.

The LA-ICP-MS method provides the possibility of quick analysis of the metal content in the particulate matter. The results showed a different metal composition pattern between biodiesel and diesel. In view of the results, it is possible to conclude LA-ICP-MS offers a good alternative for metal analysis when limited sample is provided. Zn was chosen as the internal standard for the laser ablation; however it is not the best due to the variation among different size fractions. Additionally, Zn is known to fractionate strongly from most other elements during laser ablation. The fractionation factor is 2.5 during a continuous prolonged laser-ablation sampling of NBS 610 glass, while the other elements' fractionation factors detected in this experiment are in the range of 1 to 1.8. Although the high concentration of Zn may compensate for the fractionation issue, using Zn as an internal standard requires well characterized secondary standards (Danyushevsky et al., 2011; Fryer et al., 1995). The next step of this experiment was to find an appropriate internal standard with more consistency, in this case carbon-13.

V.5.5 Metal content when ^{13}C used as the internal standard using LA-ICP-MS method.

Significant emissions of Zn were detected in both diesel and biodiesel samples, which is consistent with the previous results (Figure 30). Zn from diesel emissions likely came from the combusted fuel and lubricating oil used. The lubrication oil has been shown to play an important role in emission of metal contents, particularly for Zn (Wang, et al., 2003). Zn may also be introduced to the biodiesel through the production process. Zn concentration decreased with increasing particle size, with the highest concentration of 243 ppm. For diesel particulates, the Zn concentrations increased with size in the smallest fractions. They reached the maximum concentrations in the particle size range of 0.060 and 0.108μm, then remained constant in larger fractions.

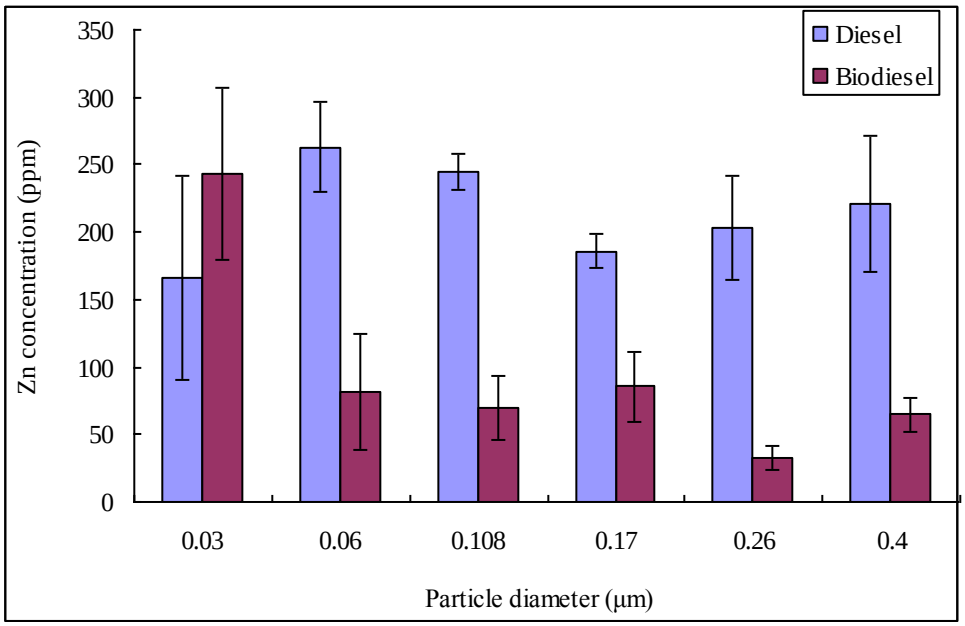

Figure 30: Zn concentration in diesel and biodiesel particles (Error bar indicate one standard deviation of the uncertainty)

The other metals present in both diesel and biodiesel particles are Sr, Sn and Ba (Figure 31 and 32). There was no substantial difference in the Ba concentration of less

than about 1 ppm for diesel particles of diameter less than 0.26 μm, but concentration increased to 3.6 ppm when the particle diameter increased to 0.4 μm. Biodiesel had a much higher Ba concentration, which was greatest when the particles were less than 0.06 μm.

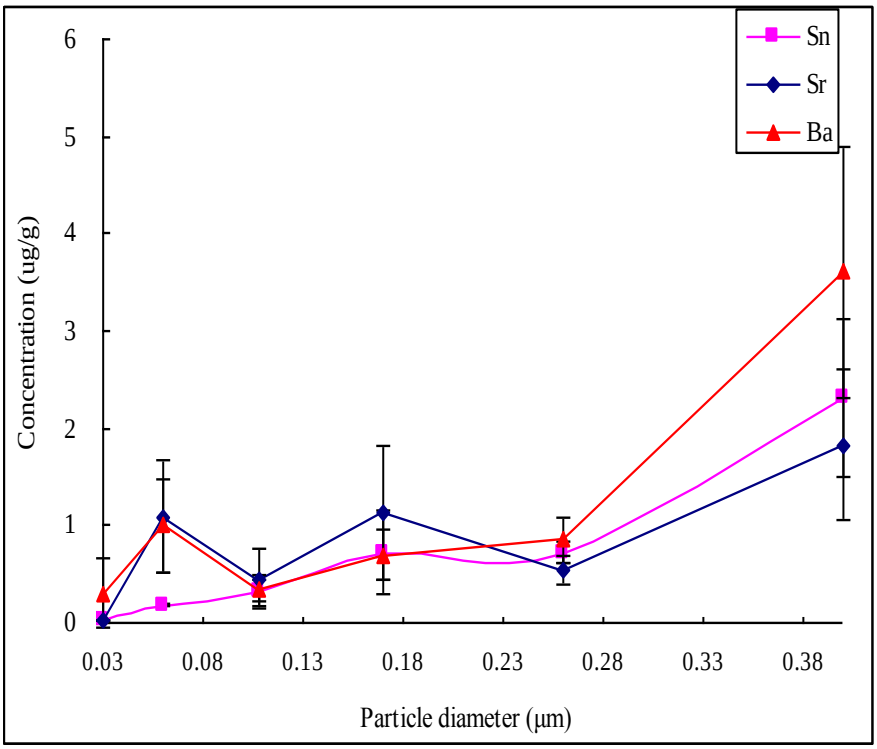

Figure 31: Sr, Sn and Ba concentration in diesel particles (Error bar indicate one standard deviation of the uncertainty)

Sr and Sn concentrations in the biodiesel samples followed the same trend. The concentrations decreased with the increasing particle size and were much higher in biodiesel particulates than in diesel particulates. In diesel samples, there was no apparent trend for Sr with particle size, but Sn concentrations increased steadily with increasing particle size in diesel samples.

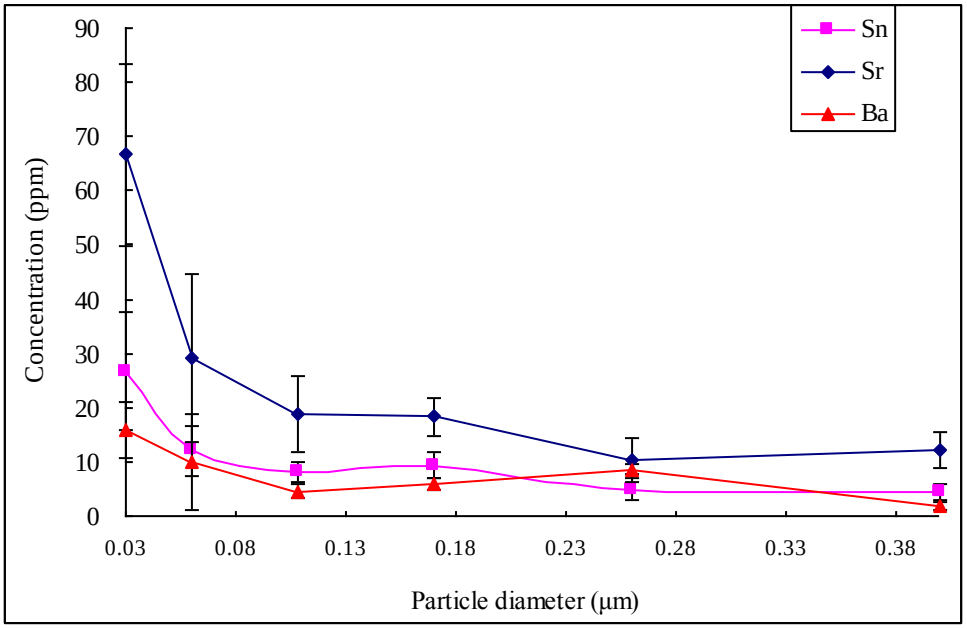

Figure 32: Sr, Sn and Ba concentration in biodiesel particles (Error bar indicate one standard deviation of the uncertainty)

Cu concentrations increased with the diameter of diesel particles (Table 24). There was no apparent trend for biodiesel samples. For stages 2 and 4, Cu concentrations were below the detection limit. Cd and Mg concentrations in diesel particulates increased with the increasing particle size. Mg concentrations were higher in biodiesel samples than in diesel samples (Dwivedi, et al., 2006).

Table 24: Cu, Mg and Cd in diesel and biodiesel samples

Element	Cu (ppm)		Mg (ppm)		Cd (ppm)	
Particle size (µm)	Diesel	Biodiesel	Diesel	Biodiesel	Diesel	Biodiesel
0.03	0.15	13.08	-	551.4	0.01	1.53
0.06	0.15	0.34	-	241.8	0.12	0.01
0.108	0.89	20.19	10.2	180	0.07	0.38
0.17	2.97	0.85	35.4	180.6	0.08	0.37
0.26	3.23	19.70	28.2	-	0.34	0.84
0.4	8.90	0.85	92.4	-	1.00	0.04

Table 25: Trace metals only exist in diesel samples

Diameter μm	Fe ppm	Rb ppm	Cd ppm	Sb ppm	Cs ppm	W ppm	Pb ppm
0.03	-	0.04	0.01	0.01	0.00	0.00	0.20
0.06	91.00	1.24	0.12	0.03	0.10	0.06	1.93
0.108	89.44	0.04	0.07	0.04	0.06	0.02	4.27
0.17	153.22	0.22	0.08	0.14	0.30	0.02	11.41
0.26	231.78	0.19	0.34	0.25	0.07	0.07	35.86
0.4	504.78	1.06	1.00	0.22	0.12	0.13	55.76

Compared with biodiesel samples, the diesel samples had a greater range of metals but with lower concentrations except for Zn. Table 25 and Appendix J show the metals that existed only in diesel samples. Pb is the most abundant metal in this category. It may be emitted from several sources, including fuel and motor oil combustion (Lough, et al., 2005). The detection limits of this method are shown in Appendix K.

V.6 Conclusion.

For a better understanding of the health- and environmental-related air quality issues regarding air particulates, great importance is attached to the identification of the sources, and to the quantification of mass, size, and particle-bound toxics of ambient particles of different sources. In this section, LA-ICP-MS was used to rapidly analyze diesel and biodiesel samples, and to quantify the metal content in particulates collected from a diesel generator at different running conditions. This method provides a new direction for the determination of trace metals in air particulates.

The crucial part of the LA-ICP-MS method is to find the appropriate internal standard, because the absolute amount of material ablated during each run varies from

one sample to another due to the differences in the sample matrix and the related absorption behavior of the wavelength used for the ablation. For the initial experiment, Zn was used as the internal standard. However, the Zn concentrations were determined by dissolving the particles by acid digestion followed by the ICP-MS analysis. There might be some silicate-bound Zn that could not be extracted. Also, due to the heterogeneous properties of the diesel and biodiesel particulates, there were some variations in Zn concentration from stage to stage, which affected detection limits.

After the preliminary experiment, ^{13}C was selected as the internal standard since it is the most abundant element in diesel engine particulates and exists in both reference standards. The results showed biodiesel generated more ultrafine particles than diesel fuel, and levels for all determined elements were low except Zn. Diesel samples have a greater range of metals but with comparatively lower concentrations. This method is still in its initial phase, but shows excellent promise as a method for rapid, accurate assessment of metals in diesel or biodiesel combustion products.

Chapter VI. Conclusions

VI.1 Summary of Results

The goal of this work was to investigate the effects of biodiesel and biodiesel blends, and the resulting changes in fuel properties on emissions of criteria pollutants and particle-bound metal emissions from off-road diesel engines, including a lawn mower, a diesel generator, and a switching locomotive.

The first section of this research uses biodiesel produced from waste cooking oil feedstocks at the University of Kansas. Multiple batches of WCO biodiesel were analyzed to determine physical and chemical properties and to assess elemental composition and hydrocarbon content. One batch of the WCO biodiesel was then blended with #2 diesel to create fuels with 5-100 percent biodiesel by volume. These fuels were used to power two off-road diesel engines. Exhaust emissions from both engines were analyzed to determine concentrations of CO_2, CO, NO_X, and THC. The results were used to evaluate the suitability of WCO biodiesel blends for related off-road applications and to assess the relative importance of fuel makeup and engine operations on pollutant emissions.

The physical properties of the six WCO biodiesel batches produced by the KU Biodiesel Initiative showed very little variation. While there was some change in chemical composition from batch-to-batch, H: C ratios and oxygen contents were very similar, and could be estimated well from GC-MS analysis. Increased blending of biodiesel from waste cooking oil into the B5 fuel currently used by KU produced lower emissions of total hydrocarbons in both engines. These decreases are consistent

with similar results from other studies of waste cooking oil biodiesel, and most likely are related to the observed differences in fuel composition, particularly the higher oxygen level and lower aromatic content.

The relationship between biodiesel content and both CO and NO_X emissions, by contrast, varied substantially between the two engines. The generator results followed typical patterns for biodiesel, with decreased CO and increased NO_X production. In the lawn mower, however, increased biodiesel content resulted in decreased NO_X emissions and had no effect on CO. This difference is likely related to differences in fuel injection strategies between the two engines that resulted from changes in emissions regulation for off-road engines implemented over the last two decades. Overall, these results indicate that the use of this WCO biodiesel at 5-20% blends with #2 diesel could result in decreased emissions of partial combustion products (likely including particulate matter) in the KU landscaping fleet, but with NO_X increase. This effect is expected to be much less consistent for older equipment, which will be less likely to have fuel injection systems optimized for emissions control.

In the second section of this research, a soy- and tallow-based biodiesel fuel was blended with ULSD to create 10% (B10) and 20% (B20) biodiesel blends. These blends were then tested in a switching locomotive owned by the Iowa Interstate Railroad. Each soy biodiesel blend was used exclusively in the locomotive for a 90-day period during normal operation. Emissions monitoring was performed at the beginning and end of the testing period to determine emissions of regulated pollutants from the different fuel blends. The results of the operations and emissions tests were

used to assess the suitability of biodiesel as a “drop in” replacement for petroleum diesel from both a performance and air quality standpoint.

These tests showed that up to 20 percent biodiesel can be successfully used for extended periods of time in currently operating locomotives without engine modifications. Both the B10 and B20 blends caused no performance or maintenance issues for the GP38 locomotive under Iowa summer and winter conditions. The 30-minute static load test results show that biodiesel blends may produce slightly lower horsepower output for the same quantity of fuel. From an emissions standpoint, the biodiesel blends produced lower amounts of combustion byproducts, including soot and total hydrocarbons, but appeared to increase the amount of NO_X released.

WCO, soybean and tallow biodiesel can be used in these three non-road diesel engines without causing any performance issue. There were subtle changes in CO_2 emissions for any engine type or fuel used. Biodiesel decreased THC and CO emissions for the tests. While NO_X emissions depended on not only the engine types but also the fuel used, NO_X emissions increased with increasing biodiesel percentage in the test fuel, NO_2 comprised less than half of the total NO_X. emissions increased with increasing biodiesel percentage in the test fuel.

In the final section, a LA-ICP-MS method was used to quantify the metal content in biodiesel and diesel particulates from a diesel generator at different running conditions, which provided a new direction for the determination of trace metals in exhaust and atmospheric particulates. The crucial step in the LA-ICP-MS method is to find the appropriate internal standard, because the absolute amount of material ablated

during each run varies from one to another due to the differences in the sample matrix and the related absorption behavior of the wavelength used for the ablation. For our initial experiment, Zn was used as the internal standard. However, the Zn concentrations were determined by dissolving the particles by acid digestion. This method produced significant variations in stage to stage results. In the final experiments, ^{13}C was selected as the internal standard since it is the most abundant element in diesel engine particulates and exists in both reference standards.

The results showed that biodiesel generated more ultrafine particles than diesel fuel, and levels for all determined elements were low except for Zn. Diesel samples have more kinds of metals but with comparatively lower concentrations. This method is still in its initial phase and will need further refinement, but shows promise for rapid assessment of exhaust particulates with minimal pretreatment.

VI.2 Research Implications and Future Studies

The following are other specific areas of possible future research based on questions which arose during this study:

1. Biodiesel composition

In the first section, the criteria pollutant emissions were only compared at the zero engine loading, which is not the normal working conditions for these two off-road diesel engines. Tests also should be conducted at higher engine loadings.

The biodiesel feedstocks have a large effect on the emissions. Research has indicated that biodiesels with more unsaturated fatty acids tend to have lower NO_X emissions. As the WCO biodiesel used here had only small batch-to-batch variation,

this issue could not be addressed in this study. Research should be done to investigate the composition of different biodiesel feedstocks to find a better biodiesel mixture to reduce both NO_X and PM emissions. There are also sparse data focusing on the biodiesel nitrogen's effects on diesel engine NO_X emissions.

The limited number of tests conducted for the switching locomotive did not allow for a full assessment of the effects of all relevant variables, such as ambient temperature conditions, on exhaust emissions. Additional testing with a greater variety of engine types is also recommended, as engine design parameters could affect the production of NO_x and partial combustion products. Additional mechanisms for NO_x reductions with biodiesel, such as biodiesel production from alternative feedstocks and engine injection-timing modifications, should be explored in future studies.

2. Particulate composition

It is essential to know the sources of biodiesel metals, whether they are from the production process or the degradation of contacted metals. In order to fully assess the benefit of the biodiesel usage, particle-bound PAHs and other toxic organics also need to be investigated.

3. Broad implications: what trends will be expected if biodiesel is used?

Due to the nature of diesel engines, there is a trade-off between NO_X and PM. Most research has shown that biodiesel content can reduce PM emissions, but with increases in NO_X emissions. EGR is the traditional method to reduce NO_X emissions in diesel engines, which might be a useful way to reduce NO_X formation when

biodiesel is used. In order to use biodiesel in diesel engines, a more complete picture of its effects on exhaust emissions and air quality is highly desirable for planning and regulatory purposes.

Chapter VII. Reference

Abd-Alla, G. H. (2002). Using Exhaust Gas Recirculation in Internal Combustion Engines: A Review. [doi: DOI: 10.1016/S0196-8904(01)00091-7]. *Energy Conversion and Management, 43*(8), 1027-1042

AltIn, R., Çetinkaya, S., & Yücesu, H. S. (2001). The Potential of Using Vegetable Oil Fuels as Fuel for Diesel Engines. [doi: DOI: 10.1016/S0196-8904(00)00080-7]. *Energy Conversion and Management, 42*(5), 529-538

Ang-Olson, J., & Ostria, S. (2005). Assessing the Effects of Freight Movement on Air Quality at the National and Regional Level. Fairfax, VA.

Arimoto, R. (1989). Atmospheric Deposition of Chemical Contaminants to the Great Lakes. *Journal of Great Lakes Research, 15*(2), 339-356

ASTM international. (2008). Astm D6751 - Biodiesel Standards and Testing Methods.

Baulig, A., Poirault, J.-J., Ausset, P., Schins, R., Shi, T., Baralle, D., Dorlhene, P., Meyer, M., Lefevre, R., Baeza-Squiban, A., & Marano, F. (2004). Physicochemical Characteristics and Biological Activities of Seasonal Atmospheric Particulate Matter Sampling in Two Locations of Paris. [doi: 10.1021/es049476z]. *Environmental Science & Technology, 38*(22), 5985-5992

Beary, E. S., & Paulsen, P. J. (1993). Selective Application of Chemical Separations to Isotope Dilution Inductively Coupled Plasma Mass Spectrometric Analyses of Standard Reference Materials. *Analytical Chemistry, 65*(11), 1602-1608

Birmili, W., Allen, A. G., Bary, F., & Harrison, R. M. (2006). Trace Metal Concentrations and Water Solubility in Size-Fractionated Atmospheric Particles and Influence of Road Traffic. [doi: 10.1021/es0486925]. *Environmental Science & Technology, 40*(4), 1144-1153

Bishop, G. A., & Stedman, D. H. (2008). A Decade of on-Road Emissions Measurements. [doi: 10.1021/es702413b]. *Environmental Science & Technology, 42*(5), 1651-1656

Boehman, A. L., Morris, D., Szybist, J., & Esen, E. (2004). The Impact of the Bulk Modulus of Diesel Fuels on Fuel Injection Timing. *Energy & Fuels, 18*(6), 1877-1882

Borrás, E., & Tortajada-Genaro, L. A. (2007). Characterisation of Polycyclic Aromatic Hydrocarbons in Atmospheric Aerosols by Gas Chromatography-Mass Spectrometry. [doi: DOI: 10.1016/j.aca.2006.10.043]. *Analytica Chimica Acta, 583*(2), 266-276

Bourotte, C., Curi-Amarante, A.-P., Forti, M.-C., A. Pereira, L. A., Braga, A. L., & Lotufo, P. A. (2007). Association between Ionic Composition of Fine and Coarse Aerosol Soluble Fraction and Peak Expiratory Flow of Asthmatic Patients in São Paulo City (Brazil). [doi: DOI: 10.1016/j.atmosenv.2006.11.004]. *Atmospheric Environment, 41*(10), 2036-2048

Brown, W. J., Gendernalik, S. A., Kerley, R. V., & Marsee, F. J. (1970). *Effects of Engine Intake-Air Moisture on Exhaust Emissions*. Paper presented at the Automotive Engineering Congress and Exposition, Detroit, Michigan.

Calculations; exhaust emissions. (1986). *Title 40 Code of Federal Regulations*.

California Environmental Protection Agency. (1998). *Proposed Identification of Diesel Exhaust as a Toxic Air Contaminant: Health Risk Assessment for Diesel Exhaust*. Sacramento, CA.

Cardone, M., Prati, M. V., Rocco, V., Seggiani, M., Senatore, A., & Vitolo, S. (2002). *Brassica Carinata* as an Alternative Oil Crop for the Production of Biodiesel in Italy: Engine Performance and Regulated and Unregulated Exhaust Emissions. *Environmental Science & Technology, 36*(21), 4656-4662

Cecrle, E., Depcik, C., Guo, J., & Peltier, E. (Submitted). Analysis of the Effects of Reformate (Hydrogen/Carbon Monoxide) as an Assistive Fuel on the Performance and Emissions of Used Canola-Oil Biodiesel. *International journal of hydrogen energy*

Chang, D., Van Gerpen, J., Lee, I., Johnson, L., Hammond, E., & Marley, S. (1996). Fuel Properties and Emissions of Soybean Oil Esters as Diesel Fuel. [10.1007/BF02523523]. *Journal of the American Oil Chemists' Society, 73*(11), 1549-1555

Charron, A., & Harrison, R. M. (2005). Fine (Pm2.5) and Coarse (Pm2.5-10) Particulate Matter on a Heavily Trafficked London Highway: Sources and Processes. [doi: 10.1021/es050462i]. *Environmental Science & Technology, 39*(20), 7768-7776

Chillrud, S. N., Grass, D., Ross, J. M., & Coulibaly, D. (2005). Steel Dust in the New York City Subway System as a Source of Manganese, Chromium, and Iron Exposures for Transit Workers. *Journal of Urban Health, 82*(1), 33-42

Chisti, Y. (2007). Biodiesel from Microalgae. [doi: DOI: 10.1016/j.biotechadv.2007.02.001]. *Biotechnology Advances, 25*(3), 294-306

Corley, J. (2002). Best Practices in Establishing Detection and Quantification Limits for Pesticide Residues in Foods *Handbook of Residue Analytical Methods for Agrochemicals*: John Wiley & Sons Ltd.

Dagher, Z., Garçon, G., Billet, S., Gosset, P., Ledoux, F., Courcot, D., Aboukais, A., & Shirali, P. (2006). Activation of Different Pathways of Apoptosis by Air Pollution Particulate Matter (Pm2.5) in Human Epithelial Lung Cells (L132) in Culture. [doi: DOI: 10.1016/j.tox.2006.04.038]. *Toxicology, 225*(1), 12-24

Danyushevsky, L., Robinson, P., Gilbert, S., Norman, M., Large, R., McGoldrick, P., & Shelley, M. (2011). Routine Quantitative Multi-Element Analysis of Sulphide Minerals by Laser Ablation Icp-Ms: Standard Development and Consideration of Matrix Effects. *Geochemistry: Exploration, Environment, Analysis, 11*(1), 51-60

Demirbas, A. (2007). Importance of Biodiesel as Transportation Fuel. [doi: DOI: 10.1016/j.enpol.2007.04.003]. *Energy Policy, 35*(9), 4661-4670

Department of Health and Human Services. (2007). Toxicological Profile for Lead. Retrieved October 22, 2009, from http://www.atsdr.cdc.gov/toxprofiles/tp13.html

Di, Y., Cheung, C. S., & Huang, Z. H. (2009). Experimental Investigation on Regulated and Unregulated Emissions of a Diesel Engine Fueled with Ultra-Low Sulfur Diesel Fuel Blended with Biodiesel from Waste Cooking Oil. *Science of the Total Environment, 407*(2), 835-846

Diaz-Sanchez, D. (1997). The Role of Diesel Exhaust Particles and Their Associated Polyaromatic Hydrocarbons in the Induction of Allergic Airway Disease. *Allergy, 52*, 52-56

Diaz-Sanchez, D., Tslen, A., Casillas, A., Dotson, A. R., & Saxon, A. (1999). Nasal Challenge with Diesel Exhaust Particles Can Induce Sensitization to a Neoallergen in the Human Mucosa. *Journal of allergy clinical immunology, 104*, 1183-1188

DieselNet. (2007). Heavy-Duty Trucks and Bus Engines. Retrieved September 12, 2009, from http://www.dieselnet.com/standards/us/hd.php

Dodge, L. G., Callahan, T. J., & Ryan, T. W. (2003). Humidity and Temperature Correction Factors for No_x Emissions from Diesel Engines: Final Report. San Antonio, TX: Southwest Research Institute.

Donaldson, K., Brown, D. M., Mitchell, C., Dineva, M., Beswick, P. H., Gilmour, P., & MacNee, W. (1997). Free Radical Activity of Pm10: Iron-Mediated Generatioin of Hydroxyl Radicals. *Environmental Health Perspectives, 105*(suppl 5), 1285-1289

Donaldson, K., Brown, D. M., Mitchell, C., Dineva, M., Beswick, P. H., Gilmour, P., & MacNee, W. (1997). Free Radical Activity of Pm10: Iron-Mediated Generation of Hydroxyl Radicals. *Environmental Health Perspectives, 105*,

1285-1290

Dorado, M. P., Ballesteros, E., Arnal, J. M., Gomez, J., & Lopez, F. J. (2003). Exhaust Emissions from a Diesel Engine Fueled with Transesterified Waste Olive Oil. *Fuel, 82*(11), 1311-1315

Durbin, T. D., Collins, J. R., Norbeck, J. M., & Smith, M. R. (2000). Effects of Biodiesel, Biodiesel Blends, and a Synthetic Diesel on Emissions from Light Heavy-Duty Diesel Vehicles. [doi: 10.1021/es990543c]. *Environmental Science & Technology, 34*(3), 349-355

Dwivedi, D., Agarwal, A. K., & Sharma, M. (2006). Particulate Emission Characterization of a Biodiesel Vs Diesel-Fuelled Compression Ignition Transport Engine: A Comparative Study. *Atmospheric Environment, 40*(29), 5586-5595

Economic Census. (1999). *Vehicle Inventory and Use Survey*. Washington, DC.

Eggins, S. M. (2003). Laser Ablation Icp-Ms Analysis of Geological Materials Prepared as Lithium Borate Glasses. *Geostandards Newsletter, 27*(2), 147-162

EnviroTools. (2002). Nitrogen Oxides. Retrieved May 24, 2009, from http://www.envirotools.org/factsheets/comtaminants/nitrogenoxides.shtml

Espinosa, A. J. F., Ternero Rodríguez, M., Barragán de la Rosa, F. J., & Jiménez Sánchez, J. C. (2001). Size Distribution of Metals in Urban Aerosols in Seville (Spain). [doi: DOI: 10.1016/S1352-2310(00)00403-9]. *Atmospheric Environment, 35*(14), 2595-2601

Faiz, A., Weaver, C. S., & Walsh, M. P. (1996). *Air Pollution from Moter Vehicles: Standards and Technologies for Controlling Emissions*. Washington, DC: World bank publications.

Ferguson, C. R., & Kirkpatrick, A. T. (2001). *Internal Combustion Engines Applied Thermosciences* (Second ed.). New York: John Wiley & Sons, Inc.

Fernando, S., Hall, C., & Jha, S. (2005). Nox Reduction from Biodiesel Fuels. [doi: 10.1021/ef050202m]. *Energy & Fuels, 20*(1), 376-382

Fluent Inc. (2001). Thermal Nox Formation Retrieved Mar 23, 2010, from http://www.imp.cnrs.fr/intranet/fluent6.0/help/html/ug/node581.htm

Freedman, B., & Bagby, M. (1990). Predicting Cetane Numbers of N-Alcohols and Methyl Esters from Their Physical Properties. *Journal of the American Oil Chemists' Society, 67*(9), 565-571

Freedman, B., Butterfield, R., & Pryde, E. (1986). Transesterification Kinetics of

Soybean Oil 1. [10.1007/BF02679606]. *Journal of the American Oil Chemists' Society, 63*(10), 1375-1380

Fritz, S. G. (2004). Evaluation of Biodiesel Fuel in Emd Gp38-2 Locomotive. San Antonio, Texas: Southwest research institue.

Fryer, B. J., Jackson, S. E., & Longerich, H. P. (1995). The Design, Operation and Role of the Laser-Ablation Microprobe Coupled with an Inductively Coupled Plasma-Mass Spectrometer (Lam-Icp-Ms) in the Earth Sciences. *The Canadian Mineralogist, 33*, 303-312

Gable, C., & Gable, S. (2010). What Is Common Rail Direct Injection (Crd)? *hybrid cars & alternative fuel.* Retrieved November 12, 2010, from http://alternativefuels.about.com/od/dieselbiodieselvehicles/a/dieselcrd.htm

Gavrich, D., Grady, B., Chernich, D., Burnitzki, M., Riemersma, R., Sobieralski, W., Quan, H., & Holve, D. (2008). Sfbr Biodiesel Test Study - Emissions Evaluation of a 1944 Alco. S2 Switch Locomotive Operated on Biodiesel and California, Ultra Low Sulfur Diesel: California environmental protection agency air resources board.

Gerpen, J. V. (2005). Biodiesel Processing and Production. [doi: DOI: 10.1016/j.fuproc.2004.11.005]. *Fuel Processing Technology, 86*(10), 1097-1107

Ghio, A. J., Jacqueline, D., Richards, J. H., Brighton, L. E., Lay, J. C., & Devlin, R. B. (1998). Disruption of Normal Iron Homeostasis after Instillation of an Iron Homeostasis after Instillation of an Iron-Containing Particle. *American Journal of Physiology, 274*, L396-L403

Gillies, J. A., Gertler, A. W., Sagebiel, J. C., & Dippel, W. A. (2001). On-Road Particulate Matter (Pm2.5 and Pm10) Emissions in the Sepulveda Tunnel, Los Angeles, California. [doi: 10.1021/es991320p]. *Environmental Science & Technology, 35*(6), 1054-1063

Gleit, A. (1985). Estimation for Small Normal Data Sets with Detection Limits. *Environmental Science & Technology, 19*(12), 1201-1206

Glikin, P. E. (1985). Fuel Injection in Diesel Engines. *Proceedings of the Institution of Mechanical Engineers, Part D: Transport Engineering, 199*(34), 161-174

Goering, C. E., Schwab, A. W., Daugherty, M. J., Pryde, E. H., & Keakin, A. J. (1981). *Fuel Properties of Eleven Vegetable Oils*.

Golledge, N. (2009). [Ku Dining Vegetable Comsumption.].

Gomez, M. E. G., Howard-Hildige, R., Leahy, J. J., O'Reilly, T., Supple, B., & Malone,

M. (2000). Emission and Performance Characteristics of a 2 Litre Toyota Diesel Van Operating on Esterified Waste Cooking Oil and Mineral Diesel Fuel. [10.1023/A:1006446326210]. *Environmental Monitoring and Assessment, 65*(1), 13-20

Graboski, M. S., & McCormick, R. L. (1998). Combustion of Fat and Vegetable Oil Derived Fuels in Diesel Engines. [doi: DOI: 10.1016/S0360-1285(97)00034-8]. *Progress in Energy and Combustion Science, 24*(2), 125-164

Granum, B., & Løvik, M. (2002). The Effect of Particles on Allergic Immune Responses. *Toxicological Sciences, 65*(1), 7-17

Haas, M. J., Scott, K. M., Alleman, T. L., & McCormick, R. L. (2001). Engine Performance of Biodiesel Fuel Prepared from Soybean Soapstock: A High Quality Renewable Fuel Produced from a Waste Feedstock ‖ . [doi: 10.1021/ef010051x]. *Energy & Fuels, 15*(5), 1207-1212

Hanć, A., Komorowicz, I., Iskra, M., Majewski, W., & Barałkiewicz, D. (2011). *Application of Spectroscopic Techniques: Icp-Oes, La-Icp-Ms and Chemometric Methods for Studying the Relationships between Trace Elements in Clinical Samples from Patients with Atherosclerosis Obliterans*.

Harrison, R. M., Shi, J. P., Xi, S., Khan, A., Mark, D., Kinnersley, R., Yin, J., & Philos, T. (2000). Measurement of Number, Mass and Size Distribution of Particles in the Atmosphere. *Philosophical transactions of the royal society A: mathematical, physical & engineering sciences, 358*, 2567-2580

He, M. Z., Zheng, J. G., Li, X. R., & Qian, Y. L. (2007). Environmental Factors Affecting Vegetation Composition in the Alxa Plateau, China. *Journal of Arid Environments, 69*(3), 473-489

Health and Satety Executive. (1999). Diesel Engine Exhaust Emissions. Retrieved October 28, 2009, from http://www.hse.gov.uk/pubns/indg286.htm

Hemmerlin, M., & Mermet, J. M. (1996). Determination of Elements in Polymers by Laser Ablation Inductively Coupled Plasma Atomic Emission Spectrometry: Effect of the Laser Beam Wavelength, Energy and Masking on the Ablation Threshold and Efficiency. [doi: DOI: 10.1016/0584-8547(95)01451-9]. *Spectrochimica Acta Part B: Atomic Spectroscopy, 51*(6), 579-589

Heywood, J. B. (1988). *Internal Combustion Engine Fundementals*. New York: McGraw-Hill, Inc.

Hilliard, J. C., & Wheeler, R. W. (1979). Nitrogen Dioxide in Engine Exhaust. *SAE technical paper:790691*

Hu, Q., Sommerfeld, M., Jarvs, E., Ghirardi, M., Posewitz, M., Seibert, M., & Darzins, A. (2008). Microalgal Triacylglycerols as Feedstocks for Biofuel Production: Perspectives and Advances. *Plant Journal, 54*(4), 621-639

International Carbon Bank and Exchange. (2000). Calculating Greenhouse Gases Emissions. Retrieved April 12, 2009, from http://www.icbe.com/emissions/calculate.asp

International Organization for Standardization. (1998). Iso Dp 10054: Internal Combustion Compression Ignition Engines-Apparatus for Measurement of Smoke from Diesel Engines Operating under Steady State Conditions-Filter Type Smoke Meter Berlin: Beuth Verlag.

Ito, K., Hasebe, N., Sumita, R., Arai, S., Yamamoto, M., Kashiwaya, K., & Ganzawa, Y. (2009). La-Icp-Ms Analysis of Pressed Powder Pellets to Luminescence Geochronology. *Chemical Geology, 262*(3-4), 131-137

Jakubowski, N., Moens, L., & Vanhaecke, F. (1998). Sector Field Mass Spectrometers in Icp-Ms. *Spectrochimica Acta Part B: Atomic Spectroscopy, 53*(13), 1739-1763

Jarvis, K. E., Williams, J. G., Parry, S. J., & Bertalan, E. (1995). Quantitative Determination Fo the Paltinum-Group Elements and Gold Using Nis Fire Assay with Laser Ablation-Inductively Coupled Plasma-Mass Spectrometry (La-Icp-Ms). *chemical geology, 124*, 37-46

Jones, A. M., & Harrison, R. M. (2004). The Effects of Meteorological Factors on Atmospheric Bioaerosol Concentration-a Review. *Science of the Total Environment, 326*(1-3), 151-180

Knothe, G. (2001). Historical Perspectives on Vegetable Oil-Based Diesel Fuels. *Industry Oils, 12*(11), 1103-1107

Knothe, G., & Steidley, K. R. (2009). A Comparison of Used Cooking Oils: A Very Heterogeneous Feedstock for Biodiesel. [doi: DOI: 10.1016/j.biortech.2008.11.064]. *Bioresource Technology, 100*(23), 5796-5801

Kocak, M. S., Ileri, E., & Utlu, Z. (2007). Experimental Study of Emission Parameters of Biodiesel Fuels Obtained from Canola, Hazelnut, and Waste Cooking Oils. *Energy & Fuels, 21*(6), 3622-3626

Krause, S. R. (1971). *Effect of Engine Intake-Air Humidity, Temperature, and Presure on Exhaust Emissions*. Paper presented at the National Truck, Powerplant, Fuels and Lubricants Meeting, St. Louis, MO.

Kulkarni, P., Chellam, S., Flanagan, J. B., & Jayanty, R. K. M. (2007). Microwave Digestion--Icp-Ms for Elemental Analysis in Ambient Airborne Fine

Particulate Matter: Rare Earth Elements and Validation Using a Filter Borne Fine Particle Certified Reference Material. [doi: DOI: 10.1016/j.aca.2007.08.014]. *Analytica Chimica Acta, 599*(2), 170-176

Lüdke, C., Hoffmann, E., & Skole, J. (1994). Comparative Studies on Metal Determination in Airborne Particulates by La-Icp-Ms and Furnace Atomization Non-Thermal Excitation Spectrometry. [10.1007/BF00322481]. *Fresenius' Journal of Analytical Chemistry, 350*(4), 272-276

Lamaison, L., Alleman, L. Y., Robache, A., & Galloo, J. C. (2009). Quantification of Trace Metalloids and Metals in Airborne Particles Applying Dynamic Reaction Cell Inductively Coupled Plasma Mass Specrometry. *Applied spectroscopy, 63*(1), 87-91

Lapuerta, M., Armas, O., & Rodríguez-Fernández, J. (2008). Effect of Biodiesel Fuels on Diesel Engine Emissions. *Progress in Energy and Combustion Science, 34*(2), 198-223

Lee, C. S., Park, S. W., & Kwon, S. I. (2005). An Experimental Study on the Atomization and Combustion Characteristics of Biodiesel-Blended Fuels. *Energy & Fuels, 19*(5), 2201-2208

Leung, D. (2001). Development of a Clean Biodiesel Fuel in Hong Kong Using Recycled Oil. *Water, Air, & Soil Pollution, 130*(1), 277-282

Lin, C.-C., Chen, S.-J., Huang, K.-L., Hwang, W.-I., Chang-Chien, G.-P., & Lin, W.-Y. (2005). Characteristics of Metals in Nano/Ultrafine/Fine/Coarse Particles Collected Beside a Heavily Trafficked Road. [doi: 10.1021/es048182a]. *Environmental Science & Technology, 39*(21), 8113-8122

Lin, Y. F., Wu, Y. P. G., & Chang, C. T. (2007). Combustion Characteristics of Waste-Oil Produced Biodiesel/Diesel Fuel Blends. *Fuel, 86*(12-13), 1772-1780

Lipsett, M., & Campleman, S. (1999). Occupational Exposure to Diesel Exhaust and Lung Cancer: A Meta Analysis. *american journal of public health, 89*(7), 1009-1017

Liu, K.-S. (1994). Preparation of Fatty Acid Methyl Esters for Gas-Chromatographic Analysis of Lipids in Biological Materials. *Journal of the American Oil Chemists' Society, 71*(11), 1179-1187

Lloyd, A. C., & Cackette, T. A. (2001). Diesel Engines: Environmental Impact and Control. *Journal of the Air & Waste Management Association, 51*(6), 809-847

Longerich, H. P., Jackson, S. E., & Gunther, D. (1996). Laser Ablation Inductively Coupled Plasma Mass Spectrometric Transient Signal Data Acquisition and

Analyte Concentration Calculation. *journal of analytical atomic spectrometry 11*(9), 899-904

Lough, G. C., Schauer, J. J., Park, J.-S., Shafer, M. M., DeMinter, J. T., & Weinstein, J. P. (2005). Emissions of Metals Associated with Motor Vehicle Roadways. [doi: 10.1021/es048715f]. *Environmental Science & Technology, 39*(3), 826-836

Manos, M. J., Bozek, J. W., & Huls, T. A. (1972). *Effect of Laboratory Ambient Conditions on Exhaust Emissions*. Paper presented at the Automotive Engineering Congress and Exposition, Detroit, MI.

Marchetti, J. M., Miguel, V. U., & Errazu, A. F. (2007). Possible Methods for Biodiesel Production. [doi: DOI: 10.1016/j.rser.2005.08.006]. *Renewable and Sustainable Energy Reviews, 11*(6), 1300-1311

Marissiu, F., & Varga, B. (2010). Improvement the Cold Start Process of Ic Engines Fueled with Biodiesel. *Research journal of agricultural science, 42*(1), 630-635

Marshall, J., Franks, J., Abell, I., & Tye, C. (1991). Determination of Trace Elements in Solid Plastic Materials by Laser Ablation–Inductively Coupled Plasma Mass Spectrometry. *Journal of Analytical Atomic Spectroscopy*(6), 145-150

McCormick, R. L., Graboski, M. S., Alleman, T. L., Herring, A. M., & Tyson, K. S. (2001). Impact of Biodiesel Source Material and Chemical Structure on Emissions of Criteria Pollutants from a Heavy-Duty Engine. [doi: 10.1021/es001636t]. *Environmental Science & Technology, 35*(9), 1742-1747

McCormick, R. L., Ross, J. D., & Graboski, M. S. (1997). Effect of Several Oxygenates on Regulated Emissions from Heavy-Duty Diesel Engines. [doi: 10.1021/es9606438]. *Environmental Science & Technology, 31*(4), 1144-1150

McCormick, R. L., Williams, A., Ireland, J., Brimhall, M., & Hayes, R. R. (2006). Effects of Biodiesel Blends on Vehicle Emissions. Golden, CO: National Renewable Energy Laboratory.

McKenna, D., Bhatia, K., Hesketh, R., Rowen, C., Baughn, T., & Marchese, A. (2008). *Evaluation of Emissions and Performance of Diesel Locomotives with B20 Biodiesel Blends: Static Test Results.* Paper presented at the ASME Rail Transportation Division Fall Technical Conference, Wilmington, DE.

Mittelbach, M., & Gangl, S. (2001). Long Storage Stability of Biodiesel Made from Rapeseed and Used Frying Oil. [10.1007/s11746-001-0306-z]. *Journal of the American Oil Chemists' Society, 78*(6), 573-577

Monyem, A., & H. Van Gerpen, J. (2001). The Effect of Biodiesel Oxidation on Engine Performance and Emissions. [doi: DOI:

10.1016/S0961-9534(00)00095-7]. *Biomass and Bioenergy, 20*(4), 317-325

Mulawa, P. A., Cadle, S. H., Knapp, K., Zweidinger, R., Snow, R., Lucas, R., & Goldbach, J. (1997). Effect of Ambient Temperature and E-10 Fuel on Primary Exhaust Particulate Matter Emissions from Light-Duty Vehicles. [doi: 10.1021/es960514r]. *Environmental Science & Technology, 31*(5), 1302-1307

Murayama, T., Fujiwara, Y., & Noto, T. (2000). Evaluating Waste Vegetable Oils as a Diesel Fuel. Proceedings of the Institution of Mechanical Engineers. Part D. *Journal of Automobile Engineering, 214*(2), 141-148

Nwafor, O. M. I. (2004). Emission Characteristics of Diesel Engine Operating on Rapeseed Methyl Ester. [doi: DOI: 10.1016/S0960-1481(03)00133-2]. *Renewable Energy, 29*(1), 119-129

Ohura, T., Amagai, T., Sugiyama, T., Fusaya, M., & Matsushita, H. (2004). Characteristics of Particle Matter and Associated Polycyclic Aromatic Hydrocarbons in Indoor and Outdoor Air in Two Cities in Shizuoka, Japan. [doi: DOI: 10.1016/j.atmosenv.2004.01.038]. *Atmospheric Environment, 38*(14), 2045-2054

Ottley, C. J., & Harrison, R. M. (1991). The Atmospheric Input Flux of Trace Metals to the North Sea; a Review and Recommendations for Research. *The Science of The Total Environment, 100*, 301-318

Pöschl, U. (2002). Formation and Decomposition of Hazardous Chemical Components Contained in Atmospheric Aerosol Particles. *Journal of Aerosol Medicine, 15*(2), 203-212

Peterson, C. L. (1986). Vegetable Oil as a Diesel Fuel: Status and Research Priorities. *Transactions of ASAE, 29*(5), 1413-1422

Pinto, A. C., Guarieiro, L. L. N., Rezende, M. J. C., Ribeiro, N. M., Torres, E. A., & Lopes, W. A. (2005). Biodiesel, an Overview. *Journal of Brazilian Chemical Society, 16*(6B), 1313-1330

Pope III, C. A., Thun, M. J., Namboodiri, M. M., Dockery, D. W., Evans, J. S., Speizer, F. E., & Heath Jr, C. W. (1995). Particulate Air Pollution as a Predictor of Mortality in a Prospective Study of U.S. Adults. *American Journal of Respiratory and Critical Care Medicine, 151*(3), 669-674

Prakash, C. B. (1998). A Critical Review of Biodiesel as a Transportation Fuel in Canada. Retrieved June 8, 2008, from http://www.ec.gc.ca/cleanair-airpur/CAOL/transport/publications/biodiesel/biodiesel4.htm

Pugazhvadivu, M., & Jeyachandran, K. (2005). Investigations on the Performance and

Exhaust Emissions of a Diesel Engine Using Preheated Waste Frying Oil as Fuel. [doi: DOI: 10.1016/j.renene.2005.02.001]. *Renewable Energy, 30*(14), 2189-2202

Radich, A. (2004). Biodiesel Performance, Costs, and Use. Retrieved March 25, 2008, from http://www.eia.doe.gov/oiaf/analysispaper/biodiesel/index.html.

Reed, T. B., Graboski, M. S., & Gaur, S. (1992). Development and Commercialization of Oxygenated Diesel Fuels from Waste Vegetable Oils. [doi: DOI: 10.1016/0961-9534(92)90048-U]. *Biomass and Bioenergy, 3*(2), 111-115

Samaras, C., & Meisterling, K. (2008). Life Cycle Assessment of Greenhouse Gas Emissions from Plug-in Hybrid Vehicles: Implication for Policy. *Environmental Science & Technology, 42*(9), 3170-3176

Schwab, A. W., Bagby, M. O., & Freedman, B. (1987). Preparation and Properties of Diesel Fuels from Vegetable Oils. [doi: DOI: 10.1016/0016-2361(87)90184-0]. *Fuel, 66*(10), 1372-1378

Sensors Inc. (2006). Semtech-Ds User Manual, Revision 1.11 (pp. 191-206). Saline, MI: Sensors, Inc.

Shah, S. D., Cocker, D. R., Miller, J. W., & Norbeck, J. M. (2004). Emission Rates of Particulate Matter and Elemental and Organic Carbon from in-Use Diesel Engines. *Environmental Science & Technology, 38*(9), 2544-2550

Sharma, M., Agarwal, A. K., & Bharathi, K. V. L. (2005). Characterization of Exhaust Particulates from Diesel Engine. [doi: DOI: 10.1016/j.atmosenv.2004.12.047]. *Atmospheric Environment, 39*(17), 3023-3028

Shorter, J. H., Herndon, S., Zahniser, M. S., Nelson, D. D., Wormhoudt, J., Demerjian, K. L., & Kolb, C. E. (2005). Real-Time Measurements of Nitrogen Oxide Emissions from in-Use New York City Transit Buses Using a Chase Vehicle. [doi: 10.1021/es048295u]. *Environmental Science & Technology, 39*(20), 7991-8000

Spandler, C., Mavrogenes, J., & Hermann, J. (2007). Experimental Constraints on Element Mobility from Subducted Sediments Using High-P Synthetic Fluid/Melt Inclusions. *Chemical Geology, 239*(3-4), 228-249

Stokes, S., Ingram, S., Aitken, M. J., Sirocko, F., Anderson, R., & Leuschner, D. (2003). Alternative Chronologies for Late Quaternary (Last Interglacial-Holocene) Deep Sea Sediments Via Optical Dating of Silt-Sized Quartz. *Quaternary Science Reviews, 22*(8-9), 925-941

Stone, R. (1992). *Introduction to Internal Combustion Engines* (Second ed.). Warrendale, PA: Society of automotive engineers, Inc.

Strong, C., Erickson, C., & Shukla, D. (2004). Evaluation of Biodiesel Fuel: Literature Review.

Szybist, P., Song, J., Alam, M., & Boehman, A. (2007). Biodiesel Combustion, Emissions and Emission Control. [doi: DOI: 10.1016/j.fuproc.2006.12.008]. *Fuel Processing Technology, 88*(7), 679-691

The History of Diesel. (2009). The History of Diesel. Retrieved November 15, 2010, from http://www.talktalk.co.uk/motoring/diesel/history.html

Toliyat, H. A., & Kliman, G. B. (2004). *Handbook of Electric Motors*. New York: Marcel Dekker Inc.

Turns, S. R. (1995). Understanding Nox Formation in Nonpremixed Flames: Experiments and Modeling. *Progress in Energy and Combustion Science, 21*(5), 361-385

U.S. Department of Transportation. (1999). *Transportation Statistics Annual Report: Bts99-03*. Washington, DC.

U.S. Energy Information Administration. (2003). In Demand. Retrieved November 18, 2009, from http://www.eia.doe.gov/pub/oil_gas/petroleum/analysis_publications/oil_market_basics/demand_text.htm#Measuring%20Oil%20Consumption

U.S. Environmenal Protection Agency (2001). *Control of Air Pollution from New Motor Vehicles: Heavy-Duty Engine and Vehicle Standards and Highway Diesel Fuel Sulfur Control Requirements-Final Rule*.

U.S. Environmental Protection Agency. (2002). *A Comprehensive Analysis of Biodiesel Impacts on Exhaust Emissions*. (EPA 420-P-02-001). Washington, DC: Assessment and Standard Division, Office of Transportation and Air Quality, USEPA.

U.S. Environmental Protection Agency. (2008). *Control of Emissions of Air Pollution from Nonroad Diesel Engines and Fuel: Final Rule, 40 Cfr Parts 9, 85*.

U.S. Environmental Protection Agency. (2009). *Clean Air Nonroad Diesel - Tier 4 Final Rule*

U.S. Environmental Protection Agency. (2010). *Epa Finalizes Regulations for the National Renewable Fuel Standard Program for 2010 and Beyond.*

U.S. Environmental Protection Agency. (2010). *Ground-Level Ozone: Health and Environment*.

U.S. Environmental Protection Agency. (2010). *Mtbe/ Oxygenates*.

U.S. Environmental Protection Agency. (2010). *National Ambient Air Quality Standards*.

Uchida, N., Daisho, Y., Saito, T., & Sugano, H. (1993). Combined Effects of Egr Ans Superchargine on Diesel Combustion and Emissions. *SAE technical paper: 930601*

UIC Inc. (2008). Cm 5015 Co2 Coulometer. Retrieved March 1, 2011, from http://www.uicinc.com/CarbonSystems.htm

Usta, N. (2005). Use of Tobacco Seed Oil Methyl Ester in a Turbocharged Indirect Injection Diesel Engine. [doi: DOI: 10.1016/j.biombioe.2004.06.004]. *Biomass and Bioenergy, 28*(1), 77-86

Utlu, Z., & Kocak, M. S. (2008). The Effect of Biodiesel Fuel Obtained from Waste Frying Oil on Direct Injection Diesel Engine Performance and Exhaust Emissions. *Renewable Energy, 33*(8), 1936-1941

Valavanidis, A., Salika, A., & Theodoropoulou, A. (2000). Generation of Hydroxyl Radicals by Urban Suspended Particulate Air Matter. The Role of Iron Ions. *Atmospheric Environment, 34*(15), 2379-2386

Vallero, D. (2008). *Fundementals of Air Pollution* (Fourth ed.). Burlington, MA: Academic press.

Vallyathan, V., Castranova, V., Weber, K., & Dalal, N. (1994). Oxygen Radicals and Lung Injury. *Environmental Health Perspectives, 102*(Suppl 10), 1-212

Wang, W. G., Lyons, D. W., Clark, N. N., Gautam, M., & Norton, P. M. (2000). Emissions from Nine Heavy Trucks Fueled by Diesel and Biodiesel Blend without Engine Modification. [doi: 10.1021/es981329b]. *Environmental Science & Technology, 34*(6), 933-939

Wang, Y.-F., Huang, K.-L., Li, C.-T., Mi, H.-H., Luo, J.-H., & Tsai, P.-J. (2003). Emissions of Fuel Metals Content from a Diesel Vehicle Engine. [doi: DOI: 10.1016/j.atmosenv.2003.07.007]. *Atmospheric Environment, 37*(33), 4637-4643

Waynick, J. A. (2005). *Characterization of Biodiesel Oxidation and Oxidation Products*. (08-10721).

Weckwerth, G. (2001). Verification of Traffic Emitted Aerosol Components in the Ambient Air of Cologne (Germany). *Atmospheric Environment, 35*(32), 5525-5536

Wichmann. (2007). Diesel Exhaust Particles. *Inhalation toxicology, 19*(s1), 241-244

Woods, G. D., & Fryer, B. J. (2007). Direct Elemental Analysis of Biodiesel by Inductively Coupled Plasma-Mass Spectrometry. *Analytical and Bioanalytical Chemistry, 389*(3), 753-761

Wu, L., & Wang, R. (2005). Carbon Monoxide: Endogenous Production, Physiological Functions, and Pharmacological Applications. *Pharmacological Reviews, 57*(4), 585-630

Wu., S., Wang., X., Yan., J., Zhang., M., & Hong, H. (2010). Diurnal Variations of Particle-Bound Pahs at a Traffic Site in Xiamen, China. *Aerosol and air quality research, 10*, 497-506

Yahya, A., & Marley, S. J. (1994). Performance and Exhaust Emissions of a Compression Ignition Engine Operating on Ester Fuels at Increased Injection Pressure and Advanced Timing. [doi: DOI: 10.1016/0961-9534(94)90070-1]. *Biomass and Bioenergy, 6*(4), 297-319

Yang, H.-H., Hsieh, L.-T., Liu, H.-C., & Mi, H.-H. (2005). Polycyclic Aromatic Hydrocarbon Emissions from Motorcycles. [doi: DOI: 10.1016/j.atmosenv.2004.09.054]. *Atmospheric Environment, 39*(1), 17-25

Yang, H.-H., Lo, M.-Y., Chi-Wei Lan, J., Wang, J.-S., & Hsieh, D. P. H. (2007). Characteristics of Trans,Trans-2,4-Decadienal and Polycyclic Aromatic Hydrocarbons in Exhaust of Diesel Engine Fueled with Biodiesel. [doi: DOI: 10.1016/j.atmosenv.2006.12.028]. *Atmospheric Environment, 41*(16), 3373-3380

Zhang, Y., Dubé, M. A., McLean, D. D., & Kates, M. (2003). Biodiesel Production from Waste Cooking Oil: 1. Process Design and Technological Assessment. [doi: DOI: 10.1016/S0960-8524(03)00040-3]. *Bioresource Technology, 89*(1), 1-16

Zhang, Z. L., Hong, H. S., Zhou, J. L., & Yu, G. (2004). Phase Association of Polycyclic Aromatic Hydrocarbons in the Minjiang River Estuary, China. *Science of the Total Environment, 323*(1-3), 71-86

Appendix A: The correction factor for the biodiesel molecular weight

Fuel	Semtech Formula	Molecular Weight	Corrected Formula	Corrected Molecular Weight	Correction Factor
Diesel	$CH_{1.80}$	13.8254	$CH_{1.80}$	13.83	1.00
B5	$CH_{1.80}$	13.8254	$CH_{1.80}O_{0.005}$	13.91	0.99
B20	$CH_{1.81}$	13.83548	$CH_{1.81}O_{0.02}$	14.16	0.98
B50	$CH_{1.84}$	13.86572	$CH_{1.84}O_{0.051}$	14.68	0.94
B75	$CH_{1.85}$	13.8758	$CH_{1.85}O_{0.076}$	15.09	0.92
B100	$CH_{1.87}$	13.89596	$CH_{1.87}O_{0.102}$	15.53	0.89

Appendix B: The response factor of different fatty acid in the calibration standards

Name	Retention time(min)	RF 1	RF 2	RF 3	RF 4	RF 5	RF 6	RF 7	RF 8	RF 9	RF 10	Average RF
Decanoic acid,	3.247	0.3013	0.2524	0.2810	0.2846	0.2823	0.3895	0.4367	0.4255	0.4222	0.3963	0.3472
Dodecanoic acid,	5.818	0.4821	0.4459	0.4291	0.4453	0.4464	0.4323	0.4880	0.4788	0.4685	0.4456	0.4562
Methyl	8.846	0.5209	0.4942	0.4623	0.4726	0.4832	0.4687	0.5175	0.5029	0.5003	0.4772	0.4900
Hexadecanoic acid,	11.98	0.5535	0.5440	0.4942	0.4968	0.5176	0.4974	0.5440	0.5360	0.5259	0.5131	0.5222
9-Hexadecenoic acid,	12.41	0.5167	0.4995	0.4634	0.4451	0.4590	0.4463	0.4817	0.4805	0.4720	0.4590	0.4723
Octadecanoic acid,	16.19	0.5548	0.5599	0.5140	0.4999	0.5168	0.5037	0.5286	0.5333	0.5090	0.5121	0.5232
9-Octadecenoic acid (Z)-,	16.65	0.4995	0.5765	0.4838	0.4893	0.4805	0.4722	0.5026	0.5168	0.4797	0.4973	0.4998
Ethyl Stearate	17.09	1.0000	1.0000	1.0000	1.0000	1.0000	1.0000	1.0000	1.0000	1.0000	1.0000	1.0000
9,12-Octadecadienoic acid,	17.85	0.4907	0.4749	0.4375	0.4248	0.4334	0.4260	0.4424	0.4438	0.4355	0.4283	0.4437
9,12,15-Octadecadienoic acid,	19.68	0.4477	0.4784	0.4315	0.4118	0.4164	0.4089	0.4324	0.4310	0.4192	0.4200	0.4297
Eicosanoic acid,	22.01	0.5528	0.5748	0.5252	0.5172	0.5357	0.5041	0.5252	0.5388	0.5188	0.5132	0.5306
Docosanoic acid,	27.56	0.6188	0.6730	0.5655	0.5369	0.5473	0.5186	0.5337	0.5484	0.4929	0.5335	0.5569
13-Docosanoic acid,	27.95	0.6557	0.7067	0.5309	0.5397	0.5056	0.4852	0.5038	0.5242	0.4799	0.5062	0.5438
Tetracosanoic acid,	32.04	0.6659	0.6705	0.5721	0.5717	0.5725	0.5618	0.5536	0.5591	0.5283	0.5490	0.5804

Appendix C: Summary table of ambient conditions and emissions from generator

Date	Fuel blends	Order Of fuel	Ambient temperature deg C	Exhaust Temperature deg C	CO2 g/kg fuel	CO g/kg fuel	NO g/kg fuel	NO2 g/kg fuel	NOx g/kg fuel	THC g/kg fuel	O2 g/kg fuel
2009-7-31	0	1	22.80	100.57	3120.21	53.36	5.61	6.83	12.45	14.55	22968.86
2009-7-31	0	2	23.03	99.79	3130.10	50.66	6.68	7.33	14.01	14.76	25510.37
2009-7-25	5	3	23.34	99.43	3142.09	46.55	8.24	9.85	18.10	10.32	28168.82
2009-7-26	5	3	24.00	101.42	3131.61	46.24	7.80	7.61	15.41	10.73	24389.12
2009-7-27	5	4	24.30	97.48	3119.08	48.49	6.19	6.73	12.92	12.45	24190.99
2009-7-28	5	1	23.19	95.24	3109.35	51.98	5.81	8.40	14.21	13.27	23391.11
2009-7-31	5	2	23.99	97.36	3108.64	51.05	6.34	7.25	13.59	14.94	24710.09
2009-7-25	20	4	23.88	102.12	3113.15	35.06	8.73	9.48	18.22	7.00	27662.65
2009-7-26	20	1	24.00	103.09	3103.15	34.04	9.72	6.12	15.84	7.60	23825.77
2009-7-27	20	3	24.00	101.93	3090.14	39.24	8.71	9.59	18.30	7.73	23222.38
2009-7-28	20	2	23.81	99.95	3086.33	38.44	7.76	5.78	13.54	9.68	23551.27
2009-7-25	50	1	23.00	98.65	3011.33	29.36	9.90	6.52	16.42	5.63	26328.23
2009-7-26	50	3	23.00	99.31	2992.18	31.08	8.48	6.45	14.93	6.79	22411.90
2009-7-27	50	2	23.00	98.19	2998.03	31.51	10.35	10.09	20.44	6.34	23297.89
2009-7-28	50	4	23.00	96.81	2985.56	33.94	8.80	6.35	15.15	7.34	22104.28
2009-7-30	50	3	23.90	123.45	2972.95	33.69	8.54	5.87	14.41	7.10	16751.94
2009-7-30	75	2	23.76	107.00	2906.32	29.84	9.87	5.69	15.56	5.92	19220.19
2009-7-30	75	4	24.00	119.26	2896.45	31.23	8.93	5.96	14.89	6.46	16902.09
2009-7-26	100	1	22.77	93.69	2841.69	27.86	10.36	7.83	18.20	4.24	21476.34
2009-7-27	100	1	23.37	106.58	2834.25	27.72	9.26	6.69	15.95	4.37	19600.18
2009-7-28	100	3	24.00	103.44	2831.76	28.79	9.15	5.60	14.75	5.22	20303.06
2009-7-30	100	2	23.57	107.74	2830.34	29.33	9.90	6.46	16.36	4.86	19600.16

Appendix D: Summary table of ambient conditions and emissions from Mower

Date	Fuel blends	Order of fuel	Ambient temperature deg C	Exhaust Temperature deg C	CO2 g/kg fuel	CO g/kg fuel	NO g/kg fuel	NO2 g/kg fuel	NOx g/kg fuel	THC g/kg fuel	O2 g/kg fuel
2008-10-16	B5	1	17.35	84.21	2988.67	49.59	51.53	15.40	66.93	45.18	14278.07
2008-10-20	B5	1	24.00	84.50	3009.47	46.87	50.68	15.66	66.33	40.32	14532.96
2008-10-27	B5	4	17.82	77.43	3037.42	43.85	61.23	14.89	76.12	32.85	14070.30
2008-10-28	B5	2	17.24	73.28	3038.96	43.84	61.13	14.81	75.95	35.75	14070.30
2008-10-29	B5	3	21.33	86.92	3008.19	45.10	53.98	14.93	68.91	41.53	16201.08
2008-10-31	B5	4	24.83	87.74	2971.07	48.54	47.94	15.41	63.35	52.02	16402.10
2008-10-16	B20	2	20.24	84.48	2926.27	53.50	50.13	15.93	66.06	45.20	14246.89
2008-10-20	B20	3	22.17	81.02	2971.53	42.94	51.07	14.75	65.82	36.10	13915.26
2008-10-27	B20	3	15.62	77.67	2985.70	43.07	58.52	14.18	72.69	31.59	13585.71
2008-10-28	B20	4	16.69	73.15	2983.87	44.56	58.22	14.39	72.61	31.58	14870.61
2008-10-29	B20	4	22.00	85.28	2950.57	47.54	52.55	16.17	68.72	40.90	16178.32
2008-10-31	B20	1	27.43	84.03	2944.54	48.82	46.70	15.54	62.24	41.75	15399.01
2008-10-16	B50	3	25.78	83.27	2842.74	48.57	48.44	15.60	64.03	38.35	13715.44
2008-10-20	B50	4	23.47	86.63	2859.06	44.12	49.15	14.88	64.03	35.40	13509.69
2008-10-27	B50	2	15.00	76.74	2879.61	40.97	55.91	13.18	69.09	29.23	12789.91
2008-10-28	B50	3	15.70	80.47	2873.29	42.12	53.27	13.91	67.18	31.84	14051.90
2008-10-29	B50	1	19.12	82.31	2860.47	46.28	47.16	14.03	61.18	33.68	14778.17
2008-10-31	B50	3	23.40	84.41	2849.84	43.40	46.62	14.50	61.12	39.04	15245.83
2008-10-16	B100	4	26.38	78.25	2696.45	53.05	38.37	15.51	53.88	29.80	12716.89
2008-10-20	B100	2	23.00	83.41	2696.95	47.67	38.04	14.24	52.28	32.08	12062.57
2008-10-27	B100	1	13.36	76.01	2721.69	44.33	45.22	13.48	58.71	26.01	11934.96
2008-10-28	B100	1	14.48	78.83	2715.03	44.76	43.51	13.05	56.55	28.20	13158.15
2008-10-29	B100	2	20.00	81.64	2714.00	47.77	40.78	14.08	54.86	26.97	14087.40
2008-10-31	B100	2	23.00	83.86	2691.20	48.90	37.16	14.26	51.42	33.67	13909.09

Appendix E: Minitab results from generator and mower tests

General Linear Model: CO_2, CO, NO, NO_2, THC versus fuel blends for generator

```
Factor      Type   Levels  Values
Fuel blends  fixed      6  0, 5, 20, 50, 75, 100


Analysis of Variance for CO2, using Adjusted SS for Tests

Source             DF  Seq SS  Adj SS  Adj MS      F      P
Ambient temperature   1     203      37      37   0.30  0.594
Exhaust temperature   1      24     562     562   4.56  0.052
Absolute humidity     1     720      84      84   0.68  0.423
Fuel blends           5  267840  267840   53568  434.67  0.000
Error                13    1602    1602     123
Total                21  270390


S = 11.1013   R-Sq = 99.41%   R-Sq(adj) = 99.04%


Term           Coef  SE Coef      T      P
Constant      3031.1    124.2  24.41  0.000
Ambient temp   -9.75    17.85  -0.55  0.594
Exhaust temp  -0.9807   0.4593  -2.14  0.052
Absolute hum   5.405    6.537   0.83  0.423


Analysis of Variance for CO, using Adjusted SS for Tests

Source             DF   Seq SS   Adj SS  Adj MS      F      P
Ambient temperature   1     1.78     0.02    0.02   0.00  0.949
Exhaust temperature   1    32.40    12.63   12.63   3.36  0.090
Absolute humidity     1    29.13     1.32    1.32   0.35  0.563
Fuel blends           5  1605.49  1605.49  321.10  85.41  0.000
Error                13    48.87    48.87    3.76
Total                21  1717.67


S = 1.93897   R-Sq = 97.15%   R-Sq(adj) = 95.40%


Term           Coef  SE Coef      T      P
Constant      57.27    21.69   2.64  0.020
Ambient temp   0.202    3.118   0.06  0.949
Exhaust temp  0.14702  0.08023   1.83  0.090
Absolute hum  -0.678    1.142  -0.59  0.563


Analysis of Variance for NO, using Adjusted SS for Tests

Source             DF   Seq SS   Adj SS  Adj MS     F      P
Ambient temperature   1   0.7782   0.1001  0.1001  0.15  0.704
Exhaust temperature   1   2.6971   1.7360  1.7360  2.62  0.130
Absolute humidity     1   0.7916   0.0187  0.0187  0.03  0.869
Fuel blends           5  32.5124  32.5124  6.5025  9.81  0.000
Error                13   8.6143   8.6143  0.6626
Total                21  45.3935


S = 0.814026   R-Sq = 81.02%   R-Sq(adj) = 69.35%


Term           Coef  SE Coef      T      P
Constant      -2.675    9.106  -0.29  0.774
Ambient temp   0.509    1.309   0.39  0.704
```

```
Exhaust temp  -0.05452  0.03368  -1.62  0.130
Absolute hum   0.0806   0.4793   0.17  0.869


Analysis of Variance for NO2, using Adjusted SS for Tests

Source             DF  Seq SS  Adj SS  Adj MS     F      P
Ambient temperature   1   0.008   0.431   0.431  0.17  0.685
Exhaust temperature   1   1.545   0.462   0.462  0.18  0.674
Absolute humidity     1   0.002   0.269   0.269  0.11  0.748
Fuel blends           5   8.488   8.488   1.698  0.68  0.647
Error                13  32.513  32.513   2.501
Total                21  42.554


S = 1.58145   R-Sq = 23.60%   R-Sq(adj) = 0.00%


Term            Coef  SE Coef     T      P
Constant        2.72    17.69   0.15  0.880
Ambient temp    1.056    2.543   0.42  0.685
Exhaust temp  -0.02814  0.06543  -0.43  0.674
Absolute hum   -0.3055   0.9312  -0.33  0.748


Analysis of Variance for THC, using Adjusted SS for Tests

Source             DF   Seq SS   Adj SS  Adj MS     F      P
Ambient temperature   1    0.002    0.129   0.129   0.09  0.769
Exhaust temperature   1    7.076    1.434   1.434   1.00  0.335
Absolute humidity     1    7.173    0.500   0.500   0.35  0.564
Fuel blends           5  225.286  225.286  45.057  31.50  0.000
Error                13   18.594   18.594   1.430
Total                21  258.131


S = 1.19597   R-Sq = 92.80%   R-Sq(adj) = 88.36%


Term           Coef  SE Coef     T      P
Constant      14.10    13.38   1.05  0.311
Ambient temp   0.577    1.923   0.30  0.769
Exhaust temp  0.04955  0.04948   1.00  0.335
Absolute hum  -0.4166   0.7043  -0.59  0.564
```

General Linear Model: CO_2, CO, NO, NO_2, THC versus fuel blends for mower

```
Factor      Type   Levels  Values
Fuel blends  fixed      4  5, 20, 50, 100


Analysis of Variance for CO2, using Adjusted SS for Tests

Source             DF  Seq SS  Adj SS  Adj MS       F      P
Ambient temperature   1    1006     233     233    2.41  0.139
Exhaust temperature   1     976    2136    2136   22.06  0.000
Absolute humidity     1   15244     857     857    8.85  0.009
Fuel blends           3  311552  311552  103851  1072.50  0.000
Error                17    1646    1646      97
Total                23  330424


S = 9.84026   R-Sq = 99.50%   R-Sq(adj) = 99.33%


Term           Coef  SE Coef     T      P
```

```
Constant     3138.12    46.82  67.02  0.000
Ambient temp   1.789    1.153   1.55  0.139
Exhaust temp  -3.1187   0.6640  -4.70  0.000
Absolute hum  -0.8861   0.2979  -2.97  0.009


Analysis of Variance for CO, using Adjusted SS for Tests

Source             DF   Seq SS  Adj SS  Adj MS     F      P
Ambient temperature  1   73.020   9.036   9.036   2.23  0.153
Exhaust temperature  1    0.978   6.297   6.297   1.56  0.229
Absolute humidity    1   49.743  51.885  51.885  12.83  0.002
Fuel blends          3   48.381  48.381  16.127   3.99  0.025
Error               17   68.741  68.741   4.044
Total               23  240.862


S = 2.01087   R-Sq = 71.46%   R-Sq(adj) = 61.39%


Term           Coef  SE Coef      T      P
Constant      30.665    9.569   3.20  0.005
Ambient temp  -0.3521   0.2355  -1.49  0.153
Exhaust temp   0.1693   0.1357   1.25  0.229
Absolute hum  0.21808  0.06088   3.58  0.002



Analysis of Variance for NO, using Adjusted SS for Tests

Source             DF   Seq SS  Adj SS  Adj MS     F      P
Ambient temperature  1   208.50    5.20    5.20   1.37  0.258
Exhaust temperature  1    15.47   69.54   69.54  18.31  0.001
Absolute humidity    1    34.91    3.25    3.25   0.86  0.368
Fuel blends          3   762.86  762.86  254.29  66.95  0.000
Error               17    64.57   64.57    3.80
Total               23  1086.31


S = 1.94895   R-Sq = 94.06%   R-Sq(adj) = 91.96%


Term           Coef  SE Coef      T      P
Constant      103.014    9.274  11.11  0.000
Ambient temp   -0.2671   0.2283  -1.17  0.258
Exhaust temp   -0.5627   0.1315  -4.28  0.001
Absolute hum  -0.05460  0.05901  -0.93  0.368


Analysis of Variance for NO2, using Adjusted SS for Tests

Source             DF   Seq SS  Adj SS  Adj MS     F      P
Ambient temperature  1   7.6334  0.0076  0.0076   0.05  0.825
Exhaust temperature  1   0.1012  0.0506  0.0506   0.34  0.570
Absolute humidity    1   0.6375  1.4751  1.4751   9.79  0.006
Fuel blends          3   5.7645  5.7645  1.9215  12.76  0.000
Error               17   2.5606  2.5606  0.1506
Total               23  16.6972


S = 0.388101   R-Sq = 84.66%   R-Sq(adj) = 79.25%


Term           Coef  SE Coef     T      P
Constant      11.741    1.847  6.36  0.000
Ambient temp  0.01019  0.04546  0.22  0.825
Exhaust temp  0.01518  0.02619  0.58  0.570
Absolute hum  0.03677  0.01175  3.13  0.006
```

Analysis of Variance for THC, using Adjusted SS for Tests

Source	DF	Seq SS	Adj SS	Adj MS	F	P
Ambient temperature	1	237.78	4.46	4.46	0.57	0.460
Exhaust temperature	1	212.51	144.79	144.79	18.59	0.000
Absolute humidity	1	1.90	23.08	23.08	2.96	0.103
Fuel blends	3	380.04	380.04	126.68	16.26	0.000
Error	17	132.44	132.44	7.79		
Total	23	964.66				

S = 2.79116 R-Sq = 86.27% R-Sq(adj) = 81.43%

Term	Coef	SE Coef	T	P
Constant	-31.31	13.28	-2.36	0.031
Ambient temp	-0.2473	0.3269	-0.76	0.460
Exhaust temp	0.8119	0.1883	4.31	0.000
Absolute hum	0.14545	0.08451	1.72	0.103

Appendix F: Laser ablation element menu.

Element name	Symbol	Mass	Abundance
Beryllium	Be	9	100
Carbon	C	13	1.1
Magnesium	Mg	25	10.1
Aluminum	Al	27	100
Calcium	Ca	42	0.6
Scandium	Sc	45	100
Titanium	Ti	49	5.5
Vanadium	V	51	99.8
Chromium	Cr	53	9.5
Iron	Fe	57	2.2
Cobalt	Co	59	100
Nickel	Ni	60	26.2
Copper	Cu	65	30.9
Zinc	Zn	66	27.8
Germanium	Ge	73	7.8
Arsenic	As	75	100
Selenium	Se	82	8.8
Rubidium	Rb	85	72.1
Strontium	Sr	88	82.6
Molybdenum	Mo	95	14.8
Silver	Ag	107	51.3
Palladium	Pd	108	26.7
Cadmium	Cd	114	28.8
Tin	Sn	120	33
Antimony	Sb	121	57.2
Caesium	Cs	133	100
Barium	Ba	138	71.7
Lanthanum	La	139	99.9
Tungesten	W	182	26.3
Platinum	Pt	195	33.7
Mercury	Hg	202	29.8
Lead	Pb	204	1.4

Appendix G: Metal content in Nist 1648 and JA 1.

Element	Symbol	Unit	Nist 1648	JA 1
Carbon	C	ppm	[4312]	na
Copper	Cu	ppm	609±27	43
Barium	Ba	ppm	737	311
Iron	Fe	%	3.91±0.1	4.95
Lead	Pb	%	0.655±0.008	6.55
Magnesium	Mg	%	[0.8]	0.95
Antimony	Sb	ppm	[45]	0.22
Strontium	Sr	ppm	297.33*	263
Sodium	Na	%	0.425±0.002	2.85
Aluminum	Al	%	3.42±0.11	8.06
Potassium	K	%	1.05±0.01	0.64
Chromium	Cr	ppm	403±12	7.83
Nichel	Ni	ppm	82±3	[3.49]
Zinc	Zn	%	0.476±0.014	90.9
Silver	Ag	ppm	[6]	[0.033]
Vanadium	V	ppm	127±7	105
Beryllium	Be	ppm	na	0.5
Molybdenum	Mo	ppm	24.99*	1.59
Cobalt	Co	ppm	[18]	12.3
Titanium	Ti	%	[0.4]	0.51
Cadmium	Cd	ppm	75±7	0.11
Tin	Sn	ppm	115±10	[1.16]
Platinum	Pt	ppm	na	[0.5]
Calcium	Ca	%	na	4.07
Selenium	Se	ppm	27±1	[0.0088]
Arsenic	As	ppm	115±10	2.78
Rubidium	Rb	ppm	[52]	12.3
Cesium	Cs	ppm	[3]	0.62
Scandium	Sc	ppm	[7]	28.5
Lanthanum	La	ppm	[42]	5.24
Tungsten	W	ppm	[4.8]	[0.34]
Germanium	Ge	ppm	na	1.33

Note: The number in [] is noncertified

* There is no value for Mo and Sr in Nist 1648, JA was used to certify the numbers.

Appendix H: Detection limit for ICP-MS method

	Co 59	Ni 60	Cu 65	Zn 66	Sr 88	Mo 95	Cd 114	Sn 120	Sb 121	Ba 138	Pb 208
Calibration using 10, 1, blank on NON-blank subtracted results											
S 100ppb-a	445884.6	99326.98	107612.5	77389.06	637425.5	115005	206461.3	292818.8	299990.3	634270.9	357366.6
S 100 ppb -b	459644.6	101989.3	110598	78725.78	650254.2	116313.9	206217.6	292611.7	297981.1	633026.7	370571.8
DCS 10ppb h	44710.58	11316.25	10961.92	7910.038	63290.58	10267.92	19990.86	29250.24	29591.55	61056.75	36472.86
S 1 ppb-a	3761.42	2185.169	1005.356	787.0991	5368.52	1116.139	1741.805	3172.425	2982.066	5343.656	4833.029
S 1 ppb b	4008.759	2518.185	1061.233	849.1011	5574.104	1165.356	1717.675	3229.167	2903.608	5369.817	4869.278
Blank-a	99.29164	1464.915	180.9895	204.8511	187.0873	83.32667	21.22592	400.877	39.18805	161.7359	6037.626
Blank b	104.7898	1864.466	157.7615	195.4103	254.7967	82.27478	42.07913	411.8153	101.3898	180.9344	1364.674
Slope	0.000219	0.001004	0.000904	0.001262	0.000155	0.000843	0.000489	0.000344	0.000335	0.00016	0.000287
intercept	-0.013323	-1.592504	-0.121095	-0.221051	-0.01768	-0.045384	-0.007858	-0.138732	-0.024528	-0.02027	-0.784049
rsq	0.999974	0.99772	0.999915	0.999894	0.999975	0.999934	0.999995	0.999997	0.999992	0.999997	0.983355
Intercept DL (2 sigma):	0.001015	0.540547	0.023486	0.014747	0.007662	0.000815	0.007322	0.005281	0.030697	0.003212	1.39995

Appendix I: Acid digestion for Zn

Sample name	Bottle weight (g)	Before dilution (g)	Net weight after digestion(g)	After dilution (g)	Net weight after dilution(g)	Partice weight(mg)
Acid blank	10.602	10.602	0	60.1988	49.5968	0
Filter blank 1	10.5444	10.5444	0	60.093	49.5486	0
Filter blank 2	10.7049	10.7049	0	60.9835	50.2786	0
Biodiesel 1	10.6402	12.3426	1.7024	61.41	50.7698	3.07
Biodiesel 2	10.6323	10.6323	0	59.9534	49.3211	7.811
Biodiesel 3	10.6578	12.0378	1.38	61.8806	51.2228	6.923
Biodiesel 4	10.5623	11.3595	0.7972	62.3549	51.7926	10.009
Biodiesel 5	10.6006	10.9455	0.3449	60.8372	50.2366	4.987
Biodiesel 6	10.7055	10.7055	0	60.6695	49.964	0.769
Diesel 1	10.6829	10.6829	0	60.71	50.0271	2.783
Diesel 2	10.5851	11.7816	1.1965	60.8408	50.2557	4.969
Diesel 3	10.5604	13.2183	2.6579	61.7876	51.2272	4.158
Diesel 4	10.6796	12.4804	1.8008	61.1136	50.434	6.422
Diesel 5	10.706	12.5314	1.8254	60.897	50.191	4.067
Diesel 6	10.5899	11.7023	1.1124	60.6223	50.0324	2.195

Appendix J: Metal concentration using C as the internal standard

Sample	C ppm	Mg ppm	Al ppm	Ti ppm	V ppm	Fe ppm	Co ppm	Cu ppm	Zn ppm	As ppm	Se ppm	Rb ppm
diesel 1	9020	0	0	0		0			166.08			
diesel 2	9020	0	0	6		91.00			262.86			1.24
diesel 3	9020	10.2	0	16.2		89.44		0.89	244.62			0.04
diesel 4	9020	35.4	27	6		153.22		2.97	185.71			0.22
diesel 5	9020	28.2	69.35	3.6		231.78		3.23	203.40	0.52		0.19
diesel 6	9020	92.4	99.53	17.4		504.78	0.96	8.90	221.09	1.01	1.38	1.06
biodiesel 1	9350	551.4	0	0		0		13.08	243.43			
biodiesel 2	9350	241.8	0	0		0			81.49			
biodiesel 3	9350	180	0	0		0		20.19	69.77			
biodiesel 4	9350	180.6	0	15		0			85.70			
biodiesel 5	9350	0	0	0		0		19.70	32.62			
biodiesel 6	9350	0	0	0		0			64.92			

Appendix K: Trace metals detection limit for LA-ICP-MS

Element	C	MgO	Al2O3	TiO2	V	FeO
Unit	ppm	wt%	wt%	wt%	ppm	wt%
Concentration	81.3-107	0.001	0.001	0.001	0.049-0.051	0.001
Element	Sr	Mo	Ag	Cd	Sn	Sb
Unit	ppm	ppm	ppm	ppm	ppm	ppm
Concentration	0.006	0.025-0.027	0.003	0.006	0.009	0.003
Element	Co	Cu	Zn	As	Se	Rb
Unit	ppm	ppm	ppm	ppm	ppm	ppm
Concentration	0.065-0.069	0.15-0.159	0.056-0.065	0.029-0.032	0.068-0.072	0.012
Element	Cs	Ba	La	W	Pb	
Unit	ppm	ppm	ppm	ppm	ppm	
Concentration	0.002	0.002-0.004	0.003	0.002	0.087-0.092	